Technical University of Munich

A Data- and Demand-Based Approach at Identifying Accessible Locations for Urban Air Mobility Stations

Thesis submitted in partial fulfillment for the degree of
Master of Science in Transportation Systems

Submitted by	Secundino Arellano III
Academic Advisor	Prof. Dr.-Ing Rolf Moeckel
	Technical University of Munich
External Advisor	Raoul Rothfeld
	Bauhaus Luftfahrt e. V.
Submitted on	January 15, 2020

ABSTRACT

Urban air mobility (UAM), the concept of providing transportation in urban settings via flying vehicles, has captured the attention of research related to on-demand mobility. The concept is expected to provide speedier, time-reducing travel with vehicles envisioned to be cleaner, cheaper and more efficient than presently available short-distance crafts. Integration, by way of UAM station placement, is comparatively less understood than the benefits and vehicular designs of the concept. Therefore, this thesis consisted of developing a semi-automated procedure for allocating UAM stations in the Metropolitan Region of Munich. The work done in this thesis largely followed a geographic information system (GIS) multi-criteria decision analysis framework and consisted of gathering factors considered to be influential in UAM station placement, prioritizing said factors and then allocating stations with a process that had an objective of maximizing coverage for all demand points. The evaluation of the networks consisted of determining demand per number of stations and travel time comparisons with typical ground transportation. Additionally, the thesis networks were compared to a previous study's manually chosen UAM networks. The results indicated the thesis' UAM networks had a comparatively higher UAM demand, but lower travel time savings than the manually chosen networks. Spatial distribution and appropriate placement were found to be influential for both demand and travel time savings.

ACKNOWLEDGEMENTS

I would like to thank my external advisor Raoul Rothfeld who gave me the opportunity to conduct this thesis in conjunction with Bauhaus Luftfahrt e. V. I am very grateful for everything I learned under his supervision, for always entertaining my ideas, providing insightful advice and always being patient.

I am also very grateful for my academic advisor Prof. Dr.-Ing Rolf Moeckel who provided very considerate advice, patiently explained useful concepts and was always very genuine and realistic with expectations.

Special thanks to Carlos Llorca from the Modeling Spatial Mobility research group at the Technical University of Munich for quickly responding and answering all my questions about MITO.

To my family, friends and girlfriend, thank you for always checking in on me and providing ample encouragement.

CONTENTS

List of Tables

List of Figures

LIST OF APPENDICES

1 INTRODUCTION

Urban air mobility (UAM), the process of providing transportation via flying vehicles in an urban setting, has in recent years been the focus of some research concerning future mobility trends and/or on-demand mobility. The concept, however, is not intrinsically new given there have already been such systems in operation during the first half of the 20th century. The Los Angeles Airway's helicopter service, in operation between the late 1940s and early 1970s, provided flight connections to several locations in the Los Angeles region. Similarly, New York Airways, in operation between the late 1940s and 1970s, provided helicopter flight services to the city's airports. Unfortunately, both airway companies ceased services due to fatal crashes and financial hardship. Presently, other helicopter shuttle services, such as BLADE in New York or Voom in São Paulo and Mexico City, continue to accommodate demand for UAM [1, 2].

The introduction of UAM on a wide scale is envisioned to provide travel time reductions for daily commuters. By providing access to a third dimension (i.e. airspace), UAM has the potential to increase the supply of existing metropolitan transportation systems; supplies that are reaching or at capacity. The potential for high-speed travel, flexible paths and ability to fly to distant locations while bypassing ground obstructions are examples of benefits literature has envisioned UAM to provide [3, 4]. Some of the main differences between the reinvigorated UAM concept and previous/present UAM services are the vehicles and scale at which it is anticipated to operate. Future UAM services are envisioned to provide flight service via vertical take-off and landing (VTOL) likely utilizing electric (eVTOL) propulsion [5]. Some claim such vehicles would be quieter, more efficient, less impactful to the environment and more affordable than helicopters or other small aircrafts [3]. While initial UAM operations are anticipated to provide service on low-density networks and with slower speeds [1], proposed future use-cases include high-density on-demand, point-to-point air taxi services, airport shuttle services and intercity connections [4, 6].

In addition to the potential benefits, vehicular concepts and operations for UAM, integration must equally be considered and understood for implementation [2, 5]. Rather than introducing UAM as a mode of travel running in parallel to other mobility systems, UAM has the potential to act as a complimentary service to existing transportation systems [2, 7, 8].

1.1 Motivation

An important element of UAM integration relates to the design of networks, which would primarily consist of stations [1]. At the time of this thesis, UAM, as a wide scale on-demand mobility service, was still a relatively new research topic and only a handful of studies were dedicated to the exploration of UAM station allocation. While some studies had coinciding methodologies, there was yet to be a proven best practice for finding suitable locations (or even establishing what suitable locations consist of) for UAM stations. Therefore, this thesis was considerably motivated by the fact that UAM station placement was still a misunderstood, new topic and aimed at providing a varied, alternative approach.

Furthermore, there were 2 previous studies this thesis aimed to expand given their study areas coincided with that of this thesis and their work primarily consisted of [7], or at least included [8], a method for UAM station placement. The work done in these studies were frequently consulted, compared and mentioned throughout this thesis.

1.2 Objectives and Research Questions

The main goal of this thesis was to develop a procedure for allocating stations in the Metropolitan Region of Munich. The chosen, semi-automated procedure was developed using a multi-criteria decision analysis framework that considered several factors. The objective for the allocation procedure was to generate UAM networks in such a way that stations were spatially distributed to accommodate all demand while maximizing the coverage of each station. Such objectives were consistent with German spatial planning practices, which strive to provide equal living conditions and services to all municipalities regardless of size or demand [9].

The evaluation of said objectives included a comparison of the resulting semi-automated UAM networks with those of a previous study [8] that manually selected stations throughout the study area. The evaluation, and this thesis, aimed at answering the following research questions:

1. Is there a point at which UAM demand in the Metropolitan Region of Munich levels off as a result of incrementing stations? If so, how many stations would be required?
2. Would the introduction of UAM to the Metropolitan Region of Munich provide travel time savings to destinations such as city cores and/or the Munich Airport?
3. Is there a difference in UAM demand and travel time savings for networks defined manually versus semi-automated?

1.3 Thesis Structure

The structure of this thesis is as follows: Chapter 2 consists of a review of literature on topics such as urban air mobility, multi-criteria decision analysis and UAM station allocation studies. Chapter 3 describes the study area, factors found to be influential for UAM station allocation and the general data collection process. Chapter 4 described the methodology and analytical procedures employed in this thesis. Chapter 5 consists of the evaluation of the UAM networks developed in this thesis. Finally, Chapter 6 was the conclusion where research questions were addressed, limitations acknowledged, and future work proposed.

2 LITERATURE REVIEW

2.1 Urban Air Mobility Background

Simply put, urban air mobility is the concept of providing transportation via a flying vehicle within an urban setting [10]. Though not a new concept (think helicopters), there has been a technological push to produce flying vehicles that would be cheaper and cleaner than what is currently available in the market. Given these vehicles would potentially operate in dense, urban settings, they would require to take-off and land vertically likely with electric propulsion [5]. There are already a multitude of companies invested in UAM/VTOL development programs [3, 11] and if the trends continue, the technology will likely improve and come to fruition.

2.1.1 Use Cases

There are several proposed uses for UAM. In their study, Baur et al. [6] suggest 3 cases: (1) air taxis, (2) airport shuttles, and (3) intercity flights. Under the air taxi case, UAM vehicles would provide on-demand, point-to-point flight service between stations located inside a defined area (most likely confined to a metropolitan area). Trips are not envisioned to surpass 50 km and the expected number of passengers would be 1 or 2. Under the airport shuttle case, flight routes and schedules would most likely be fixed. Service would be limited to flights between a metropolitan area and an airport (or airports). Flight distances are believed to be on par or longer than those under the air taxi case. Under the intercity flights case, flight service would be provided between nearby cities too close for conventional airline flights. Like the airport shuttle case, flight routes and schedules would be fixed. The expected number of passengers would be between 2 and 4 and UAM vehicles would require the capacity to travel further (up to 250 km).

In addition to the cases listed in Baur et al.'s study, Thipphavong et al. [1] proposed UAM use cases outside of passenger-specific travel. This includes transportation for cargo, emergency and rescue, law enforcement, and monitoring for weather, news and ground traffic.

The UAM use case assumed for this thesis most closely resembles the air taxis case. However, trips to the airport and other cities, while not fixed to a schedule, were also considered.

2.1.2 Vehicle Types

As was shown in the previous section, different use cases would require different seat and range capacities. Liu et al. [12] consider VTOL and short take-off and landing (STOL) capabilities for personal air vehicles. They indicate VTOL would be suitable for intra-city trips and STOL for thin-haul trips. Propulsion for the former would likely be fully or hybrid electric while the latter would be distributed fully or hybrid electric. There are several advantages that come with electric propulsion: lower emissions, lower noise, and higher motor efficiency. Further, due to less moving parts than a conventional engine, electric motors would likely require less maintenance costs [1]. Distributed electric propulsion systems in particular have an added safety advantage due to their redundant design [3]. If one of the motors were to suddenly fail, there would simply be a reduction in both speed and climbing capabilities rather than a more disastrous outcome.

Baur et al. [6] identified 5 classifications for UAM vehicles currently under development: (1) multicopters, (2) quadcopters, (3) hybrids, (4) tilt-wings, and (5) fixed wing vectored thrust. As the name implies, multicopters have multiple (more than 4) fixed propellers and can cruise at speeds between 80 and 100 km/h. The wingless vehicle can accommodate between 2 and 4 passengers and would be well-suited for an air taxi use case. According to Thipphavong et al. [1], multicopters are expected to perform well for hovering stages, but are expected to have relatively lower cruise speeds. Quadcopters have 4 fixed propellers and are expected to cruise at speeds between 120 and 150 km/h. The wingless vehicle can accommodate between 2 and 6 passengers and would be well-suited for an air taxi and airport shuttle use case. A hybrid design would have both forward and upward facing propellers for thrust and lift, respectively. These types of vehicles are expected to cruise at speeds between 150 and 200 km/h, accommodate between 2 and 4 passengers and be well-suited for all use cases identified in Baur et al [6]. A tilt-wing design would consist of multiple propellers or fans that would be able to rotate depending on whether the vehicle is in hover or cruise stage. This type of vehicle is expected to cruise at speeds between 180 and 250 km/h, accommodate between 2 and 4 passengers, and, like the hybrid design, be well-suited for all use cases. According to Thipphavong et al. [1], articulated UAM vehicles would require more time, space and altitude to accommodate transition stages. Such vehicles would probably have lower hovering efficiency but would likely have higher flight speeds. Finally, a fixed wing vectored thrust design consists of multiple groups of fans that can rotate depending on whether the vehicle is in hover or cruise stage. This type of vehicle is expected to cruise at speeds between 200 and 300 km/h, accommodate between 2 and 4 passengers and be well-suited for airport shuttle and intercity use cases [6].

2.1.3 Modelling and Simulation

In their study, Rothfeld et al. [5] explained that while UAM vehicular technology has been under research for some years, integration is still not fully understood. Integration meaning the interaction between UAM (vehicles and infrastructure) and already existing transportation systems. The authors therefore developed a model that provides a medium by which the effects and performance of UAM systems can be simulated and analyzed. The model is an extension to the well-established multi-agent transportation simulation framework MATSim [13]. With the UAM extension, 3 key UAM features can be set: vehicles, nodes and links [5]. Parameters such as range, capacity, cruise speed and VTOL speed can be set for vehicles. Nodes primarily serve as either stations or link connectors and can have their locations set for 3 dimensions: longitude, latitude and height. Finally, links are the conduits through which UAM vehicles traverse between nodes. Link parameters such as capacity, free-flow speed and length can be set. In addition to setting UAM network elements, operational features, such as routing and dispatching, can also be set. By introducing and connecting UAM-specific elements onto a network with conventional transportation system elements (i.e. roads and intersections), integration effects can be observed and tested for practically any city and/or scenario.

One of the earliest use cases for the MATSim UAM extension was a study based in Sioux Falls, South Dakota [14]. The authors tested several UAM-related parameters including cruise speed, VTOL speed, processing time, vehicle capacity, fleet size and networks (i.e. different number of stations). The UAM service was assumed to be shared and available to passengers on-demand rather than individual ownership and/or operating on a fixed schedule. Results showed that travel time savings was among the leading factors for UAM adoption from passengers. Any updates to parameters that decreased UAM travel time resulted in a higher UAM mode share. Among the most influential parameters was also processing time, which corresponds to the time segment between arriving at a UAM station and vertical take-off. Another factor that greatly influenced UAM usage was the number of UAM stations. For example, decreasing the number of stations from 10 to 4 lead to a 55% reduction in UAM passengers.

The MATSim UAM extension was used on a larger scale for a study based in the metropolitan region of Munich, Germany [8]. The study is known as OBUAM for Oberbayern (Upper Bavaria) UAM. In the study, the introduction of UAM, as a complement service to public transportation, to the Upper Bavaria region was explored. The performance of UAM was evaluated by determining demand for such a service in the region. Much like the Sioux Falls study [14], adjustments to UAM-related parameters were tested and resulted in varying mode shares. In order to determine UAM demand, the agent- and trip-based model Microsimulation Transport Orchestrator (MITO) [15] was enhanced so that its mode choice model would include UAM. This was done by integrating MITO with the MATSim UAM extension.

MITO starts by taking a synthetic population as an input [15]. In the case of OBUAM, the synthetic population utilized was created using census data for the metropolitan region of Munich [16]. The model utilizes the synthetic population to generate travel demand for every household; this step is known as trip generation. Next, both mandatory and discretionary (i.e. not mandatory) trips for each household are determined. While mandatory trips must be completed, discretionary trips are assigned if the household’s travel time budget allows it. After trip purposes are determined, destination and mode choice are calculated using logit models. Trip(s) time of day (arrival and departure time) are determined and dependent on the chosen mode. The final step is trip assignment, which is handled by MATSim [15]. A graphical representation is shown below in Figure 1.

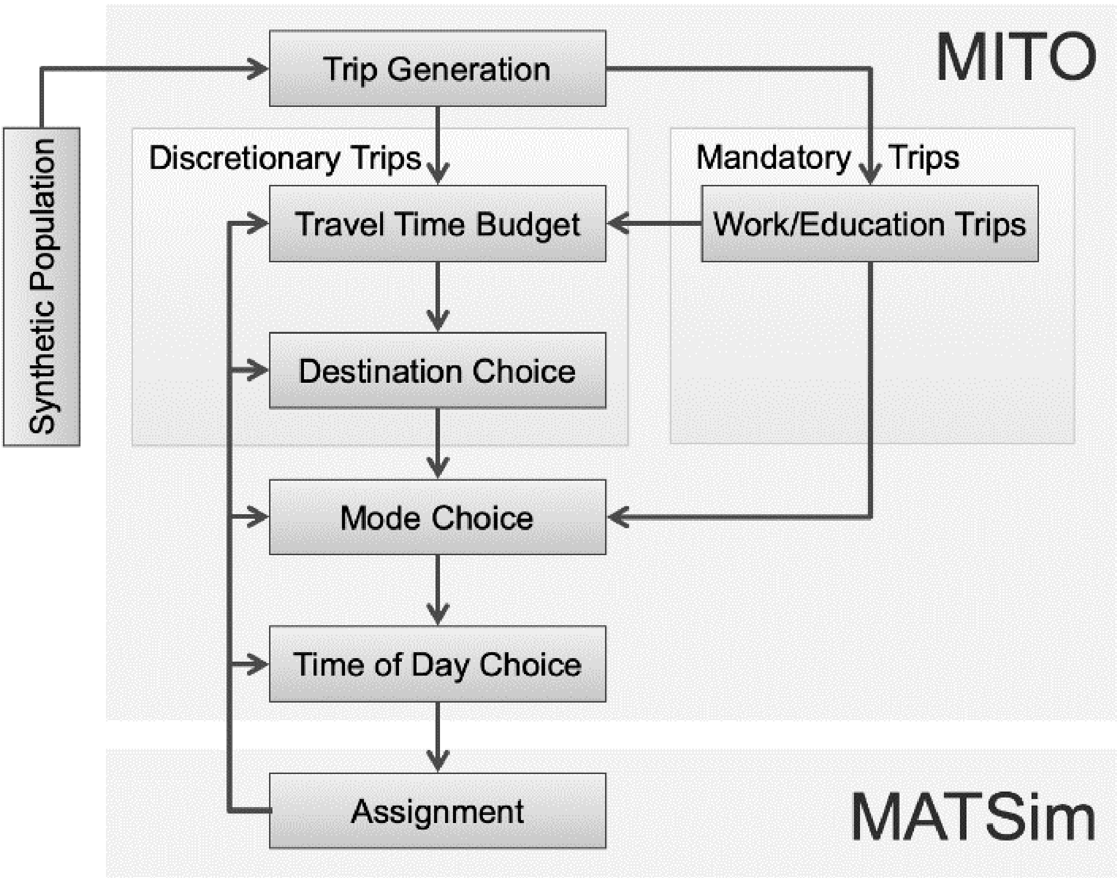

Figure 1 MITO Flowchart [8]

It was in the traffic assignment step where the MATSim UAM extension was integrated with MITO. This integration allowed iterative feedback between the UAM extension and MITO. After traffic assignment is simulated in MATSim, UAM users can reconsider if they want to choose UAM as their mode of travel. If a UAM user experienced excessive wait time for UAM, then the probability said user would again choose UAM in the next loop/iteration would be low. Ideally, an equilibrium between supply and demand would be reached after going through a number of iterations. A graphical representation of this feedback loop is shown below in Figure 2.

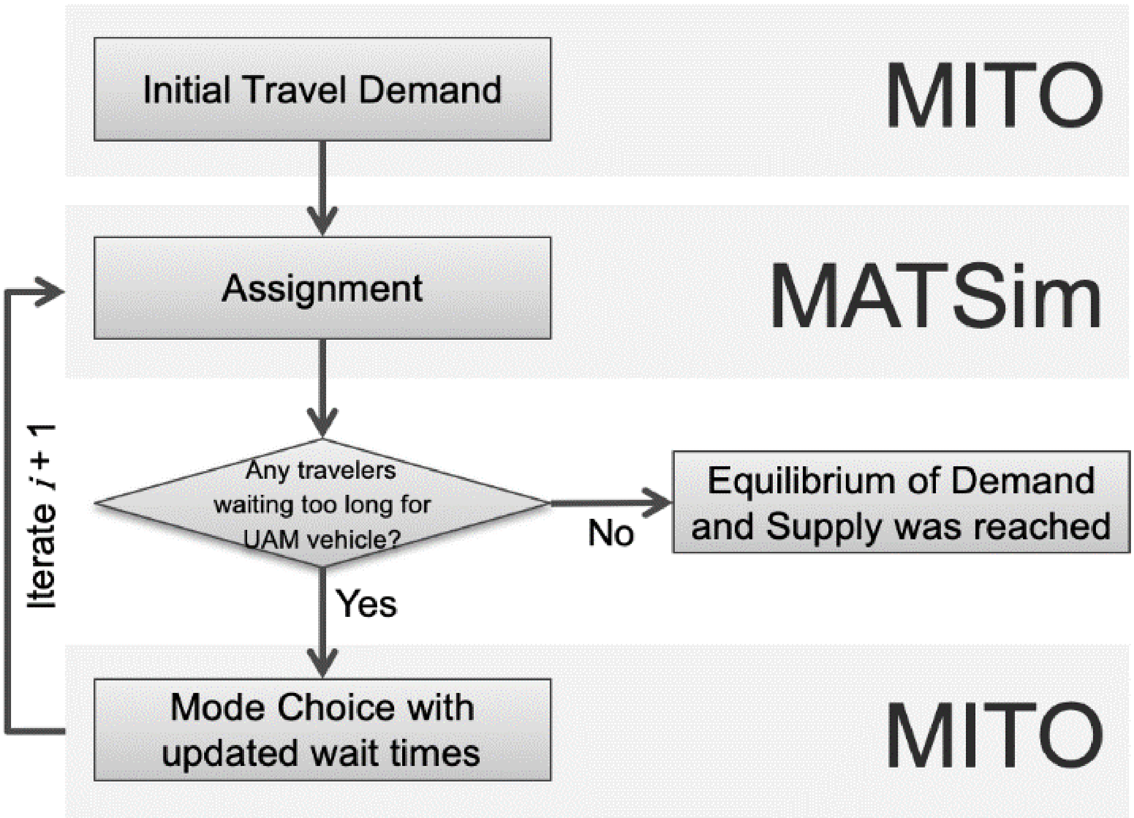

Figure 2 MITO MATSim Feedback Loop [8]

2.2 Urban Air Mobility Station Allocation

2.2.1 Existing Infrastructure and Suitability

Several studies have already utilized different methods and provided rationales for identifying locations for UAM stations. For example, Antcliff, Moore, and Goodrich [17] identified potential station locations depending on land-use types in Silicon Valley: freeway cloverleaf interchanges for general urban settings, water barges for metropolitan settings, and private tech company campuses for private land-use settings. The authors indicated cloverleaf interchanges are favorable due to them being widespread, government owned, adequately separated from private land-use, and located in high-noise areas. The water-barge option was proposed for the denser, bay-surrounded areas of Silicon Valley due to a lower count of cloverleaf interchanges (lesser land-consuming diamond interchanges prevail here). This option is of course only viable for cities surrounded by bodies of water. Finally, the authors expect tech companies to be early users of UAM and therefore placing stations at tech company campuses was found to be a suitable proposition.

A study by Otte et. al [18] proposed using existing airfields within the North Rhine-Westphalia German state for UAM stations. In total, 47 airfields were identified and consisted of passenger airports, public airfields, and special-purpose airfields. The study stated that with that many stations, 25 out of the 29 cities (equating to about 87% of the population) in North Rhine-Westphalia would have access to a station within 15 km (from city centers). The authors also proposed using appropriately dimensioned rooftops for future UAM stations within denser areas. Using the city of Cologne, Germany as an example, a total of 5 rooftops were identified to be suitable sites for future UAM stations and were all within 6 km of the city center.

In his thesis, Fadhil [7] found suitable areas for UAM station placement by applying a Geographic Information System (GIS) -based suitability analysis. Specifically, the thesis utilized multicriteria decision analysis (also known as multicriteria decision making), which generally involves evaluating alternatives based on criteria that correspond to a decision maker's preferences [19]. Multicriteria decision analysis (MCDA) can be subdivided into two groups: multi-attribute and multi-objective. Fadhil [7] employed a multi-attribute approach by combining different factors (as layers) and applying weights to each factor corresponding to their importance in the decision-making process. Fadhil identified 10 factors that could be influential in the determination of UAM ground infrastructure placement and included: population density, points of interest, major transport nodes and existing noise. The weights for each of the factors were determined by conducting an analytical hierarchy process (AHP) -Delphi analysis, which was carried out by surveying different experts of varying fields. The thesis further developed factor weights by interviewing two so-called "super experts" individually to gain their insight for factor priority. The resulting weights were then used to determine spatial suitability through a weighted linear combination process. Fadhil's results were suitability maps for the cities of Los Angles, USA and Munich, Germany. The suitability maps for each city coincided in showing high suitability scores at city centers, major transport hubs and heavily populated, high-income areas.

In another study that also considered the Munich region, Ploetner et al. [8] identified stations by conducting workshops that had experts manually choose where to place stations. The experts identified stations by considering trip purposes such as commuting, business trips, tourism and leisure trips. A total of 3 networks were created with varying numbers of UAM stations: 24 (low density), 74 (medium density) and 130 (high density). Stations were generally placed near or at city centers, major transportation nodes and high population and employment areas. Rural regions with low accessibility were also considered. The networks were evaluated using a mode-choice and traffic assignment model that consider UAM. Results showed a UAM market share of about 0.5% indicating the introduction of UAM may not significantly alter mobility patterns. Further, most UAM trips were found to be for relatively short distances with 55% of UAM trips being less than 20 km in length. In the research gap section, the authors stated that future goals include developing a more automated process (rather than manual selection) for station placement. Such a process would consider different spatial attributes that could be combined to find stations that would maximize coverage; a process that was consistent with the work done in this thesis.

2.2.2 Demand-Based

While some studies [17, 18] proposed solutions that primarily make use of existing infrastructure for station placement, other studies took a more objective approach by utilizing existing travel demand. For example, Lim and Hwang [20] gathered existing commute data for the Seoul metro area and identified three main routes (all towards Seoul). They used a k-means clustering algorithm to identify centroids for commute origins and proposed said centroids as suitable locations for vertiports. In total, the study set up 18 network schematics ranging between 2 and 36 (in increments of 2) UAM station. The authors found that location was more important than the number of UAM stations when trying to improve travel times. Rath and Chow [21] found that Lim and Hwang's [20] approach was limiting in that no objective function (e.g. minimizing travel cost, maximize travel time savings) was set up. In their study, Rath and Chow [21] identified UAM station locations around New York City by setting up an optimization problem to solve for minimum travel cost between origin and destination pairs. For every origin and destination pair, the optimization problem compared travel cost between ground transportation (i.e. car) and UAM. The aim of the study was to find a suitable number of UAM stations that would provide access to the three major airports in New York City: Newark, La Guardia, and JFK. Their results indicated that at about 6 UAM stations, the amount of incoming demand begins to stagnate, however, about 9 UAM stations would be needed for approximately 10% market penetration.

Syed et. al [22] also employed a k-means clustering algorithm to find UAM landing sites. Their study areas were the Northern California and Washington D.C. – Baltimore regions. Their k-means clustering algorithm approach differed to Lim and Hwang's [20] in that census tracts for both regions were weighted depending on population and income. With the applied weights, and objective to reduce travel time to and from stations (or intermodal travel time), the k-means algorithm favored census tracts with high population and income. Four different scenarios were tested with 200, 300, 400 and 1,000 stations. For Northern California, the authors found that 20, 25, 30 and 55% of the potential demand was within 5 minutes of a station under the 200-, 300-, 400- and 1000-station scenario, respectively. The authors used the calculated intermodal travel time (among other factors) in their self-developed mode choice model and indicated it, along with pricing, played a significant role.

In the Uber Elevate white paper, Holden and Goel [3] mention the potential to use existing infrastructure elements (e.g. cloverleaf interchanges or private company campuses) for station placement as proposed by Antcliff, Moore, and Goodrich [17], but acknowledged the limitations that arise in dense, urban areas: land is scarce and expensive. Holden and Goel approach the station allocation problem by using both a k-means clustering algorithm and network optimization, which combines approaches used by previously mentioned studies [20–22]. The study areas were the cities of Los Angeles, USA and London, England. Holden and Goel used a k-means clustering algorithm on a collection of origin and destination points to identify 100 candidate stations. Out of these 100 candidate stations, 25 were chosen through an optimization problem that solved for a maximum trip coverage objective function. Similar to Rath and Chow's [21] approach, the optimization problem compares travel time via ground transportation and air travel. A user was considered eligible for air travel if the air trip was 40% faster than a ground trip. Results indicated that with 25 stations, 60 and 35% of long-distance trips can be accommodated by UAM for Los Angeles and London, respectively.

The studies cited thus far have dealt with passenger UAM transportation, however, German et al. [23] identified locations for placing UAM stations that would be used for cargo delivery. Specifically, the study had two goals that could benefit the Amazon Prime Same Day and Amazon Prime Now services: 1) increase the number of items that could be shipped via Amazon Prime Now, and 2) extend the order time cutoff for Amazon Prime Same Day shipments. The authors chose the San Francisco Bay Area as their study area due to the high-income, tech-savvy population and geographic constraints that exist between the urban areas and the Tracy, California Amazon fulfillment center (50 miles [80 km] apart). Similar to Rath and Chow's [21] network-trip structure, inter-station connections were not considered and trips would fulfill only one trip purpose. To find the stations, the study used an optimization approach with an objective function that maximized package demand served. The study's demand was structured similar to Syed et al.'s [22] study in that census tracts were weighted on population and income under the assumption that customers with higher income are willing to pay for the premium services. The optimization problem solved 8 scenarios to determine demand served by number of stations ranging between 1 and 8 (in increments of 1). Results indicated that the first 3 stations would be placed near the San Francisco Bay Area's largest cities (San Francisco, Oakland, and San Jose) and that incremental demand served dropped for scenarios with more than 3 stations.

As an extension to German et al.'s [23] study, Daskilewicz et al. [24] considered the spatial distribution of jobs, in addition to population and income, as influential factors for identifying UAM stations. Further, the latter study aimed at providing commuter connections rather than package delivery routes [23]. To find locations for stations, Daskilewicz et al. [24] again used an optimization approach, but with an objective function of maximizing travel time savings compared to typical ground transportation (i.e. driving). Potential UAM users were assumed to be high-income (annual salaries greater than $75,000) individuals that commute to work by themselves. The authors chose the San Francisco Bay Area and Los Angeles region as their study areas. For each study area, the optimization problem solved 3 scenarios of varying sizes comprising of 10, 20 and 40 UAM stations. For the San Francisco Bay Area, results indicated that significant amount of work trips are located near the San Francisco downtown financial district while the home trips were more evenly spread out throughout the region. For the Los Angeles region, results placed stations primarily around the Santa

Monica, Burbank and downtown areas, which could be explained by the high accumulation of high-income residents in said areas. When comparing the two cities, Los Angeles showed a higher number of short trips, which could be a result of the high traffic congestion that is characteristic of the region. Both cities saw an increase in trip length for the larger network scenarios. Finally, results for both cities coincided in that a majority of UAM trips had lengths under 30 miles (48 km) with only a few going beyond 60 miles (96 km).

2.3 Multi-Criteria Decision Analysis

Fundamentally, an MCDA decision requires evaluating and choosing among different alternatives based on criteria, or factors, that have been prioritized by decision makers. According to Malczewski and Rinner [19], MCDA consists of 3 basic elements: decision makers, criteria, and decision alternatives. Decision makers can range from individuals, a group of individuals, or an organization. Typically, decisions are made by groups rather than just one person. Criteria can refer to either attributes or objectives [25]. The both are interrelated in that the successfulness of an objective can be measured by its attribute(s). For example, the object of maximizing accessibility to UAM stations can be assessed by attributes such as travel time, distance or cost. Therefore, an objective can be thought of as a goal while an attribute something that can be measured. Moving towards a desired objective requires some type of measurable change in its attribute(s). Decision alternatives are options decision makers must choose and typically relate to action and location (i.e. what to do where). Spatial decision alternatives can be either explicit or implicit [26]. An explicit alternative, for example, could be choosing a site for allocating a UAM station. Implicit alternatives relate to the consequences that arise from choosing one alternative over another. For example, choosing site A over site B for UAM station allocation could lead to poor regional connectivity at site B.

In addition to laying out the basic elements of MCDA problems, Malczewski and Rinner [19] also provided the basic procedures and concepts to conduct MCDA, which are: value scaling, criterion weighting and combination rule. They specify that while said procedures can apply to any MCDA-type problem, they are especially relevant to GIS-based MCDA.

2.3.1 Value Scaling

When criteria or factors are collected, they are usually in different measurement values and ranges. When conducting MCDA, converting the criteria to comparable values is necessary and accomplished with value scaling (also known as standardization) [19, 27]. In his book, Voogd [28] explored a variety of standardization methods all related to transforming the measurement values to a range between 0 and 1 by utilizing the raw maximum and minimum values. Voogd found that if the standardized criteria are to be prioritized, or weighted, via pairwise-comparison (the preferred method for this thesis as explained in the next section), then an appropriate method of standardization will transform the raw values so that the minimum and maximum values are 0 and 1, respectively. This method, known as linear scaling [27], is one of the simplest and is calculated as follows:

$$x_i = \frac{(R_i - R_{min})}{(R_{max} - R_{min})}$$

2-1 Linear Scaling

Where R_i is the raw value measurement of factor i, R_{min} the minimum value and R_{max} the maximum value.

2.3.2 Criterion Weighting

As Kao [29] explains, a challenging aspect of MCDA is the determination of weights for contributing criteria or factors. Typical methods for weight determination include literature review, attaining expert opinion or conducting analytical studies on the data [30]. Determining weights by conducting analytical studies may consist of using methods classified as objective, which are also known as indirect explication or posteriori weights. Under objective methods, weights are determined by the data [29] and by using mathematical models with little to no input from decision makers and hence omit subjective judgement. Examples of commonly used objective weighting methods include entropy method, TOPSIS and multi-objective optimization method [31, 32]. While objective methods are less susceptible to bias due to less subjective input, Malczewski [19] explains such methods are rarely used in MCDA problems involving GIS. Finally, attaining expert opinion can include weighting methods classified as subjective and are also known as direct explication or priori weights

[29]. Under subjective methods, weights are determined through direct input from decision makers and/or experts via questionnaires or interviews. Examples of commonly used subjective weighting methods include analytic hierarchy process, Delphi method and minimum weighted squares [31, 32]. Unlike algorithmic weight determination methods, AHP can handle both qualitative and quantitative factors [33]. Further, Malczewski [19] explains pairwise comparisons (such as AHP) are a commonly used method for MCDA problems that utilize GIS.

2.3.2.1 Analytic Hierarchy Process

First introduced by Saaty in the 1970s, the Analytic Hierarchy Process (AHP) is a decision-making tool intended to determine priority among different criteria or factors [34]. The AHP methodology consists of three main elements: structuring (or decomposition), measurement (or comparative judgements) and synthesis. Structuring relates to setting up the problem into a hierarchy which typically consists of a goal, criteria, sub-criteria and alternatives (all of which are interrelated). Measurement relates to the pairwise comparison of criteria where decision makers choose between 2 criteria at a time based on their judgement of which is more important and by how much. Synthesis, as the name implies, is the aggregation of all the participating elements and is the final step of the analysis. Under synthesis, pairwise comparisons (from measurement) are calculated into ratio-scale weights which are then utilized to determine the best alternative (from structuring) [19, 35, 36].

In his book contribution, Estoque [35] broke down the AHP into fundamental steps:

1. ***Problem Modeling***: In this initial step, the structure of the problem is set up by determining the goals and relevant criteria (or factors) that will be compared. This step encompasses the structuring/decomposition element of AHP.
2. ***Priority Determination***: This is the core of the AHP process were priority between factors are determined. The second step involves choosing between the different factors in a pairwise manner. The number of pairwise comparisons is solely dependent on the number of factors (n):

$$Number\ of\ comparisons = \frac{n(n-1)}{2}$$

2-2 Number of Pairwise Comparisons

In this step, multiple decision makers or experts can be involved. The participants choose which factor they believe is more important than the other and by how much (with a score). The complete comparison of all factors takes the form of a matrix. The scoring schematic is explained below in Table 1, as based on Saaty [37].

Intensity of Importance	Definition
1	Equal importance
3	Moderate importance
5	Strong importance
7	Very strong importance
9	Extreme importance
Reciprocal Scores	When factor A, compared to factor B, is given one of the above scores, factor B receives the reciprocal value when it is compared to factor A

Table 1 AHP Scoring Scale Description

3. ***Weight Derivation***: The third step takes the results of the pairwise comparisons (from step 2) and uses them to calculate the relative weights of all factors. The calculation consists of 2 steps: (1) calculating the normalized value for each factor, and (2) calculating the principal eigenvector, which is also known as the priority vector.
4. ***Consistency***: Once the relative weights are determined, a consistency ratio (CR) can be calculated using the following formulas:

$$CR = \frac{CI}{RI}$$

2-3 Consistency Ratio

$$CI = \frac{\lambda_{max} - n}{n - 1}$$

2-4 Consistency Index

Where CI is the consistency index, RI is the random consistency index, λ_{max} is the principal eigenvalue (from step 3) and n is the number of factors. The RI, developed by Saaty [38], is a fixed value dependent on the number of factors. Saaty suggested a suitable CR to be no more than 10%.

2.3.2.2 Group Decision Making with AHP

According to Forman and Peniwati [39], there are a number of ways to aggregate the priorities of different individuals participating in an AHP including: (1) aggregating each individual's results to the pairwise comparisons (prior to calculating priority vectors), or (2) aggregating each individual's resulting priorities. The method of aggregation depends on whether the group of decision makers are considered a homogeneous group or a collection of individuals. The former assumption leads to the method of aggregating individual judgements (AIJ) and the latter, aggregating individual priorities (AIP) [39, 40]. Each of those methods has recommended mathematical procedures for aggregation. Under AIP, for example, after the priority vectors are calculated for every individual, they are averaged using either an arithmetic or geometric mean. Alternatively, under AIJ, all individuals' pairwise comparisons are averaged using a geometric mean and the result is considered the collective group's judgement of that pairwise comparison. Under AIJ, the judgement or identify of each decision maker is diluted [39]. Ossadnik, Schinke and Kaspar [40] recommend AIP due to its ability to handle a group of any size that may have conflicting judgements.

2.3.3 Combination Rule

A combination rule is a method for evaluating and assessing the different alternatives. This can be done by either picking the best alternative and/or ranking the alternatives based on their performance. A combination rule considers both the alternatives (criteria or factors) and the priorities of the decision makers (criterion weighting) [19]. While there are numerous ways to classify combination rules, this thesis will focus on multi-attribute and multi-objective.

2.3.3.1 Multi-Attribute and Multi-Objective Methods

As stated previously, a criterion can take the form of an attribute or an objective, therefore, MCDA can be subdivided into two groups: multi-attribute and multi-objective. Under multi-attribute decision analysis, all possible solutions are predetermined and finite. Therefore, solving a multi-attribute problem is typically a selection process. Under multi-objective decision analysis, the solution is not predetermined, is continuous in that it can be located anywhere within a region of feasible solutions and typically involves optimizing different, competing objectives [19, 26, 41, 42]. The comparison of the two methods are shown below in Table 2, as based on Hwang and Yoon [42] and Malczewski [25].

Condition	**Multi-Attribute Decision Analysis**	**Multi-Objective Decision Analysis**
Criteria defined by	Attributes	Objectives
Objectives defined	Implicitly	Explicitly
Attributes defined	Explicitly	Implicitly
Constraints defined	Implicitly	Explicitly
Alternatives defined	Explicitly	Implicitly
Examples of multicriteria methods	- Weighted linear combination - AHP - Outranking methods - Ideal point methods	- Linear/integer programming - Goal programming - Compromise programming - Heuristics/metaheuristics
Examples of spatial decision problems	- Site selection - Land use/suitability - Vulnerability assessment	- Site search - Location-allocation - Transportation problem - Shortest path problem - Districting

Condition	Multi-Attribute Decision Analysis	Multi-Objective Decision Analysis
	- Environmental impact assessment	

Table 2 Comparison of Multi-Attribute and Multi-Objective Decision Analysis

As stated previously, Fadhil [7] employed a multi-attribute decision analysis in his thesis. Specifically, Fadhil utilized weighted linear combination and an AHP-type method (Delphi analysis) for attribute scoring and weighting followed by a suitability analysis for the spatial decision-making process. As Fadhil stated, multi-attribute analysis relates to finding suitable areas while multi-attribute relates to finding an exact location.

Therefore, the work done in this thesis aimed at also exploring the multi-objective aspect of MCDA by finding more exact locations for UAM station placement. To do so, the spatial decision analysis method of location-allocation was utilized.

2.4 Location-Allocation

Fundamentally, a location-allocation problem consists of maximizing or minimizing (via optimization) some objective function so that facilities are located and demand (to said facilities) is properly allocated [43].

2.4.1 Problem Types

According to Church [44], location problems consist of two types: location measurement and location search. Location measurement involves measuring, or determining, the location of something while location search (also known as location-allocation) involves searching for a suitable location for an activity or a facility. There are numerous location-allocation problem types, but among the most popular are those that attempt to locate facilities by considering: (1) weighted distance or time, and (2) maximal service distance [44, 45]. The former, more commonly known as the p-median problem type, locates p number of facilities with an objective of minimizing the weighted distance of all served demand points. Typical applications of the p-median problem include locating schools, health clinics and emergency response centers. Minimizing the weighted distance between demand points and facilities could still yield situations where some demand points must travel a long distance to reach the nearest facility. This is unfavorable for facilities such as emergency response centers [44]. Instead of considering weighted distance to locate facilities, a maximal service distance could be introduced. By utilizing a maximal service distance, no demand point must travel further than a specified, adequate distance. All demand points within the maximal service distance are assumed to be covered. Within the context of maximal service distance, two methods can be used to locate facilities: location set covering and maximal covering. Under location set covering, the number of facilities is minimized while in maximal covering, the number of covered demand points is maximized [44, 45].

In their Madrid bike-sharing station allocation study, Garcia-Palomares, Gutierrez and Latorre [46] utilized and compared both the minimize impedance and maximize coverage location-allocation problem types. Their results showed that under minimize impedance, stations were more spread out throughout the city. The authors indicated that while the minimize impedance problem type could be advantageous for spatial equity, some stations were inefficiently placed due to low demand. Under maximize coverage, stations were allocated in areas of higher potential demand, increasing efficiency. However, when the number of stations to find was low, maximize coverage found stations that were isolated and thus not very practical.

While the intended use and structure between bike-sharing and UAM is very different, the location-allocation approach is comparable. This thesis followed a similar approach by exploring both the minimize impedance and maximize coverage location-allocation problem types.

2.4.2 Solvers

There are generally two main methods for solving location-allocation problems: optimization and heuristics. Typically, optimization is done using linear programming which involves optimizing (i.e. solving for maximization or minimization) an objective function while abiding to a set of constraints. Such problems are classified as NP (non-deterministic polynomial) -hard meaning solve time is defined by a polynomial function made up of problem parameters. An increase in problem parameters (e.g. increase in facilities and/or demand points) increases the complexity and solve time of the problem. Heuristics attempt to mitigate the complexity that comes with optimization-type problems. Instead of solving for optimality, heuristics solves problems more efficiently and faster. Heuristic results are not guaranteed to be optimal but are often close [47]. As Church [44] explained it, heuristics were introduced to solve problems too large for mathematical algorithms in a faster and more cost-effective manner.

ESRI's network analyst suite is considered one of the most successful GIS environments to employ heuristics for solving location-allocation problems of varying types (including both p-median and maximize coverage) [48]. Specifically, ESRI's location-allocation problem solver uses the Teitz and Bart vertex substitution process. The Teitz and Bart procedure begins by selecting a random number of facilities *F* from the original, complete pool of facilities *P*. The facilities in *F* are removed from *P* and considered to be the initial set of solutions. The next step is to take (and remove) a single facility *S* from *P* and compare it to the facilities in *F*. If *S* performs better than any of the facilities in *F*, then it is substituted into *F*. This process continues until *P* is empty. The Teitz and Bart procedure has been found to provide good, if not optimal, solutions [44, 47]. Church and Medrano [47] described Teitz and Bart results as 1-opt, which means using one of the unused facilities, in place of one of the used facilities, would not improve results.

If the initial set of solutions *F* are not the same every time the Teitz and Bart procedure is initialized, the result will not always be the same for the same set of data [44]. To remedy this, ESRI's location-allocation solver runs a start routine that generates the same initial set of solutions *F* for the same set of data. By doing this, the same solution is generated regardless of how many times the Teitz and Bart procedure is run [49].

Before applying the Teitz and Bart vertex substitution procedure, ESRI's location-allocation solver calculates an origin-destination matrix consisting of the costs between all facilities and demand points. Afterwards, it edits this cost matrix using Hillsman editing [50]. Under Hillsman editing, the cost matrix is edited in such a way that multiple location-allocation problem types can be solved. This is beneficial because the Teitz and Bart procedure was initially developed to be used for the p-median problem. Hillsman editing calculates what are known as distance strings. A distance string, for a single node, is a collection of distances between the single node and other nodes listed in ascending order. This allows for organized, faster storage and retrieval. The editing process can generate distance strings for both demand and facility points [51].

Using GIS can have a lot of benefits including providing an environment under which dataset collection, management and visualization can be conducted. This, coupled with tools such as ESRI's location-allocation solver, allows for quicker and more stream-lined problem solving execution [49]. In their study, Mapa and Lima [52], compared a heuristic (via GIS) and optimization-type (via linear programming) location-allocation solvers and found that GIS was able to handle larger problems with more facilities and demand data. They noted that processing time was substantially different between the two procedures. For instance, all solutions generated with GIS were completed in less than 5 seconds while some of the linear-programming runs lasted almost 2 hours.

2.5 Surface Modeling

Surface modeling techniques typically involve creating a continuous surface from a collection of measured points (or control points). Some modeling techniques utilize said control points to estimate values for unmeasured locations (or unknown values) while other techniques spread out the measurement values based on their concentration and value. The former is known as spatial interpolation and the latter, density estimation. Surface modeling techniques are useful for removing boundaries from measurement values that typically aren't confined to hard borders [53].

2.5.1 Spatial Interpolation

Much like typical interpolation, the main idea behind spatial interpolation is to take known values and use them to determine unknown values. Typical uses for spatial interpolation include determining amount of precipitation, elevation differences or pollution concentration. The need for spatial interpolation is a result of not being able to collect phenomena measurements at every point within a geographic area. With spatial interpolation, estimates can be generated for all, or most, points where no measurement values were collected. The general assumption behind spatial interpolation is that nearer points are more alike than further points [53]. When conducting spatial interpolation, there are some assumptions to consider about what type of interpolation is to be run: global or local, exact or inexact and deterministic or stochastic [54]. Spatial interpolation methods are classified below in Table 3, as taken from Zhi [54].

Global		**Local**	
Deterministic	*Stochastic*	*Deterministic*	*Stochastic*
– Trend Surface (inexact)	– Regression (inexact)	– Thiessen (exact) – Density Estimation (inexact) – Inverse Distance Weighting (exact) – Splines (exact)	– Kriging (exact)

Table 3 Classification of Spatial Interpolation Methods

The main difference between global and local spatial interpolation methods is related to how many, or which, control points (i.e. known values) will be utilized to determine unknown values. Under global methods, all control points are utilized, and a single trend function is applied to determine all unknown values. Under local methods, a select (or sample) number of control points (typically within a vicinity) are utilized to determine unknown values [55]. Exact and inexact simply refers to whether the interpolated surface passes through every single point (exact) or not (inexact) [54]. Deterministic methods create interpolation surfaces based on mathematical equations and control points while stochastic methods utilize statistics for more advanced predictions and typically provide error measurements [56]. According to Setianto and Triandini [57], the local spatial interpolation methods of Inverse Distance Weighting (IDW) and Kriging provide results with very similar accuracy levels. Further, the authors stated IDW is more intuitive, simpler and requires fewer steps than Kriging. While Kriging does provide more reliable results, no substantial amount of efficiency is lost by using IDW. Therefore, IDW was the selected method to test under the surface modeling technique of spatial interpolation.

2.5.1.1 Inverse Distance Weighting

According to Childs [56], IDW should be used when there is enough density in the control points to fully capture the study area's surface variation. As the method's name implies, estimates are calculated by taking the inverse of the distance (between the control point and unknown value) and weight (of the control point). The influence of a control point diminishes if its distance is far or its weight is small. The formula for IDW [58] is as follows:

$$F(r) = \sum_{i=1}^{m} w_i z\,(r_i) = \frac{\sum_{i=1}^{m} z\,(r_i)\,/\,|r - r_i|^P}{\sum_{j=1}^{m} 1\,/\,\left|r - r_j\right|^P}$$

2-5 Inverse Distance Weighting

Where p is the power parameter that controls the influence of the distance (r minus r_i) between the control point and the unknown value; it is typically set to a value of 2. The z parameter is the weight, or measurement, of the control point. There are some limits that can be imposed onto the IDW calculation: a fixed number of points or a fixed radius. In ESRI's ArcGIS IDW tool [59], the former is called variable search radius and the latter fixed search radius. Under variable search radius, the number of control points are fixed, which leads to search radii of varying sizes depending on how close or far the control points are. Under fixed search radius, the size of the search radius is set (yet not fixed) along with minimum number of control points. Because the search radius is not fixed it can increase in size until the minimum number of control points are satisfied. A visual representation of IDW is shown below in Figure 3, as based on [60].

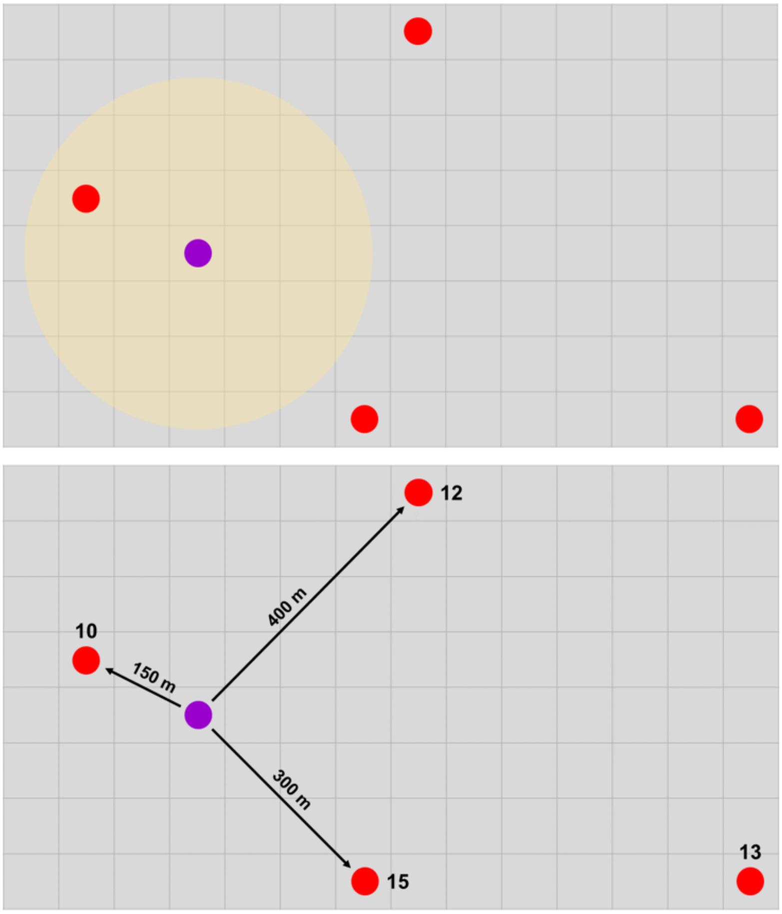

Figure 3 Inverse Distance Weighting. Fixed Search Radius (Top). Fixed Number of Points (Bottom)

As shown, under fixed search radius, the number of control points (red points) reached and utilized was just 1 while under fixed number of points, 3 points were utilized for the estimation of the unknown value (purple point).

2.5.2 Density Estimation

Simply put, to calculate density is to determine the number of phenomena within a specified area. Density can be calculated for anything that is countable such as objects or events (e.g. businesses, trees or earthquakes) and/or their respective attributes (e.g. number of employees, types of trees or earthquake magnitudes). Much like spatial interpolation, there are several methods that can be utilized to estimate density. ESRI's ArcMap, for example, provides two methods: simple and kernel. Under simple density calculations, a search radius is set around every point in the study area. All points that fall within the search radius are added and then divided by the search area. Larger search radii produce smoother surfaces. Kernel density estimation (KDE), on the other hand, sets the search radius around each control point [53]. Given the aim of using a surface modeling technique for this thesis was to determine trends around the collected data, kernel density estimation was the selected method to test under density estimation.

2.5.2.1 Kernel Density Estimation

Under KDE, density is calculated by drawing a smooth curve, or surface, over each control point. The highest calculated value is at the control point, or center of the curve, and will decrease with increased distance from the point [61]. The shape of said curve, or surface, is called the K (kernel) function. There are several K functions to choose from such as uniform, Epanechnikov, biweight or triweight (to name a few) [62]. The KDE tool provided in ESRI's ArcMap, for example, uses a biweight K function, also known as a quartic kernel [61, 62] and takes the following form:

$$\hat{f}(x) = \frac{1}{mh^2}\sum_{i=1}^{m} 3\pi^{-1}\left(1-\left(\frac{x}{h}\right)^2\right)^2$$

2-6 Quartic Kernel Function

The m parameter corresponds to the size of the sample (i.e. total number of control points) and the x parameter to the distance between the unknown value and the kernel. The h parameter is what is known as the bandwidth and corresponds to the size of the search radius drawn around each control point. While the K function does not have a substantial impact for the calculated densities, the choice of bandwidth is of much greater importance. The bandwidth is what determines how far to search for values. Too small a value yields very localized, over-fitted and jagged results while too large a value yields very homogeneous, under-fitted and over-smoothed results [62–64].

In ESRI's KDE tool [61], a bandwidth value is an optional input. If no bandwidth value is set, a default value will be calculated that is dependent on the number, intensity and spread of the control points. ESRI's bandwidth estimation is part of an algorithm that begins by first determining the mean center of all input (or control) points. It then determines the distance between each control point and the mean center. Afterwards, said distances are used to calculate a median distance. A standard distance is then calculated with two options for said calculation: weighted or unweighted. A weighted standard distance will be calculated if each control point has a corresponding intensity value, or score. The weighted standard distance takes on the following form:

$$SD = \sqrt{\frac{\sum_{i=1}^{n}(x_i - \bar{X})^2}{n} + \frac{\sum_{i=1}^{n}(y_i - \bar{Y})^2}{n}}$$

2-7 Unweighted Standard Distance

Where x_i and y_i correspond to the x and y coordinates of control point i, X and Y the coordinates for the mean center, and n the number of control points.

An unweighted standard distance will conversely be calculated in the absence of control point scores, and takes the following form:

$$SD = \sqrt{\frac{\sum_{i=1}^{n} w_i(x_i - \bar{X})^2}{\sum_{i=1}^{n} w_i} + \frac{\sum_{i=1}^{n} w_i(y_i - \bar{Y})^2}{\sum_{i=1}^{n} w_i}}$$

2-8 Weighted Standard Distance

Where w_i corresponds to the weight, or score, of control point i.

Finally, the bandwidth value can be calculated. The default bandwidth estimation formula is based on Silverman's Rule-of-thumb and takes the following form, as taken from ESRI [61]:

$$Search\ Radius = 0.9 * \min\left(SD, \sqrt{\frac{1}{\ln(2)}} * D_m\right) * n^{-0.2}$$

2-9 ESRI's Default KDE Bandwidth Estimation

Where SD is the standard distance, D_m the median distance, and n the number of control points. The min part of the equation chooses the minimum value between SD and the square root multiplication.

A visual representation is shown below in Figure 4, as based on Wasserman [64].

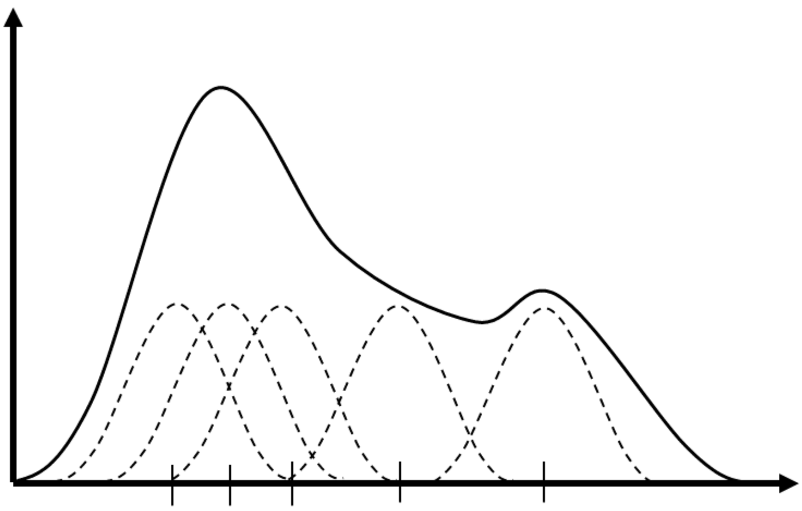

Figure 4 Kernel Density Estimation

As shown, the estimated density value (solid curve) increases with an increase in overlapping kernels (dashed curves). Each tick mark along the horizontal axis corresponds to the highest point of each kernel and represent the control points.

3 DATA COLLECTION AND PREPARATION

3.1 Study Area

The work done in this thesis was based in the Upper Bavaria region of Germany. Specifically, the study area is the Metropolitan Region of Munich, which comprises 444 municipalities of which the 5 core cities are Munich, Augsburg, Ingolstadt, Landshut and Rosenheim. The roughly 15,000 km^2 area is home to about 4.5 million inhabitants and employment is at about 1.8 million. About a third of the population lives in Munich [65].

In their OBUAM study, Ploetner et al. [8] indicated the metropolitan region of Munich was an appropriate area to explore UAM do to the high level of traffic congestion, concentration of affluent municipalities and large amount of touristic activity (more than 19 million tourist visits per year).

A digital representation (in the form of a shapefile) of the Munich metropolitan region was developed by Molloy and Moeckel [65]. In their study, they developed an algorithm that divided the study area to just under 5,000 traffic analysis zones (hereafter referred to as zones). The study's zone system served as the foundational structure by which factors were collected and analysis conducted.

A visualization of the study area is shown below in Figure 5.

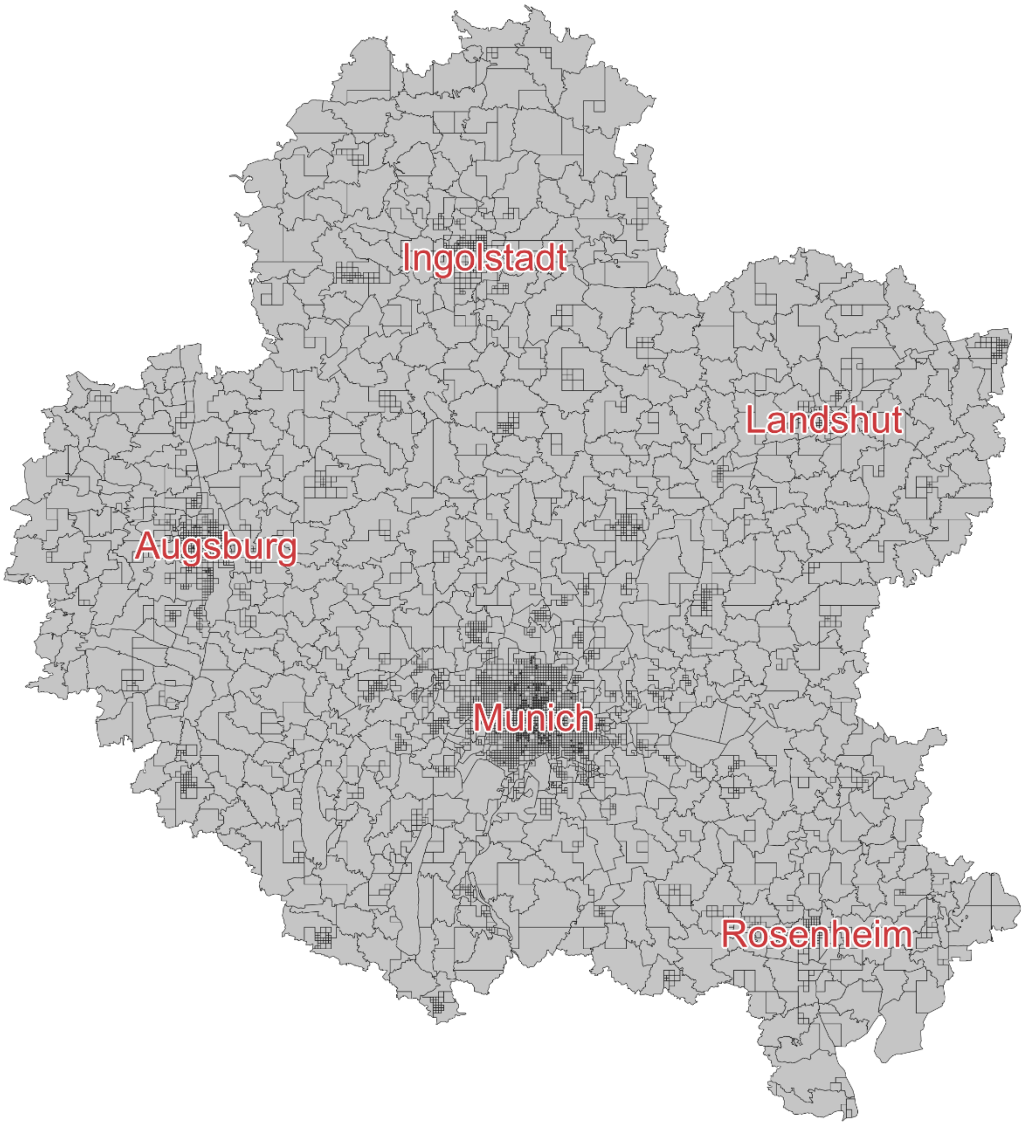

Figure 5 Metropolitan Region of Munich

The image shows the boundaries off all the region's zones. Areas of high socioeconomic and/or land-use data concentration (typically city centers) are represented with smaller zones.

3.2 Factors

There was a total of 10 factors identified and collected for the determination of UAM station allocation. Some of the factors coincided with the factors used in Fadhil's [7] study while others were more so related to modeled demand from the study area. The author took advantage of the fact that some factors had already been prioritized by experts in Fadhil's study. While not all factors utilized in Fadhil's study were utilized in this thesis, some were recycled while others inspired different factors. The prioritized factors (from an AHP-type procedure) from Fadhil’s study are presented below in Table 4 [7].

Factor	Average Weight
Population Density	5.3%
Median Income	12.7%
Office Rent Price	10.9%
Points of Interest	14.1%
Major Transport Node	14.7%
Average Total Transport Cost	12.3%
Job Density	8.5%
Number of Extreme Commuters	7.3%
Potential Supply	6.9%
Existing Noise	7.4%

Table 4 Factors Influencing UAM Ground Infrastructure Placement

As Table 4 shows, the top 3 highest scoring factors were points of interest, major transport node and median income; of which points of interest and major transport node were utilized in this thesis. Other coinciding factors that were of interest for this thesis were population density, job density and number of extreme commuters. All factors utilized in this thesis, along with data collection procedures, are presented and explained in the next sections.

3.2.1 Population

Population as an influencing factor for UAM station allocation was a commonly used factor in the studies [7, 8, 18, 20, 22–24] summarized in Section 2.2. The studies generally proposed that placing UAM stations near larger quantities of population could amount to larger quantities of patrons. While UAM is not a mode of transportation that is publicly available and/or intrinsically like any existing, typical mode of transportation, there is at least one major similarity with public transportation: stations. For users to access UAM flights, they will first have to access a UAM station. As such, public transportation station accessibility guidelines can serve as a surrogate for UAM station accessibility. Such an assumption is consistent with Ploetner et al. [8], who argued that UAM is most comparable to public transportation as a mobility system. When considering access to public transportation stations, the guidelines developed by the Transit Cooperative Research Program (TCRP) [66] indicate a station's catchment area should provide access to population. While high amounts of population would not necessarily equate to high amounts of UAM users, it does serve as a major element for a potential market. Population was therefore used as a factor for this thesis.

Population data for the metropolitan region of Munich was provided by the Technical University of Munich's Modeling Spatial Mobility research group. Specifically, the data is part of a synthetic population for the Munich metropolitan area and was developed by Moreno and Moeckel [16]. The data was conveniently included in the study area's shapefile that was developed by Molloy and Moeckel [65]. In addition to population data, each of the study area's zones also included land-use data, such as mixed-use, industrial or housing quantities.

3.2.2 Employment

Like the population factor, employment was also a commonly used factor in the studies summarized [7, 8, 20, 22, 24] in Section 2.2. In particular, the studies gathered commute data and patterns which typically consist of trips between population and employment areas. Further, as the TCRP guidelines [66] indicated, in addition to population, a public transportation's catchment area should provide access to areas of employment. Again, like population, employment distribution data can serve as an important element for a potential market. Employment was therefore used as a factor for this thesis.

Like the population data, the employment data for the metropolitan region of Munich was also obtained from the same study area shapefile [65] populated with the synthetic population developed by Moreno and Moeckel [16]. Given both the population and employment data were obtained directly from the study area's shapefile, no further manipulation or aggregation of the data were required.

3.2.3 Points of Interest

Points of interest refers to touristic attractions. As shown in Table 4, points of interest as a factor was among the highest rated factors found to influence station placement in Fadhil's [7] study. Ploetner et al. [8] indicated the region of Munich is an area of high touristic activity and further explored the use of UAM as a service to touristic areas. The TCRP guidelines [66] indicate that in addition to employment and population, a public transportation station's catchment area should provide access to major attractors. Points of interest as a factor was therefore used as in this thesis.

The points of interest data was provided by Bauhaus Luftfahrt who obtained it from TripAdvisor [67]. Specifically, the points of interest correspond to the top attractions for the Upper Bavaria region of Germany. In total there were 45 identified points of interest distributed across the study area. The popularity of an attraction on TripAdvisor is based on quality, recency and quantity [68]. Quality refers to a location's ratings given by TripAdvisor users/visitors. Recency relates to when reviews were made with older reviews counting less towards the site's overall score. Finally, quantity refers to the number of reviews.

A list of all points of interest used for this factor is provided in Appendix A.

3.2.4 Transportation Nodes

In this thesis, transportation nodes encompassed public transportation stations of systems related to longer distance travel. Transportation nodes were the highest scoring factor in Fadhil's [7] study, as shown in Table 4. While some studies [18, 22] analyzed UAM as a competing system to public transportation, most studies [3, 7, 8, 20] incorporated it as a complementary service. Finally, the TCRP accessibility guidelines [66] indicate stations should be multi-modal and should provide seamless and fast transfers between said modes. Transportation nodes as a factor was therefore used in this thesis.

The transportation nodes data was obtained from OpenStreetMap [69]. The gathered spatial data (in shapefile format) was for the entire state of Bavaria, Germany, so filtering was required to obtain data relevant for this thesis' study area. The OpenStreetMap transportation data included nodes and links, such as roads, railways and stations. Of interest for this factor were the station nodes. In particular, commuter rail, intercity rail and bus stations as such nodes represent locations related to longer distance travel. More conventional public transportation stations, such as for subway, bus or tram, were omitted due to most of them being situated within city cores. Thus, by only taking stations associated with longer distance travel, a higher spatial distribution was expected, which the author hypothesized could lead to more regional station allocation.

3.2.5 Company Headquarters

In this thesis, company headquarters encompassed employment centers and/or firms with large amounts of employees. In Antcliff, Moore and Goodrich's study [17], the authors proposed the integration of UAM to the private sector. Specifically, given the study was based in the Northern California Silicon Valley, the study suggested tech companies could be early adopters of UAM. The study investigated placing UAM stations within a tech company campus block. Said block consisted of multiple company offices which would presumably amount to a significant number of employees. The Munich region is home to several large companies including BMW, Siemens, Allianz and Audi. Like tech companies in the Silicon Valley, such companies could potentially benefit from the implementation of UAM given their workforce size. Therefore, company headquarters as a factor was used in this thesis.

The company headquarters data was provided by Bauhaus Luftfahrt who obtained it from the Bavarian Chambers of Industry and Commerce [70]. The data was queried to include companies with number of employees ranging from 200 to more than 10,000. There were just under 2,100 companies collected including headquarters, operating sites, institutions and branch offices. The raw data was presented in table format and included addresses for each of the listed companies. The addresses were geocoded using the MMQGIS [71] plug-in to QGIS [72]. After geocoding, the company locations were filtered to only include sites within this thesis' study area of which the total were about 350 company sites.

3.2.6 Travel Demand

In this thesis, travel demand encompassed total origin and destination trips per zone. Such travel demand can provide insight into travel patterns. Rath and Chow's study [21], for example, used an origin-destination demand matrix to determine number of trips per zone destined for the airports in New York City. Lim and Hwang's study [20] also used origin-destination demand data, however, instead of focusing on trips destined for airports, they explored commute trips.

Other studies [3, 22, 24] also employed similar approaches. By utilizing origin-destination data, the studies were able to determine the top demand zones and/or specific regions that would likely be suitable for UAM. Travel demand data was therefore used as a factor for this thesis.

Like the population and employment data, the travel demand data was obtained from the synthetic population developed by Moreno and Moeckel [16]. Unlike the population and employment data, the travel demand data was not included in the study area's shapefile [65]. Rather, it was provided in a separate trips file that corresponded to the number of trips occurring in the metropolitan area of Munich. Each of the entries corresponded to an agent's (or person's) trip and included information such as departure time, total travel time, trip type, origin and destination. The origin and destination information corresponded to what zone the trip originated at and was destined for. The zone IDs correspond to the zones in the study area's shapefile developed by Molloy and Moeckel [65]. In the Uber Elevate white-paper, Holden and Goel [3] indicate UAM will be most appealing to long-distance commuters. They expect long-distance commuters will benefit the most in terms of travel time and money savings. Therefore, for each zone, the collected trip data was filtered to include trips with distances of at least 32 kilometers (or 20 miles), which was a distance consistent with 2 previous UAM station allocation studies [3, 24].

3.2.7 Accessibility

Within the transportation/urban planning field, accessibility is defined several ways, though it is generally used to describe the ease with which activities can be reached. Geurs and van Wee [73] define it by taking into account the interaction between land-use and transportation and how the combination of the 2 gives people the opportunity to travel to destinations and/or engage in activities. The authors identify several different existing accessibility measures, each based on different elements such as infrastructure, location, persons and utilities. Location-based measures can further be subdivided into accessibilities that are measured by distance, contour and potential. Among the more widely used accessibility measures in urban and geographic studies is accessibility that measures potential. Hansen's [74] measure of accessibility is a well-known and established measure that considers potential. In his study, Hansen described accessibility as the “potential of opportunities for interaction” and distinguishes his measure from those that describe the ease of travel and activity interaction. Hansen explained that the accessibility at zone i to an activity located at zone j can be measured by considering the size of the activity and the travel distance, or cost, between zones i and j. In this context, such an accessibility measure is also known as a gravity-based measurement. The accessibility measurement described by Hansen is as follows, as taken from Hansen [74]:

$$A_{ij} = \frac{S_j}{T_{ij}^{x}}$$

3-1 Hansen Accessibility

Where A_{ij} is the accessibility at zone i to an activity at zone j, S_j the size of an activity at zone j, T_{ij} the travel distance or cost between zones i and j, and x is a factor describing the effect of travel time, or cost, between zones i and j. Potential accessibility can also account for more than one activity at zone j and/or more than one zones with the formula taking the following form, as taken from Geurs and van Wee [73]:

$$A_i = \sum_{j=1}^{n} D_j \mathrm{e}^{-\beta Cij}$$

3-2 Potential Accessibility with Negative Exponential Cost Function

Where A_i is the accessibility measurement for zone i to all opportunities D at zone j, c_{ij} is the travel cost between zones i and j, and β a cost sensitivity parameter. Potential accessibility measures are also known as gravity-based measures and this specific formula utilizes a negative exponential cost function. Lower values of β result in larger accessibility scores as was shown in [75]. A value of 0.2 was used for the cost sensitivity parameter β, which was consistent with several studies [76–78] that iteratively calculated the value.

According to the TCRP public transportation station accessibility guidelines [66], station access should be multi-modal. This was in accordance to Ploetner et al.’s [8] study, where the authors indicated that UAM should serve as a complementary service to public transportation. Further, the TCRP guidelines [66] recommend stations should serve both existing and potential markets by placing stations in such a way that their catchment areas serve and provide access to high densities of both population and employment. According to a TCRP station access model, the main factors found to influence station access were employment, density and parking availability. Accessibility via public transportation and car were therefore used as factors in this thesis. Specifically, there was a total of 4 accessibility factors utilized in this thesis: accessibility to employment via car, accessibility to population via car, accessibility to employment via public transportation and accessibility to employment via public transportation.

Population and employment data for each zone in the study area was obtained from the synthetic population developed by Moreno and Moeckel [16]. The car and public transportation interzonal travel time data were provided by the Technical University of Munich's Modeling Spatial Mobility research group. The raw interzonal travel time data were presented in 4953x4953 matrices with 4953 corresponding to the number of zones in the Munich metropolitan area shapefile [65]. There were multiple matrices corresponding to different travel times based on different modes, such as car, train, metro and bus, and different trip segments, such as access, egress and in-vehicle time. Given the multiple number of matrices for public transportation, merging of matrices was required. Further, for each public transportation interzonal trip, the minimum travel time across different public transportation modes (train, metro, bus) was taken. This was done because interzonal trips where public transportation as a mode was not viable were assigned with very large travel time values.

Given the large number of interzonal trips (about 25 million) for the study area, all accessibility scores were calculated using a custom R [79] script that applied Equation 3-2. For every zone, the R script calculated the sum-product of the quantity of activity (employment or population) and travel distance (via car and public transportation) to every other zone (including itself) in the study area. Hence, every zone's accessibility score consisted of 4953 products.

3.3 Aggregation

Once all the factor data were collected and mapped onto the study area, they were all aggregated at the zonal centroid level. The resulting structure was a collection of attributes indicating the total number of factor data per each of the study area's zones. At this stage, the data showed the raw factor score for each of the zones. While some of the factor data did have exact coordinates, such as travel demand, points of interest, transportation nodes or company headquarters, other factors did not, such as employment, population, and all the accessibility factors. In order to have all the factors represented in the same spatial format, all factor data was aggregated to each of the zones' centroids consequently losing spatial exactness for some factors.

Heatmaps showing the distribution of each of the factors were created and provided in Appendix B. A visualization of the study area's zone centroids is shown below in Figure 6.

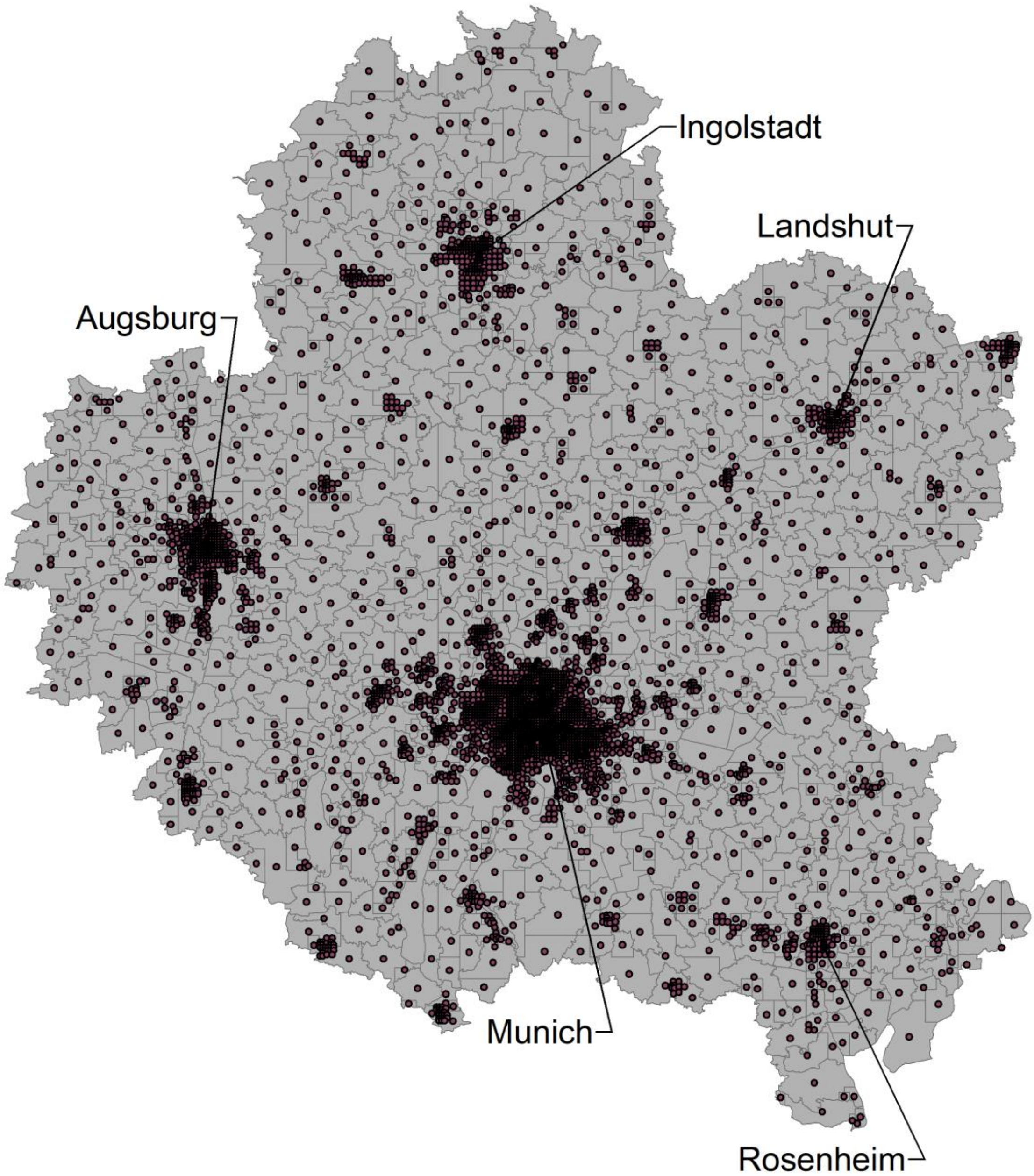

Figure 6 Study Area Zone Centroids

4 METHODOLOGY

As described in Section 2.3.3.1, MCDA can be subdivided into two general types of analysis: multi-objective and multi-attribute. Fadhil's [7] work, for example, was primarily a multi-attribute approach with elements including AHP-type criterion weighting, weighted linear combination and suitability analysis. While this thesis utilized multi-objective decision analysis (MODA) to ultimately identify station locations, it did so by first applying multi-attribute decision analysis (MADA). While MCDA was the core of this thesis, it also included other procedures. The work in this thesis began with a data collection and preparation process (Chapter 3) which consisted of gathering data related to the study area and factors. It also included a surface modeling process that transformed localized data points to a more spread-out, continuous surface. Finally, the MCDA results were evaluated (Chapter 5) using a mode choice model and travel time comparisons for car, public transport and UAM. A graphical representation of this thesis's methodology is shown below in Figure 7.

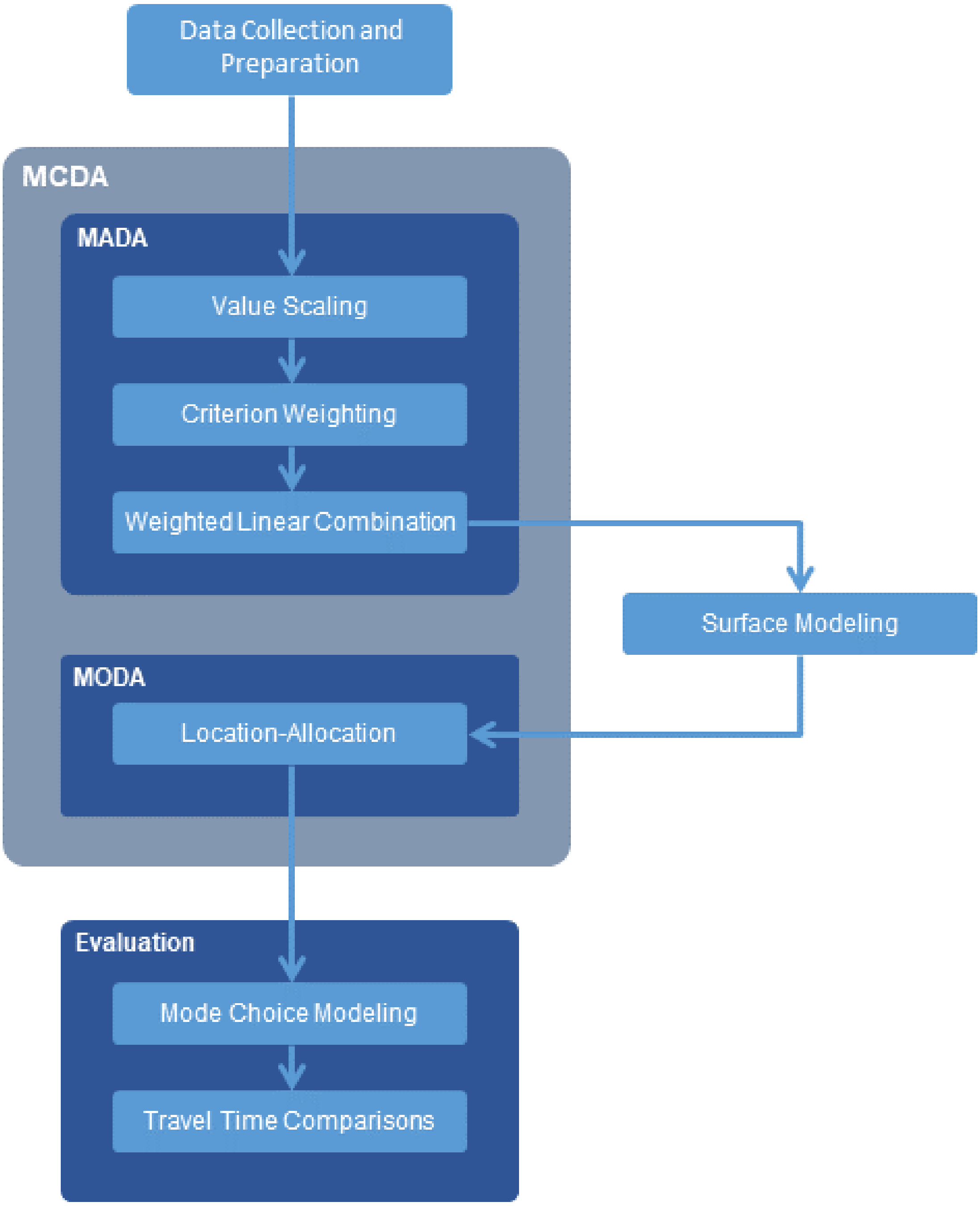

Figure 7 Methodology Flowchart

4.1 Value Scaling

The collected factors' raw scores for each zone resulted in varying ranges of values. For example, the maximum number of points of interest at a single zone was 3 while the maximum calculated car accessibility to population was well over 300,000. On the opposite spectrum, several factors had minimum values of 0 while a few had theirs in the hundreds. In order to fairly compare the factor scores, their values were converted using value scaling (also known as standardization).

Standardization is a common practice when conducting MCDA [19, 27]. As described in Section 2.3.1, the standardization method known as linear scaling is appropriate when pairwise comparison is used for factor prioritization (i.e. weight determination) [28]. In addition to complementing pairwise comparisons, the linear scaling method is considered one of the simplest to use and was therefore utilized for this thesis.

A custom R script used Equation 2-1 to convert every raw score (for each factor at each zone) to a scale ranging between 0 and 1.

4.2 Criterion Weighting

When conducting MCDA, an important element in the decision-making process is the prioritization of the attributes [19], a process Kao [29] explains to be one of the most challenging components. As was explained in Section 2.3.2, typical methods of attribute weight determination can be done through literature review, expert opinion or analytical studies on the data [30]. While some of the factors utilized in this thesis coincided with those of Fadhil's [7] study, not all of them were accounted for. Therefore, given the limited amount of studies related to UAM station allocation utilizing MCDA, a review of literature was not a suitable method for weight determination. For this thesis, expert opinion was sought for the determination of weights. Specifically, the AHP method was employed due to its ability to handle both qualitative and quantitative attributes [33], its simple, straightforward structure, moderate chance of bias [80] and well-established usage for MCDA problems utilizing GIS [19].

4.2.1 Analytic Hierarchy Process

For this thesis, an AHP process was carried out to determine the weights of all 10 factors. Often, spatial decision making processes including MCDA are done with the input of multiple decision makers, rather than just an individual [19]. The procedure was therefore carried out as a group decision making process and involved a total of 5 decision makers of varying backgrounds. According to Robbins [81], group sizes should typically range between 5 and 50 decision makers. The author took advantage of access to decision makers that had extensive knowledge or were, at the time, involved in research related to UAM. Given the decision makers' different backgrounds and fields, the author was interested in each decision maker maintaining their personal judgement without the influence of any other decision maker in the group. The AIP method (as described in Section 2.3.2.2), with an arithmetic mean, was therefore chosen for group aggregation.

Once the 5 decision makers were identified, they were each provided an AHP questionnaire that was created on Microsoft Excel using steps consistent with and developed by Saaty [37, 38]. Each decision maker completed the questionnaire individually without interacting with any other decision maker. The Excel AHP questionnaire consisted of 4 sheets:

1. The first sheet was the only sheet decision makers could edit. It was in this sheet where the pairwise comparisons of factors were performed. Given there were 10 factors, there were a total of 45 pairwise comparisons (per Equation 2-2) every decision maker had to go through. For each pairwise comparison, the decision makers were asked to choose what factor they considered to be more important (indicated by a checkbox). Afterwards, they were asked by how much the chosen factor was more important than the other factor (via a score). It was also possible to consider both factors to be of equal importance. The scoring system used was Saaty's [37] intensity of importance scale (refer to Table 1).
2. The second sheet included the comparison matrix where all pairwise comparison scores were shown in matrix format. Given there were 10 factors, the comparison matrix's size was 10x10 and additionally included a summation row at the bottom. The summation row showed the summation of each column (column sum) where each column corresponded to each of the 10 factors. As described in Saaty's [37] scoring system, if, for example, factor A is considered to be more important than factor B (when comparing A with B), then the score of factor B (when comparing B with A) receives the reciprocal value of the score (i.e. 1 over value of score). On the comparison matrix, such scores would be shown on opposite diagonal halves of the matrix (i.e. the transpose position).
3. The third sheet included the normalized relative weight matrix, which was utilized to calculate the eigenvector (or priority vector). The normalized relative weight matrix again was a 10x10 matrix with an additional column on the right showing the priority vector. The position for each cell in the

normalized relative weight matrix was consistent with the cell locations in the comparison matrix. The cells in the normalized relative weight matrix corresponded to the division of their respective comparison matrix cell by their column sum value. Once every cell in the normalized relative weight matrix was populated, the priority vector was calculated by taking the arithmetic average of every row.

4. The fourth and final sheet determined consistency. The sheet displayed the priority vector (from step 3) and the column sum (from step 2). The sum-product of these two values produces what is known as the maximum eigenvalue. The eigenvalue was in turn used in Equation 2-4 to determine the consistency index. Finally, after the consistency index was determined, it was used in Equation 2-3 to determine the consistency ratio. According to Saaty [38], a suitable consistency ratio should be less than 10%.

A copy of the AHP questionnaire, with all sheets, is provided in Appendix C.

4.2.2 Results

4.2.2.1 Consistency

The consistency ratios for the decision makers resulted in values between 10 and 22% meaning consistency was not suitable per Saaty's [38] recommendations. As Miller [82] stated in his widely cited paper, "the span of absolute judgment and the span of immediate memory impose severe limitations on the amount of information that we are able to receive, process, and remember." Miller proposed the amount of simultaneous information found to be manageable for humans is in the order of 7±2. Increasing the amount of information often leads uncertainty and/or a break in consistency. Saaty and Ozdemir [83] agreed with Miller's claim and found that when conducting AHP, inconsistencies often arose when decision makers were presented with more than 7 criteria for pairwise comparison. Nevertheless, there are times when the number of criteria goes past 7 and Saaty's 10% rule of thumb can be expanded. In his study, Wedley [84] presents acceptable and tolerable cut-off values for consistency depending on the number of criteria, which were based on Saaty's [38, 85] work. For 10 criteria, a tolerable value was found to be 20%. Per the resulting AHP questionnaires in this thesis, all but 1 (with a value of 22%) resulted in meeting the 20% tolerable cut-off value.

When dealing with inconsistent results, a possible mitigation involves asking the decision maker to reconsider their answers [83] in hopes of improving or reaching a level of acceptable consistency. Per Fadhil's study [7], having decision makers reevaluate their judgements, through several rounds, proved to be unsuccessful in reaching a target consistency. For this thesis, the author ultimately decided against such a process and accepted the decision maker's initial judgement of the factors.

4.2.2.2 Final Factor Weights

Once all the decision makers filled out their AHP questionnaires, their judgements were aggregated. In this thesis, the group decision making process was assumed to be an aggregation of individual priorities (or AIP). Under AIP, the final priority vector (i.e. factor weights) is determined by taking the arithmetic mean of every decision maker's priority vector [39, 40]. The final factor weights are shown below in Table 5.

Factors	**DM 1**	**DM 2**	**DM 3**	**DM 4**	**DM 5**	**Average Weight**
Population	2.8%	9.6%	2.3%	9.9%	17.8%	8.5%
Employment	2.8%	9.6%	4.4%	2.7%	13.2%	6.5%
Points of Interest	21.1%	17.4%	29.6%	26.7%	13.4%	21.6%
Transportation Nodes	37.7%	2.7%	6.2%	19.3%	3.5%	13.9%
Company Headquarters	15.5%	35.4%	7.4%	1.3%	8.5%	13.6%
Travel Demand	7.0%	2.3%	3.0%	16.8%	28.8%	11.6%
Accessibility to Employment via Car	3.6%	6.2%	12.8%	4.1%	3.5%	6.1%
Accessibility to Population via Car	2.2%	4.2%	7.5%	6.5%	3.8%	4.8%

Factors	DM 1	DM 2	DM 3	DM 4	DM 5	Average Weight
Accessibility to Employment via Public Transportation	4.5%	7.4%	17.6%	4.5%	3.8%	7.6%
Accessibility to Population via Public Transportation	2.9%	5.2%	9.1%	8.3%	3.8%	5.8%

DM = Decision Maker

Table 5 Final Factor Weights

As shown, the top 3 factors were found to be points of interest, transportation nodes and company headquarters. The resulting average factor weights were consistent with Fadhil's [7] results (shown in Table 4) in that points of interest and transportation nodes were considered to be important influential factors for UAM station placement.

4.3 Weighted Linear Combination

The weighted linear combination (WLC) method is among the most used combination procedures in MCDA involving GIS. It is also commonly used in combination with factors that have been weighted through a pairwise comparison process (such as AHP) [19, 35]. The WLC method consists of two main elements: criterion weights (or factor weights) and value functions (or factor scores). The value functions are typically standardized before being utilized in the WLC procedure (as was done in Section 3.2). The WLC method, known to be a straightforward combination procedure, can be calculated using the following formula, as taken from Malczewski and Rinner [19]:

$$V(A_i) = \sum_{k=1}^{n} w_k v(a_{ik})$$

4-1 Weighted Linear Combination

Where w_k is the weight for factor k, $v(a_{ik})$ is the factor score for alternative a located at i and $V(A_i)$ is the summation of all weighted factor scores at location i. The WLC method is a linear method meaning increasing the quantity of a factor score will linearly increase the overall score for alternative A_i.

The WLC for every zone was determined by using Equation 3-3 in a custom R script that calculated the sum-product of the standardized (values between 0 and 1) factor scores and the factor weights developed using AHP. Every zone's WLC score therefore consisted of a summation of 10 elements corresponding to the number of factors.

4.4 Surface Modeling

The spatial data utilized for this thesis was gathered and initially aggregated at a zonal-centroid level based on a structure developed by Molloy and Moeckel [65]. The structure they developed divided the greater Munich metropolitan area to just under 5,000 zones. In order to convert the spatial data from a centroidal (point) format to a spread-out, continuous surface, surface modeling was utilized. Two surface modeling techniques were considered for this thesis: spatial interpolation and density estimation.

All surface modeling was conducted using ESRI's ArcMap 10.7.1 [86] software. Specifically, the software's Spatial Analyst suite [56] was used given it conveniently included both inverse distance weighting and kernel density estimator tools.

4.4.1 Kernel Density Estimation

Calculating density required setting parameters and inputting data to ESRI's KDE [61] tool. The only data required for running IDW was a point shapefile with points corresponding to measurement values (or control points). The Munich metropolitan region zone shapefile [65] was used for this input given each zone had a corresponding centroid and hence, could be represented as a point shapefile. The first parameter setting required selecting the input shapefile's attribute data that would serve as the control points. The zone shapefile had at this point been modified to include all data related to factors, standardized scores, and weighted factor scores. Therefore, the weighted factor scores (calculated in Section 3.4) were used as the control points. The next parameter required setting an output raster cell size, which relates to how coarse the output raster will be generated. An output raster cell size of 1,250 meters was used. This setting proved to be important for the procedures explained in Section 3.6. The final parameter setting was the search radius, or bandwidth. As described in Section 2.5.2.1, the bandwidth determines how far to search for neighboring control points. If many control points, or kernels, fall within a single control points' search radius, the accumulation of values yields a higher density estimation. Too small a bandwidth value will result in overfitted results while too large a value will result in an oversmoothed surface [62]. The default bandwidth value (based on Equation 2-9) was used with a weighted standard distance. Here, the weights corresponded to each zone centroid weighted factor scores. The default bandwidth value (per Equation 2-8) was estimated to be about 4.3 km.

The KDE results for the Munich metropolitan region are shown below in Figure 8.

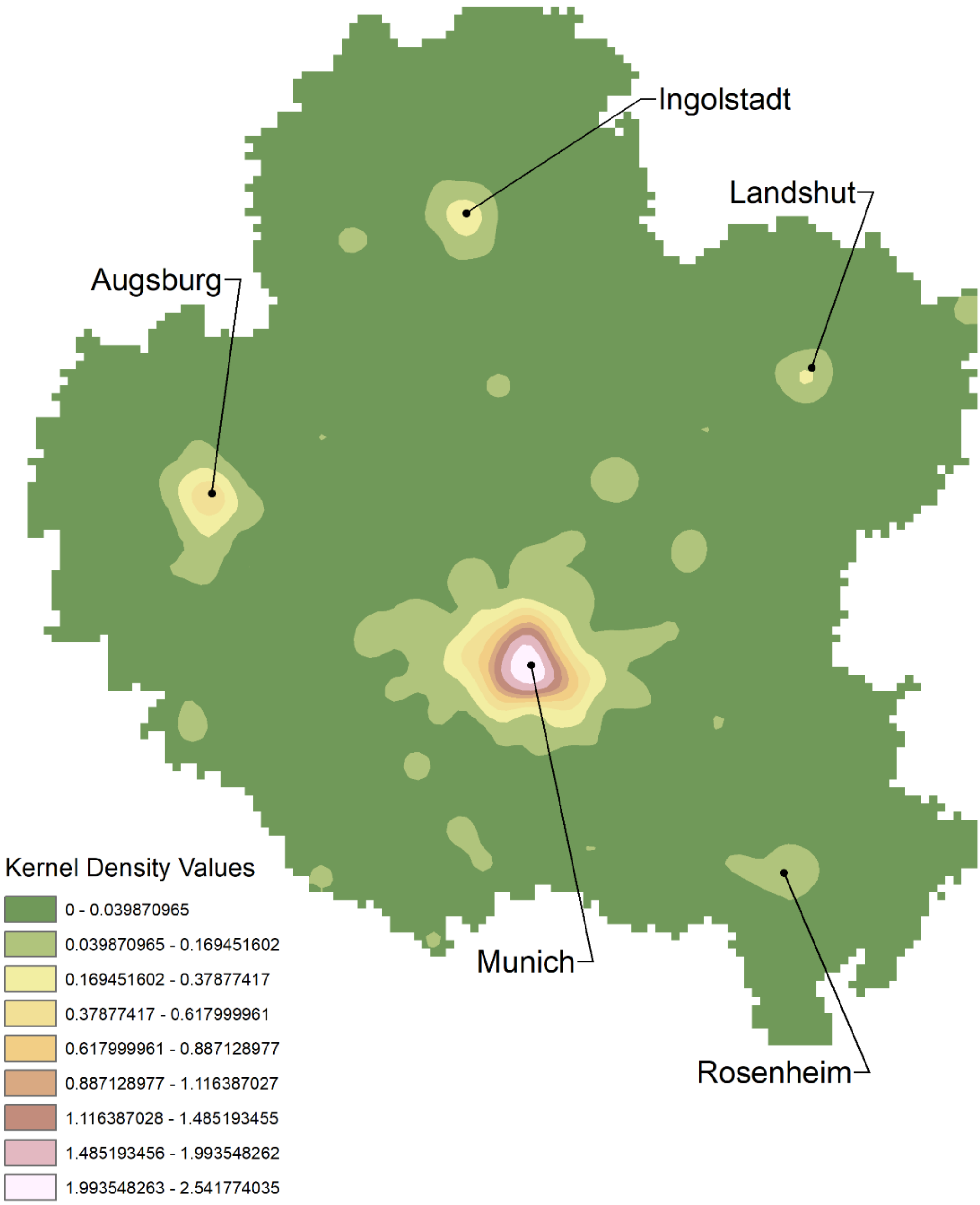

Figure 8 Kernel Density Estimation Results

The highest intensity estimates were unsurprisingly located at the city core of Munich and medium intensity estimates at the city cores of Augsburg, Ingolstadt and Landshut.

4.4.2 Inverse Distance Weighting

Interpolating for unknown values required setting parameters and inputting data to ESRI's IDW [59] tool, which were very similar to those input to the KDE tool. The only data required for running IDW was a point shapefile with points corresponding to measurement values (or control points). The Munich metropolitan region zone shapefile [65] was again used for this input given each zone had a corresponding centroid and hence, could be represented as a point shapefile.

The first parameter setting involved selecting the input shapefile's attribute data that would serve as the control points. Unlike KDE, IDW does not consider the density of control points. Unknown values are estimated based on the values of the nearest control points and cannot exceed the value of said points. This would result in areas with smaller zones (e.g. city centers), which had higher densities of scores but smaller absolute score values, to have lower interpolated values than areas with larger zones, which had lower densities of scores but larger absolute score values. The weighted factor scores (calculated in Section 3.4) for each zone were therefore transformed to density values and used as the control points. Density values were calculated by dividing the weighted factor scores by their respective zone's area.

The next parameter involved setting an output raster cell size, which relates to how coarse the output raster will be generated. The output raster cell size was set to the same value used under KDE: 1,250 meters. This setting proved to be important for the procedures explained in Section 3.6. The next parameter involved setting the power parameter, which determines how influential control points are depending on their distance from the unknown value. Higher power values diminish the influence of distant control points. A power value must be greater than 0 and ESRI recommends setting a value between 0.5 and 3. The default value of 2 was used for this setting. The final parameter setting consisted of choosing between a fixed search radius and variable search radius interpolation method (as explained in Section 2.5.1.1). Each method has two sub parameter settings [87].

Under the fixed search radius method, the first setting is the search radius distance, which corresponds to how far from the unknown point to search for neighboring control points. If no search radius is set, the IDW tool will use a search radius value that is 5 times that of the output raster cell size value [87]. The second parameter is related to setting the minimum number of points, which corresponds to the number of control points to search for and use for the interpolation estimation. The default value is 0, but if set, the search radius' size can increase until the specified number of points are satisfied.

Under the variable search radius method, the first setting is number of points, which corresponds to the number of control points to search for and use for the interpolation estimation. It searches for the nearest neighboring control points and the default value is 12. The second parameter setting is maximum distance, which is essentially a search radius and limits the distance by which to search for neighboring control points. This is an optional setting with a default value equal to the diagonal distance of the study area.

Both methods were tested, and results were noticeably different. Under the fixed search radius method, the default value for both search radius distance and minimum number of control points were used. As shown below in Figure 9, the resulting raster had missing values (indicate by white raster cells), which correspond to points that found no neighboring control points inside their search radius.

When running the variable search radius, rather than take the default value for number of points (12), a value of 7 was input. The value seemed suitable given it corresponded to the average number of neighboring zone polygons for the study area’s shapefile. The default value for maximum distance was taken. Unlike the fixed search radius method, the variable search radius had no missing values. Further, as shown in Figure 10, the resulting surface was more spread out than the one created using the fixed search radius method.

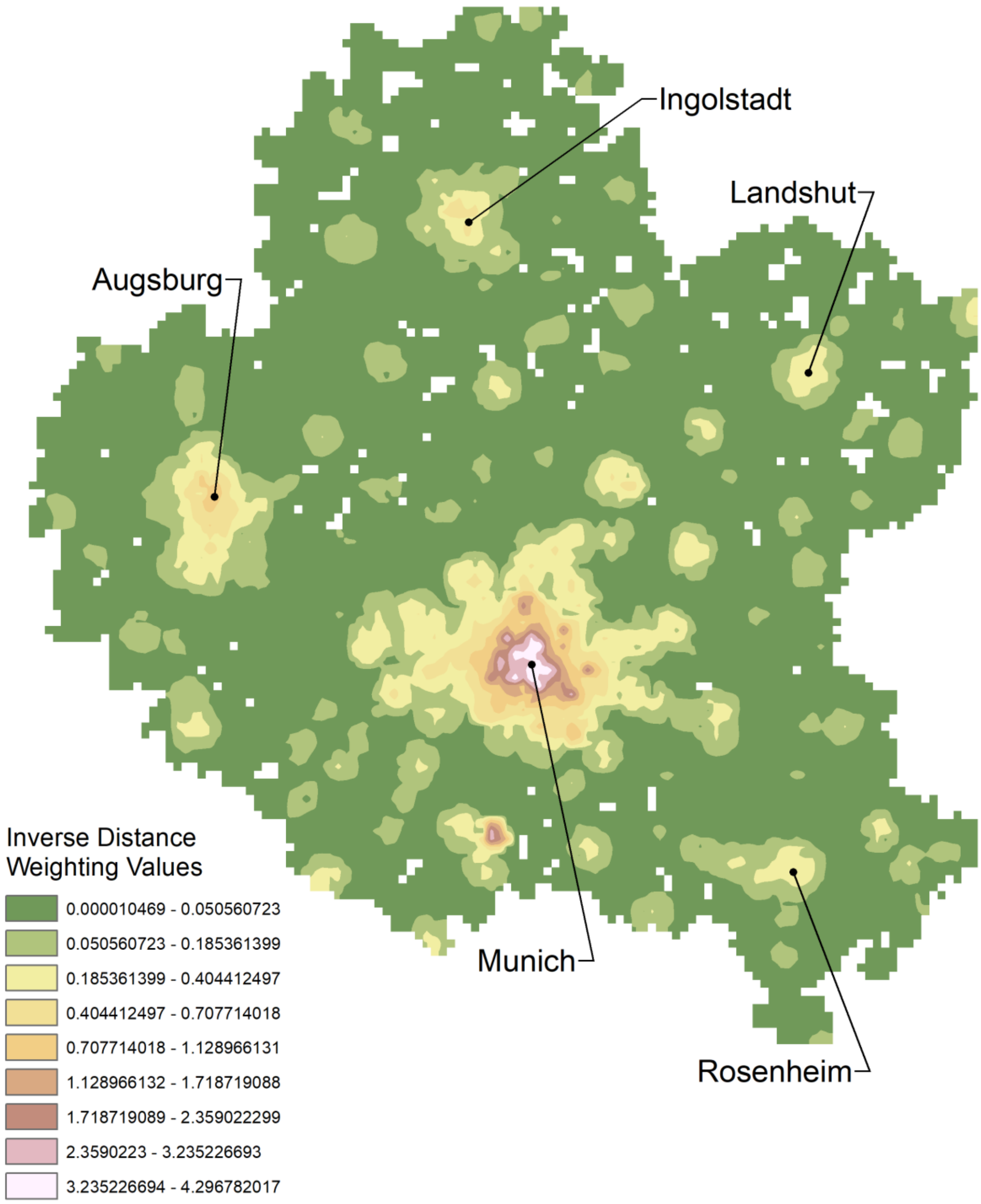

Figure 9 Inverse Distance Weighting Results using Fixed Search Radius

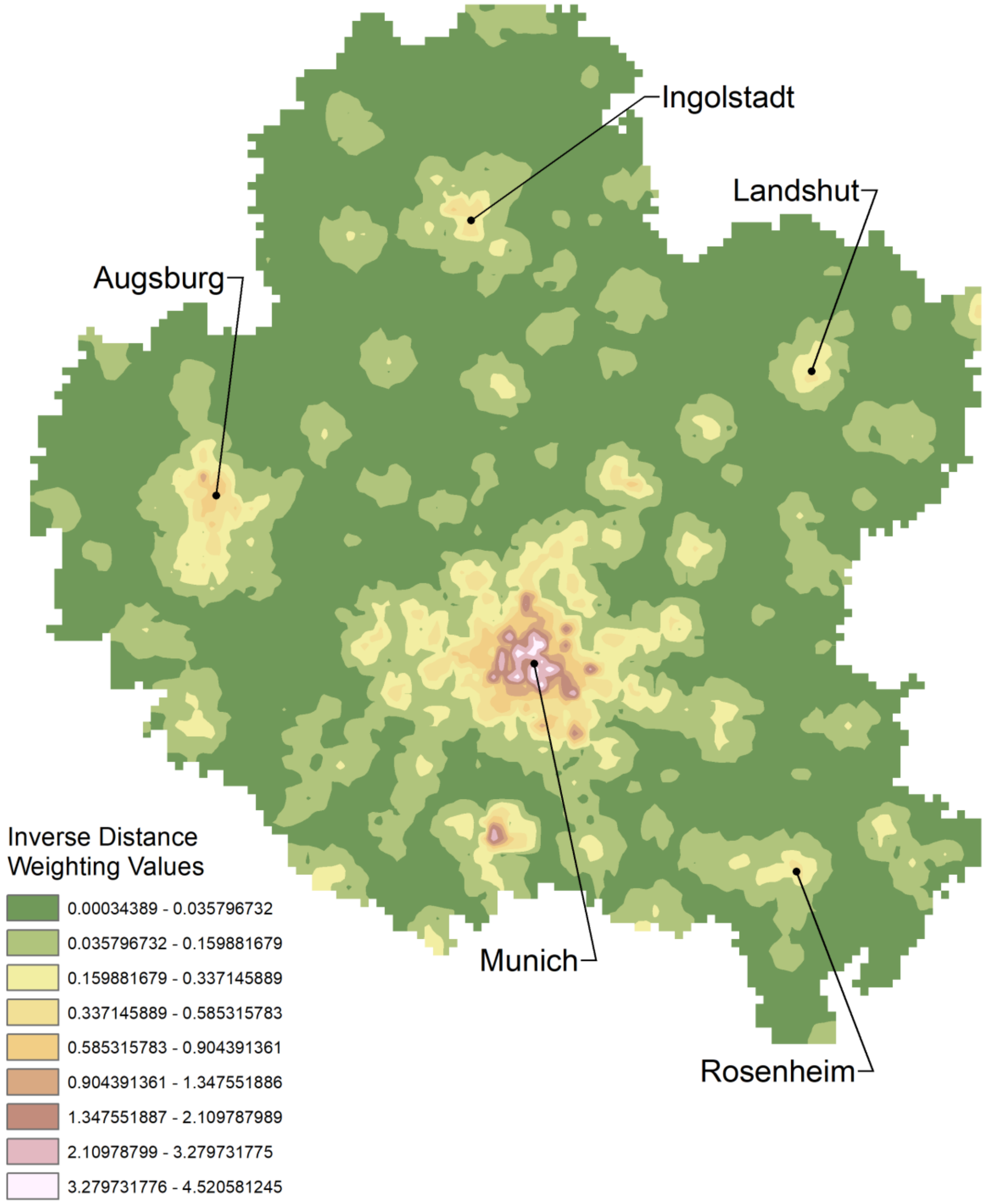

Figure 10 Inverse Distance Weighting Results using Variable Search Radius

4.4.3 Results

When comparing the KDE and 2 IDW surfaces, results were similar in showing higher intensity values at the cores of the region's larger cities. However, the KDE results were found to be overly smoothed and showing almost no variation in scores outside the city cores. The resulting surface calculated using inverse distance weighting with a variable search radius was the preferred method between both IDW approaches given it had no missing values and intensity values were more spread out throughout the region.

The IDW results indicated the highest intensity of scores were located at the city centers of the study area's largest cities. Additionally, there was a small area to the south of Munich that also had a high intensity score, as shown in Figures 9 and 10. When reviewing the individual factor heatmaps (provided in Appendix B), the area in question had relatively high activity for the travel demand, company headquarters, employment, population and transport nodes factors. The accumulation of all these factors was initially expected to be the reason for the high intensity score. However, a closer examination revealed the high score was due to a zone structure error. As shown in Figure 11, an unintended zone was drawn as a result of crooked boundaries from neighboring zones.

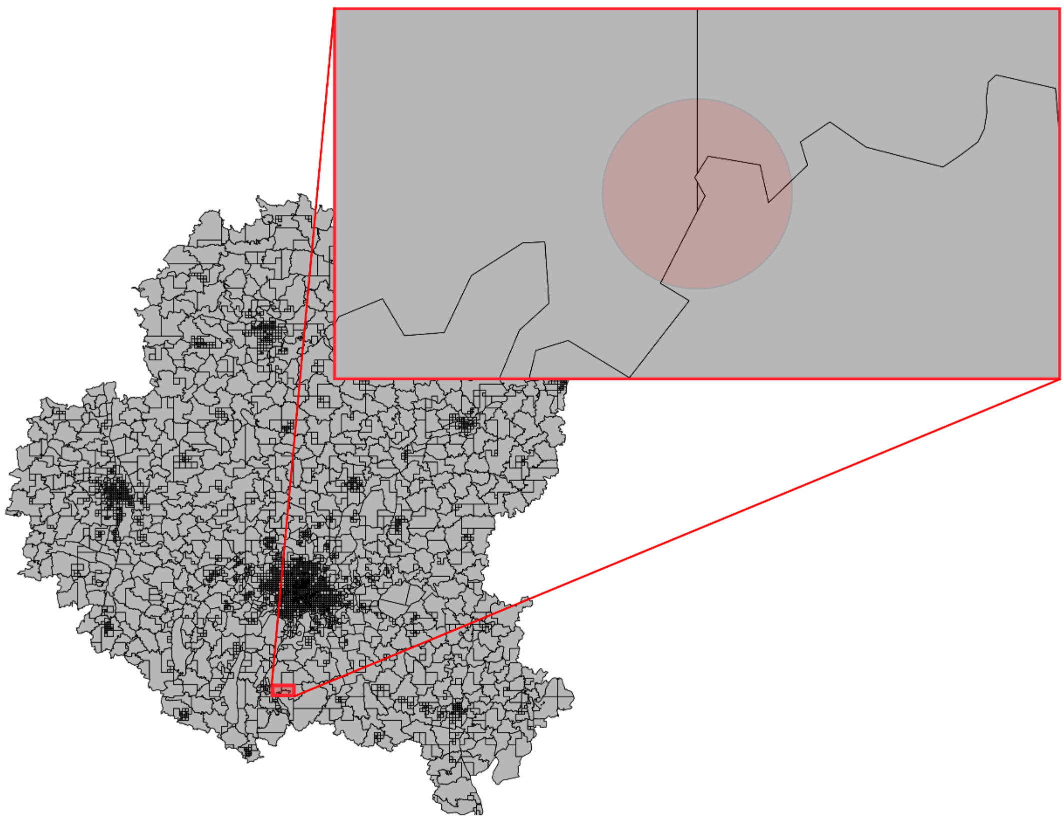

Figure 11 Zone Structure Error

The resulting zone was very small and essentially empty; it contained no land-use or socioeconomic data. When calculating accessibility scores, the obtained travel time zone matrices did have associated travel time data for the specific zone. Therefore, accessibility scores were generated for the zone. As mentioned in Section 4.4.2, the weighted zone scores for IDW were input as density scores. Although accessibility scores were relatively low for the zone, the resulting accessibility scores, in density format, were particularly high due to the zone's small area. Under location-allocation, the zone's, and consequently the area's, highly weighted demand points resulted in it being an attractive site for UAM station placement. Though location-allocation was not solved with the correction of this error, it was expected the area's high score had a considerable influence on the resulting UAM networks. A simple fix would have consisted of removing such empty zones from the original study area shapefile. This error was unfortunately identified towards the end of the thesis after all subsequent analysis and steps had been conducted.

4.5 Location-Allocation

This thesis conducted all location-allocation analysis using the GIS environment ArcMap 10.7.1 from ESRI given it provides a medium by which all relevant data can be collected, analyzed and visualized. Further, ESRI's location-allocation tool solves location problems using heuristics, which was of interest to the author given its well-established processing speed, efficiency and close to optimal solutions. ESRI's location-allocation solver is housed in the software's Network Analyst suite [88], which is able to solve multiple types of location-allocation problems. As described in Section 2.4.1, both the minimize impedance and maximize coverage problem types were considered suitable for this thesis. Under minimize impedance, locations are found in such a way that all demand points' average travel costs (e.g. time or distance) are minimized. Under maximize coverage, locations are found in such a way that the maximum amount of demand points, within an impedance cutoff value (i.e. search radius), are served. Demand points located outside the specified search radius are not assigned to any allocated facility and are considered unserved [88].

4.5.1 Data Inputs

The location-allocation solver required input data and parameter settings to be able to run. The 3 required data inputs are as follow:

- **Network Dataset**: the network dataset is essentially the infrastructure network by which demand is connected to facilities. All analysis conducted using ESRI's Network Analyst suite is done on a network dataset. Such a dataset includes information and features such as links, nodes, capacity, speed, junctions and direction of travel (i.e. one-way or two-way roads) [89]. The network dataset was created in ArcMap 10.7.1 using a road shapefile of the study area that was obtained from OpenStreetMap [69].

- **Demand Points**: demand points typically correspond to the locations that house users that will be served by the facilities [88]. ESRI's location-allocation solver can handle a maximum of 10,000 demand points [90] and must be input as a point shapefile. Demand points can contain weights, which represent a level of demand. The interpolated values calculated in Section 3.5.2 were used for this input, however, because they were produced as a raster image, a conversion of format was required. As described in Section 3.5.2, when creating the interpolated raster image, a raster output cell size of 1,250 meters was used. This value, identified through trial-and-error, determines the number of raster cells the interpolated raster surface image will contain. At an output cell size of 1,250 meters, the raster image was made up of about 9,300 raster cells. Each raster cell had an associated interpolated value estimated using the weighted factor scores. Using a built-in raster-to-shapefile tool in ArcMap, the IDW raster image was converted to a point shapefile containing about 9,300 points (evenly spaced at 1,250 meters) with their respective weights. The resulting shapefile was used as the demand points input.
- **Facilities**: facilities correspond to the sites that will be chosen by the location-allocation solver and to which the demand points are assigned. When inputting facilities, they can be classified as candidates, required or competing sites. Candidate sites make up the facilities that could be chosen by the solver, required sites are facilities that are always chosen and competing sites are facilities that will compete with other sites for market share and demand points [88]. All facilities used in this thesis were classified as candidate sites. Like demand points, facilities can also have weights assigned to them, however for this thesis, the weights were assigned to the demand points. ESRI's location-allocation solver can handle a maximum of 1,000 demand points [90] and must be input as a point shapefile. The facilities point shapefile was created using a built-in

tool in ArcMap that creates points spaced according to an input distance value. The value, identified through trial-and-error, was set to 4,000 meters (4 km) and a total of about 930 evenly spaced points were created. The resulting shapefile was used as the facilities input.

Visualizations of the study area with demand points and facilities are provided in Appendix D.

4.5.2 Parameter Settings

In addition to the aforementioned input data, ESRI's location-allocation solver has several parameters that should be set prior to running [88, 90]. The first parameter involved setting how impedance (or travel cost) between demand points and facilities would be calculated. An impedance of travel distance (in kilometers) was chosen for this parameter. Each link (or road) in the network dataset has an associated length attribute which is utilized for determining the shortest path between demand points and facilities. The next parameter involved choosing what problem type should be solved. ESRI's location-allocation solver has a total of 7 problem types to choose from: minimize impedance, maximize coverage, maximize capacitated coverage, minimize facilities, maximize attendance, maximize market share and target market share. As described previously, both the maximize coverage and the minimize impedance problem types were tested for this thesis. The next parameter involved choosing the number of facilities (i.e. UAM stations) to find. If, for example, 10 facilities were chosen, the solver would find the top 10 facilities from the approximately 930 previously input facilities. Varying number of facilities were used for this thesis. The next parameter involved setting an impedance cutoff value. This value corresponds to a search radius from each potential facility. Any demand point that fell outside this search radius was not served by the facility. Varying impedance cutoff values were used in this thesis and were dependent on the number of facilities to find. Whereas an impedance cutoff value is required under the maximize coverage problem type, for minimize impedance, the problem type finds facilities in such a way that average distance is minimized for all demand points. Therefore, the impedance cutoff for the minimize impedance problem type is optional and a value is not typically set.

As mentioned, both the number of facilities and impedance cutoff (for the maximize coverage problem type) parameters were set to varying values. From the station-allocation studies summarized in Section 2.2, there was no clear rationale or pattern for proposing number of stations. The number of stations proposed across studies varied widely with some studies allocating as few as 8 [23] while others as many as 1,000 [22]. Further, while some studies incrementally found stations [20, 21, 23], others proposed distinct networks of varying sizes [8, 22, 24]. This thesis decided to follow the incremental approach at finding stations given one of the goals was to determine a point (or range) where UAM demand leveled-off as a result of incrementing number of stations.

Therefore, in order to determine the incremental amount of UAM demand per number of stations, the location-allocation solver was solved several times iterating through the number of facilities to find. A range between 2 and 75 stations in increments of 1 were set for the parameter. The author found 75 to be a suitable ceiling given it far surpassed the number of proposed stations from other incremental approach studies. Further, it was hypothesized incrementing in single steps between 2 and 75 would provide a wide range where a noticeable UAM demand pattern would manifest.

Regarding impedance cutoff, the parameter was only required and set when running the maximize coverage problem type. Again, when referring to the work summarized in Section 2.2, there were some studies that did consider a comparable parameter. For example, in German et al.'s study [23], UAM stations were allocated by limiting service to users within a 10-minute drive to the stations. The resulting stations were primarily allocated to urban areas and indicated 10 minutes was not adequate for non-urban, more dispersed land-use. In the extension to that study, Daskilewicz et al. [24], again consider a catchment area around potential UAM stations. Their allocation solver determined stations by limiting service to users within 3 miles and a 5-minute drive to the station.

For the 2 studies, the result of imposing a catchment area around potential stations influenced results by allocating stations to areas of high population density. This thesis explored a different approach thought to be more equitable. The maximize coverage problem type was run with impedance cutoffs (i.e. catchment areas) large enough to serve every demand point in the study area and hence solved for networks where search radii were not an influential element for station allocation. This approach was considered consistent with the principles described in a German Spatial Planning Report by the Federal Office for Building and Regional Planning [9]. The report makes a reference to a law found in the German constitution (Article 72) that mandates the “preservation of equivalent living conditions.” Equivalence, as the report explains, refers to equal access to services, goods, jobs and housing. Spatial planning in Germany considers sustainability, equivalence and regional strengthening as objectives. The report also refers to the German urban planning concept of central places. German settlements are decentralized when compared to other European cities and countries. Settlement networks under the central places concept have access to all necessary and vital amenities. Under this system, rural regions too must be provided with a minimum supply of public facilities, such as access to transportation networks, in order to prevent exodus.

Given this thesis sought to create UAM networks with stations ranging between 2 and 75, tediously running the location-allocation solver 74 times was inconvenient. Therefore, using ESRI’s model builder [91], the location-allocation solver was grouped into a sequence of ESRI tools and processes. ESRI’s model builder allows multiple procedures to be run in sequence and can do so iteratively. The custom model was set up to accept all data inputs and parameter settings described in this section. The model additionally accepts iteration values, such as a start, end and increment value which correspond to the number of stations to find. Every time an iteration was commenced by the model-builder, the demand points and facility shapefiles were reloaded onto the network dataset. Given the large sizes of the input data, loading them onto the location-allocation solver required a significant amount of time. To remedy this, the built-in ArcMap tool Calculate Locations [92] was used to hard-code the demand points and facilities data onto the network dataset. By doing so, load times were significantly reduced from several minutes to a couple of seconds. A visualization of the model builder is provided in Appendix E.

4.5.3 Running the Solver

4.5.3.1 Maximize Coverage

As described in the previous section, the maximize coverage location-allocation problem type was run with an impedance cutoff large enough to serve all demand points in the study area. Networks with lower numbers of stations required larger impedance cutoff values to completely reach all demand points. Conversely, networks with higher number of stations required smaller impedance cutoff values. Solve time increased significantly with the increase in the impedance cutoff value. Therefore, to expedite the process, the solving was broken up into 3 groups of networks each with a range of UAM stations. The groups had the following ranges: 2 through 10, 11 through 25 and 26 through 75. For each group, an impedance cutoff value was determined (through trial-and-error) for the smallest network under the assumption said value would satisfy all demand points for the larger networks. The impedance cutoff values found to satisfy all demand points were 110, 50 and 40 km for the groups in ascending order.

4.5.3.2 Minimize Impedance

After maximize coverage, the minimize impedance location-allocation problem type was tested to compare differences in results. Except for the impedance cutoff values, all data inputs and parameter settings used for the maximize coverage problem type were the same for minimize impedance. As described in Section 3.6.2, impedance cutoff values are typically not set for minimize impedance as it attempts to find stations by minimizing weighted cost (here, travel distance) for all demand points.

4.5.4 Results

Every time the model builder solved a location-allocation iteration, it generated and saved 3 output shapefiles. The 3 outputs were a demand points, demand lines and facilities shapefile. Under maximize coverage, the resulting demand points shapefile typically correspond to a subset of the original input demand points corresponding to points that were successfully connected and served by a facility. In the case of this thesis, all demand points were connected. The demand points shapefile included data such as what facility it was connected to and how much of the demand points' weight was allocated to said facility. When solving for maximize coverage and minimize impedance, a demand point can only be linked to a single facility, therefore, a demand points' weight is fully allocated to the facility serving it. The demand lines output shapefile was visually a collection of straight lines between a single facility and all its served demand points. For each line, the shapefile generated information such as total travel distance and amount of demand point weight being allocated to the facility. Though the lines were visually drawn in a Euclidean format, the corresponding travel distances were network distance values. Finally, the facilities output shapefile showed the facilities that were chosen among the initial input of facilities. The shapefile included information such as total weight and total number of demand points allocated to it.

When comparing results from maximize coverage and minimize impedance, the allocated stations were unexpectedly found to be identical for all networks sizes. The author hypothesized this was due to the large impedance cutoff values set under the maximize coverage problem type. A study by Church and ReVelle [93] demonstrated the computational similarities between the p-median (or minimize impedance) and the maximal covering location problem (or maximize coverage). The authors described that by introducing a service distance (i.e. cutoff value), between the facilities and demand points, to the minimize impedance problem, the solutions can be generated using equivalent mathematical calculations to those under maximize coverage. In the final remarks of the study, the authors indicated a desire to develop a procedure that can edit the input data so that other problem types can be solved using a minimize impedance approach. As described in Section 2.4.2, such a method (known as Hillsman editing) is in fact used by ESRI's location-allocation solver. Therefore, though unexpected, the identical station allocation results between maximize coverage and minimize impedance were reasonable.

Visualizations of the location-allocation results are shown below in Figure 12.

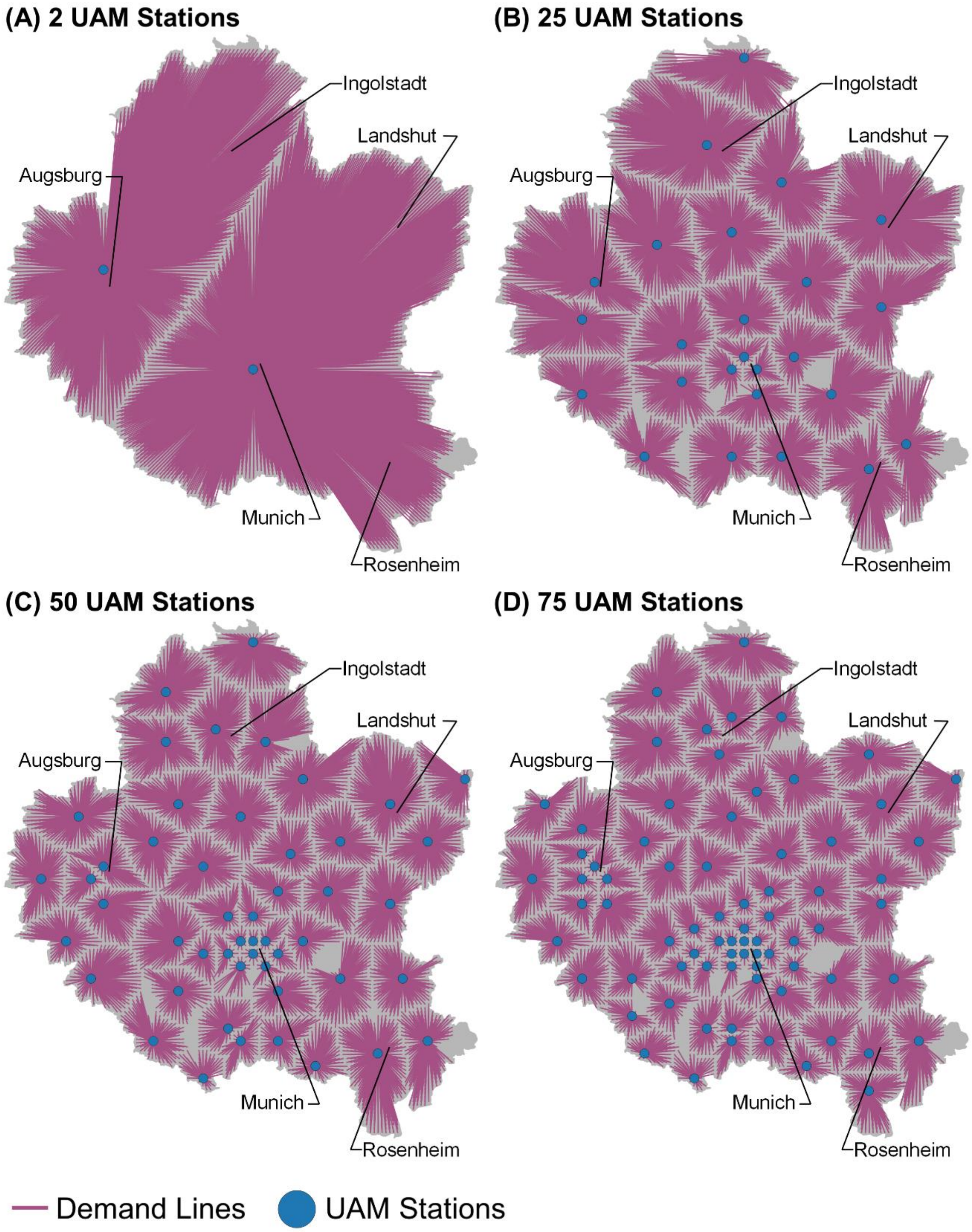

Figure 12 Location-Allocation Results

The maps, from A to D, show the results for the networks with 2, 25, 50 and 75 UAM stations. The blue points represent the allocated UAM stations while the purple lines represent the connections between the UAM stations and demand points (not shown). As mentioned, demand points were only allowed to be served by a single UAM station. Therefore, UAM station catchment area borders were clearly displayed by the maps. Patches of missing lines correspond to study area features such as lakes or forests and represent areas where UAM station placement would likely not take place.

While maps for all 74 UAM networks were not provided, Figure 12 accurately portrays the trend related to incrementing number of stations. Networks with fewer stations resulted in station allocation in areas with demand points with the highest weights. Such areas were primarily city centers as shown in map A of Figure 12 where the 2-station network resulted in the stations being allocated in the region's largest cities: Munich and Augsburg. Increasing the number of stations yielded networks with stations congregating in areas with high demand weights. Additionally, a higher number of stations resulted in a reduction of station catchment areas and hence, less travel time between demand and facilities. Both results are apparent in map D of Figure 12.

5 EVALUATION

The resulting UAM networks from the location-allocation analysis were evaluated by determining demand per number of stations and travel time comparisons. The travel demand was carried out using the mode choice model described in Section 2.1.3. The travel time evaluation involved comparing UAM, car and public transportation travel times to different destinations in the study area.

Additionally, this thesis' evaluation included a comparison between the manually created UAM networks developed in Ploetner et al.'s study [8]. The comparison seemed suitable given their study area was the same and their station allocation procedure noticeably different. Further, as described in Section 2.2.1, their study indicated a desire to explore a semi-automated process for station placement that would consider different criteria. Such a process was consistent with the work carried out in this thesis. Because their study developed UAM networks with 24, 74 and 130 stations, an additional 130-station UAM network was created using the procedures described in Chapter 4. The generated travel times for each set of networks were also compared.

A visualization of the 2 sets of networks are shown below in Figure 13. The networks on the left correspond to the networks created in this thesis (hereafter referred to as Thesis networks) while those on the right correspond to the networks created in Ploetner et al.'s study [8] (hereafter referred to as OBUAM networks). From top to bottom, the UAM network sizes are 24, 74 and 130.

As shown, the stations under the manually created networks were primarily allocated to city centers while this thesis' networks were more evenly spread out throughout the study area.

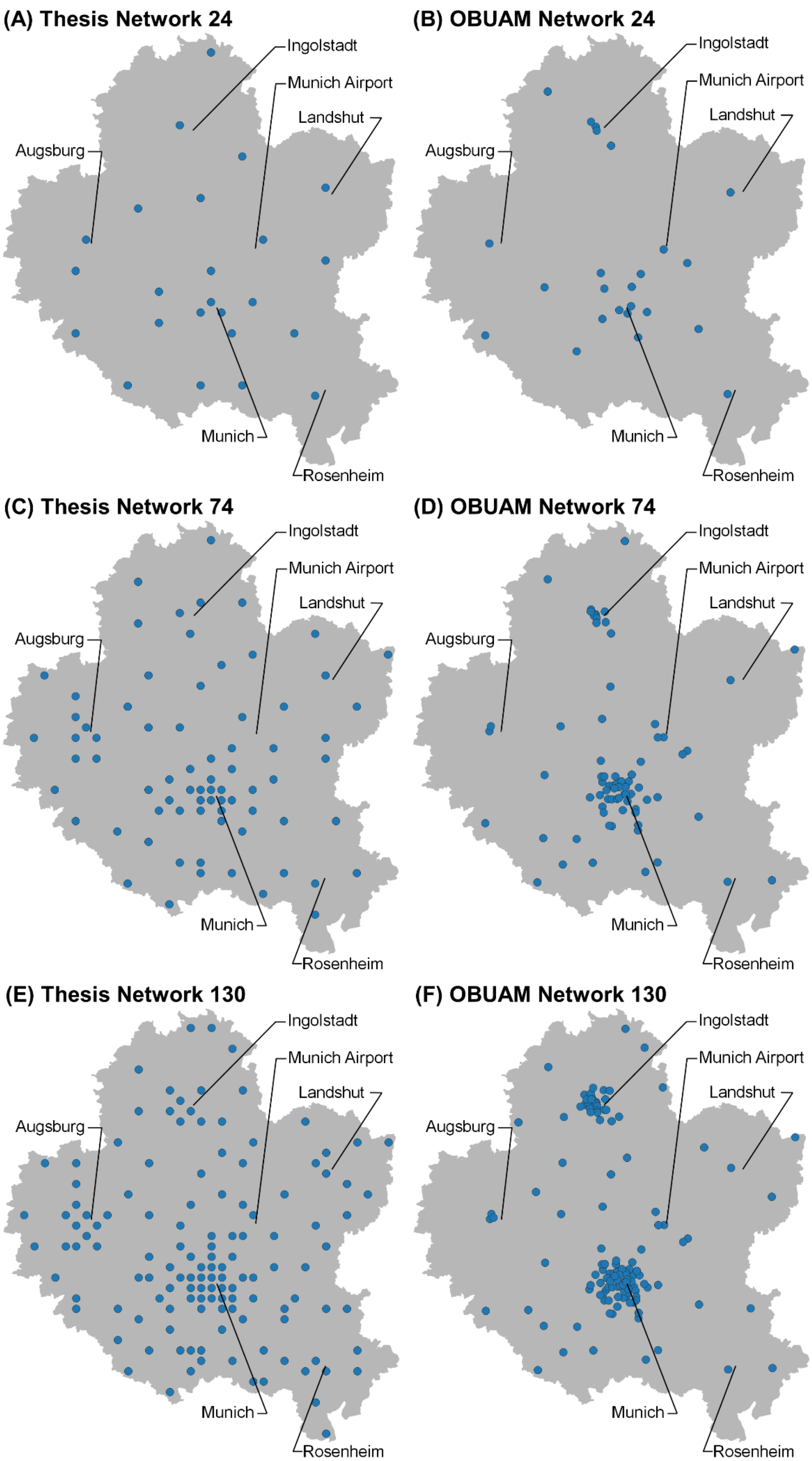

Figure 13 UAM Network Comparison

5.1 Mode Choice Modeling

In order to determine UAM demand per network size, the Thesis networks were input to a mode choice model that considered UAM as a mode of transportation. Among the required inputs, MITO [15] takes in a UAM network file. As described in Ploetner et al. [8], MITO was enhanced to consider UAM as a mode choice. Therefore, the network input must include UAM infrastructure: stations and flight links (paths). Using the MATSim UAM extension developed by Rothfeld et al. [5], UAM infrastructure was added to the study area.

5.1.1 Data Preparation

The MATSim UAM extension [94] was built and can be run using the Java object-oriented programming language. In addition to simulating UAM operations, the extension includes a multitude of Java classes that can be applied individually to create or modify UAM-related data. For this thesis, the extension's UAM scenario creator class was used to generate both a UAM network and a complimentary UAM vehicles file. The UAM vehicles file includes parameters such as station names, station coordinates, station capacity, vehicle type, vehicle capacities, and deboarding/boarding times. The MATSim UAM extension's scenario creator class accepts both a network and stations file as inputs. The stations file must contain the desired parameter settings for the UAM vehicles file and must additionally contain the UAM station coordinates, which are used to map the stations onto the network file.

Including the 3 OBUAM networks and additional 130-station network, a total of 78 UAM network and vehicles files were created. The UAM flight paths were straight lines between all stations.

5.1.2 Running MITO

Like the MATSim UAM extension, MITO was built and can be run using Java. Rather than running MITO 78 times separately on a personal computer, the cloud computing platform Amazon Web Service (AWS) was used. AWS allowed several high computing instances to run simultaneously on which separate MITO runs could be accommodated.

While MITO [95] requires multiple data inputs to run, a single command-line argument was needed: a configuration (or properties) file. The properties file points to where the input data is located and additionally includes MITO parameters that dictates what to run and how to run it. The data and parameters consist of elements such as skim matrices, socio-economic data, number of iterations, and travel patterns. The Modeling Spatial Mobility research group at the Technical University of Munich provided access to all such data corresponding to the metropolitan region of Munich.

A unique properties file was created for each UAM network where the only difference between them were the references to the UAM network and vehicles files.

5.1.3 Results

MITO results were a compilation of folders containing various outputs on the performance of the UAM networks. The output that was of interest for this thesis was the trips data. The data provided trip information for every generated trip for a single day in the study area. Generated trip information included the associated person id (i.e. who took the trip), trip purpose, origin/destination, departure time, distance and mode of travel. The trip data was provided through two files where one file contained all trips and the other, only UAM trips. The UAM trips file had additional information for each trip including origin/destination stations, access/egress modes of travel and UAM flight distance.

5.1.3.1 Thesis Networks

Total daily trips for all MITO runs were around 9.8 million. When considering only the Thesis networks (not including the 130-station network), UAM mode share ranged between 0.06 and 1%, which corresponded to just under 5,800 and 100,000 UAM trips, respectively. The UAM networks ranging between 2 and 5 stations had the largest number of trips (about 20%) in the distance range between 11 and 20 kms. Additionally, shorter trips were most dominant for the UAM networks ranging between 6 and 75 stations where trips with distances less than 10 kms made up between 30 and 58% of UAM trips. It should be noted that these distances were between the origin and destination meaning trips of less than 10 kms were present for the 2-station UAM network, which had the stations about 60 kms apart. For this reason, the number of trips were determined for total traveled distances (i.e. summation of access, egress and UAM flight distances). For total traversed distances, the UAM networks ranging between 2 and 5 stations had the largest number of trips (between 60 and 88%) for distances greater than 101 kms. Across all network sizes, trips of less than 10 kms never exceeded 1%. The larger network sizes (greater than 35 stations) had between 35 and 55% of trips in the distance range between 11 and 20 kms.

Demand per number of stations is shown below in Figure 14. The highest increase in demand was for the range between 5 and 12 stations. The range between 15 and 35 stations resulted in various fluctuations in demand. Finally, the range between 36 and 75 stations increased gradually with smaller fluctuations.

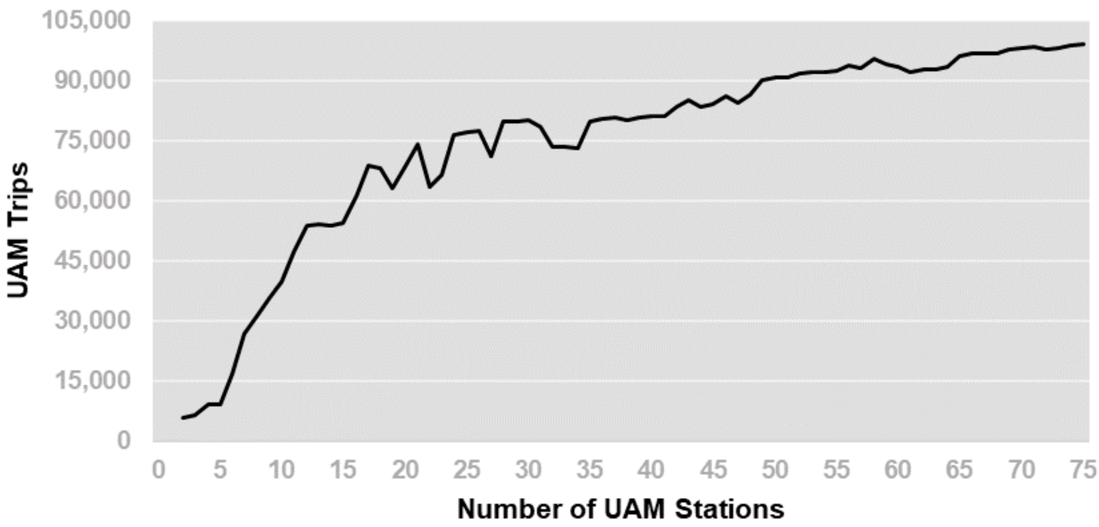

Figure 14 UAM Demand per Number of Stations

In order to determine a reason behind the high demand fluctuations for the networks ranging between 5 and 12 stations, the networks containing 21, 22 and 23 stations were mapped and compared. The MITO results indicated the 21-station network had a higher number of UAM trips than the 22- and 23-station networks, which appeared counterintuitive. As shown in Figure 15, there was a significant amount of overlap in stations allocated outside Munich's city core. A closer examination of the Munich city center showed the 21-station network allocated 3 stations in highly dense areas (as indicated by the smaller zone sizes) while the 22- and 23-station networks only had 2 stations in such areas. While the 22- and 23-station networks did have 2 additional stations within the city of Munich, they were allocated at the periphery of the city around zones that were more sparsely populated and perhaps not as well-connected to the road or public transportation networks. Except for the western region of the study area, the 22- and 23-station networks are almost identical. The 23-station network performed a bit better than the 22-station network, which could have simply been due to the extra station. A similar occurrence was observed for the networks containing 26, 27 and 28 stations (not mapped). As shown in Figure 14, there was a dip in UAM trips for the 27-station network. The 27-station network had less stations allocated in highly dense areas while still maintaining some stations at the periphery of the city.

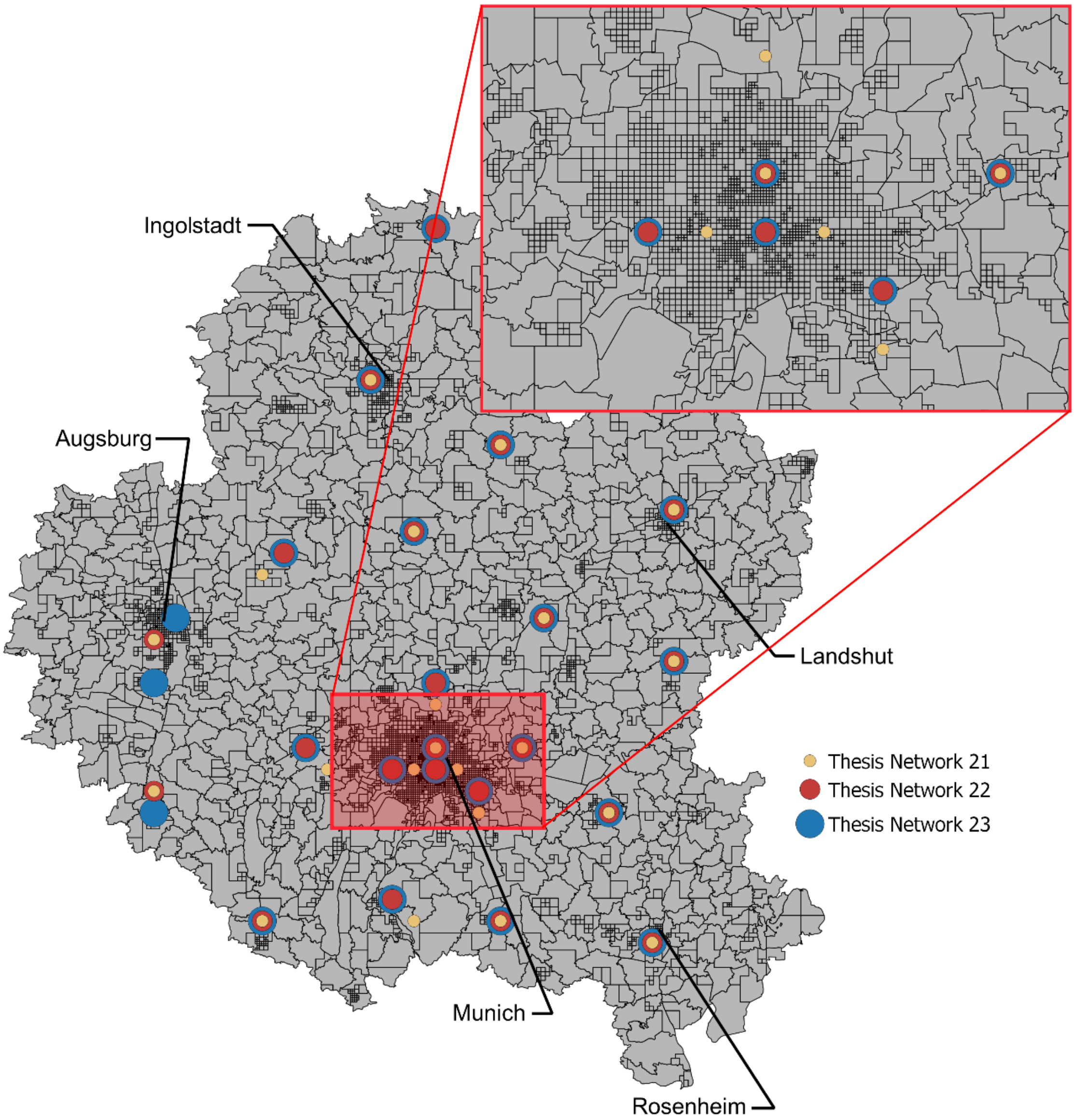

Figure 15 Station Placement Influence on Demand

5.1.3.2 Thesis and OBUAM Networks

Next, the demand between the Thesis and OBUAM networks were compared. The resulting UAM mode shares for both sets of networks ranged between 0.75 and 1.1%, which corresponded to just under 74,000 and 108,000 UAM Trips, respectively. Trip distances were very similar between the Thesis and OBUAM networks. Results showed that most trips (between 50 and 60%) were for distances of less than 10 kms. When considering total traveled distances, the Thesis and OBUAM networks coincided in showing most trips (between 54 and 60%) for the 74- and 130-station networks were for trips between 11 and 20 kms. The 24-station networks differed in showing the Thesis network had about 37% of trips between 21 and 30 kms while the OBUAM network had about 35% of trips between 11 and 20 kms.

Demand per network size is shown below in Figure 16.

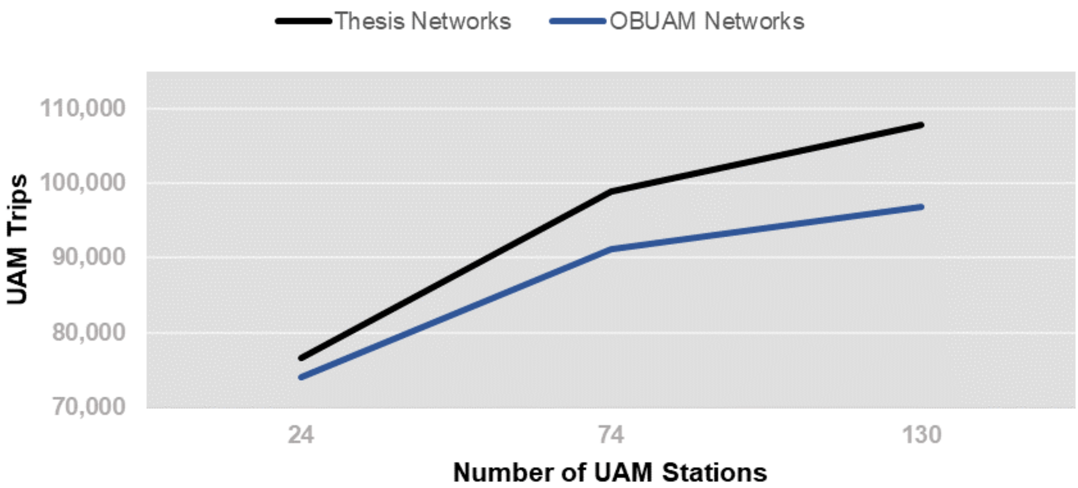

Figure 16 Thesis and OBUAM UAM Demand Comparison

For all network sizes, the results indicated the Thesis networks generated higher UAM demand than the OBUAM networks. As previously mentioned, the UAM trip information provided in the MITO results included access and egress stations. When examining such data for both the Thesis and OBUAM networks, the Thesis network stations were found to have their top performing stations attracting a significant amount of the overall UAM demand. The top 3 performing stations for each network size are tabulated below in Table 6.

	Thesis Networks		OBUAM Networks	
Network Size	*UAM Demand Served by Top 3 Stations*	*Share of Overall UAM Demand*	*UAM Demand Served by Top 3 Stations*	*Share of Overall UAM Demand*
24	56,250	73%	34,192	46%
74	23,131	23%	14,318	16%
130	20,364	19%	9,076	9%

Table 6 UAM Demand of Top 3 Stations

As shown, the top 3 performing stations for each of the Thesis' networks accommodated a higher portion of the overall UAM demand when compared to the OBUAM networks. Such results could be due to the difference in spatial distribution of UAM stations. The top 3 stations for both set of networks were primarily located in the Munich city center. As was shown in Figure 13, the station placement for this thesis was much more spatially distributed throughout the region as compared to the OBUAM networks. Higher spatial distribution, therefore, resulted in less stations allocated in areas of high demand. For the Thesis networks, this resulted in less stations taking on more UAM demand. The Thesis networks, in ascending network size, were noted to accommodate half of the generated UAM demand with 2, 9 and 15 stations, while the OBUAM networks required 4, 15 and 26 stations.

5.2 Travel Time Comparisons

To further evaluate the performances of the Thesis and OBUAM networks, travel times to different destinations in the study area were determined. For this evaluation, the MATSim UAM extension [94] was again used. Specifically, the extension's built-in travel time calculators were utilized to determine travel times for car, public transportation and UAM.

5.2.1 Data Preparation

The MATSim UAM extension [94] includes 3 travel time calculators for car, public transportation and UAM. Inputs are similar for all 3 travel time calculators.

The car travel time calculator takes in: a network file, a network-change events file and a trip inputs file. The network file contains the infrastructure (i.e. roads) by which trips will be routed and travel time calculated. The events file is a file specific to MATSim [13] that records all actions that occurred in a simulation. The events file used for the travel time calculators is intended to be an events file from a previous MATSim run where UAM is not included. By using such an events file, resulting network performances (e.g. congestion on links) can be mimicked onto the network file used for travel time calculations and hence changes the network. Therefore, when car travel time is calculated, for example, it is done so on a network that considers road congestion conditions [94]. The network-change events file was provided by Bauhaus Luftfahrt. Finally, the trips input file should include desired origin and destination coordinates and departure times.

Travel times were calculated for 3 destinations in the study area: Munich Central Station, Augsburg Central Station and the Munich Airport. Munich and Augsburg represent the largest cities in the study area and the Munich Airport is the busiest in Bavaria [96]. The travel time calculators were used to determine levels of accessibility to said destinations from all regions of the study area. Therefore, the origin coordinates in the trips input file corresponded to evenly spaced points distributed throughout the entire study area. All origin points were destined to all 3 destinations. According to TomTom's traffic index for Munich [97] and Augsburg [98], the most congested times on the roads are 5 pm. Therefore, in order to determine potential travel time savings during times of high traffic congestion, the departure time for the trips input was set to 5 pm. The same trips input file was used across all travel time calculators.

The public transportation travel time calculator takes in: a network file, a transit schedule file and a trips input file. In addition to roads, the network file should also contain infrastructure that is specific to certain public transportation types (i.e. rails for subway) that may be present in the study area. Given both car and public transportation travel times were needed, the same network input was used for both calculators. The transit schedule file contains all information on public transportation lines and schedules. The transit schedule file was provided by Bauhaus Luftfahrt.

The UAM travel time calculator takes in: a network file, a network-changes events file, a UAM vehicles file, a transit schedule file, a trips input file, a strategy name, processing time, search radius and access modes. The network file should contain infrastructure for UAM, and any other modes identified to be used for UAM access (i.e. roads, public transportation). As mentioned in Section 5.1.1, the UAM vehicles file includes parameters such as station names, station coordinates, station capacity, vehicle type, vehicle capacities, and deboarding/boarding times. The UAM network files (along with their respective UAM vehicles files) described in Section 5.1.1 were used here as inputs. The strategy name refers to the desired routing method where the options are minimum travel time, minimum distance, minimum access travel time and minimum access distance. The minimum travel time strategy was used in order to determine potential travel time savings. Processing time refers to the amount of time for the segment when passengers arrive to the station and take-off. The search radius refers to the maximum distance an agent (or person) will travel from their origin to access a UAM station. The values set for processing time and search radius were 15 minutes and 160 km, respectively. A processing time of 15 minutes was consistent with values tested by Rothfeld et al [14] and corresponded to the more conservative range of their tested values. A search radius of 160 km provided a large enough distance to cover the entire study area. Finally, access modes refer to the modes of travel (e.g. car, walk, public transportation) available to access UAM. Car, walking and public transportation were used here.

5.2.2 Running the Travel Time Calculators

Both the car and public transportation travel time calculators were run on a personal computer given they did not require substantial processing power nor time. The UAM travel time calculator, however, did require a significant amount of processing. Therefore, the AWS was again utilized to accommodate the UAM travel time calculations.

5.2.3 Results

The resulting travel time calculation files provided the same information as the input trips file, but with an additional attribute field corresponding to the resulting travel times. The results were visualized on QGIS where each origin point was assigned a color representing a value on a travel time range. The travel time range was broken up by 30-minute increments. There was a total of 3 different sets of visualizations corresponding to the number of destinations. Each set consisted of 8 maps corresponding to the different modes of travel as well as the 2 sets of UAM networks (i.e. Thesis and OBUAM).

5.2.3.1 Travel Times to Munich Central Station

The travel time results to the Munich Central Station are shown below in Figures 17A and 17B.

As shown in map A of Figure 17A, the car travel times were one among the best performing, while map B showed public transportation results to be among the worst performing. The resulting radial patterns for public transportation show travel time is dependent on proximity to transit stations. The car travel times generally performed better than all the Thesis networks, especially in the area around the destination (i.e. Munich city center) and for Ingolstadt in the north. While public transportation generally performed the worst among all the calculated travel times, it did have a slight advantage, over the 24-station Thesis network, in the area immediately surrounding the destination.

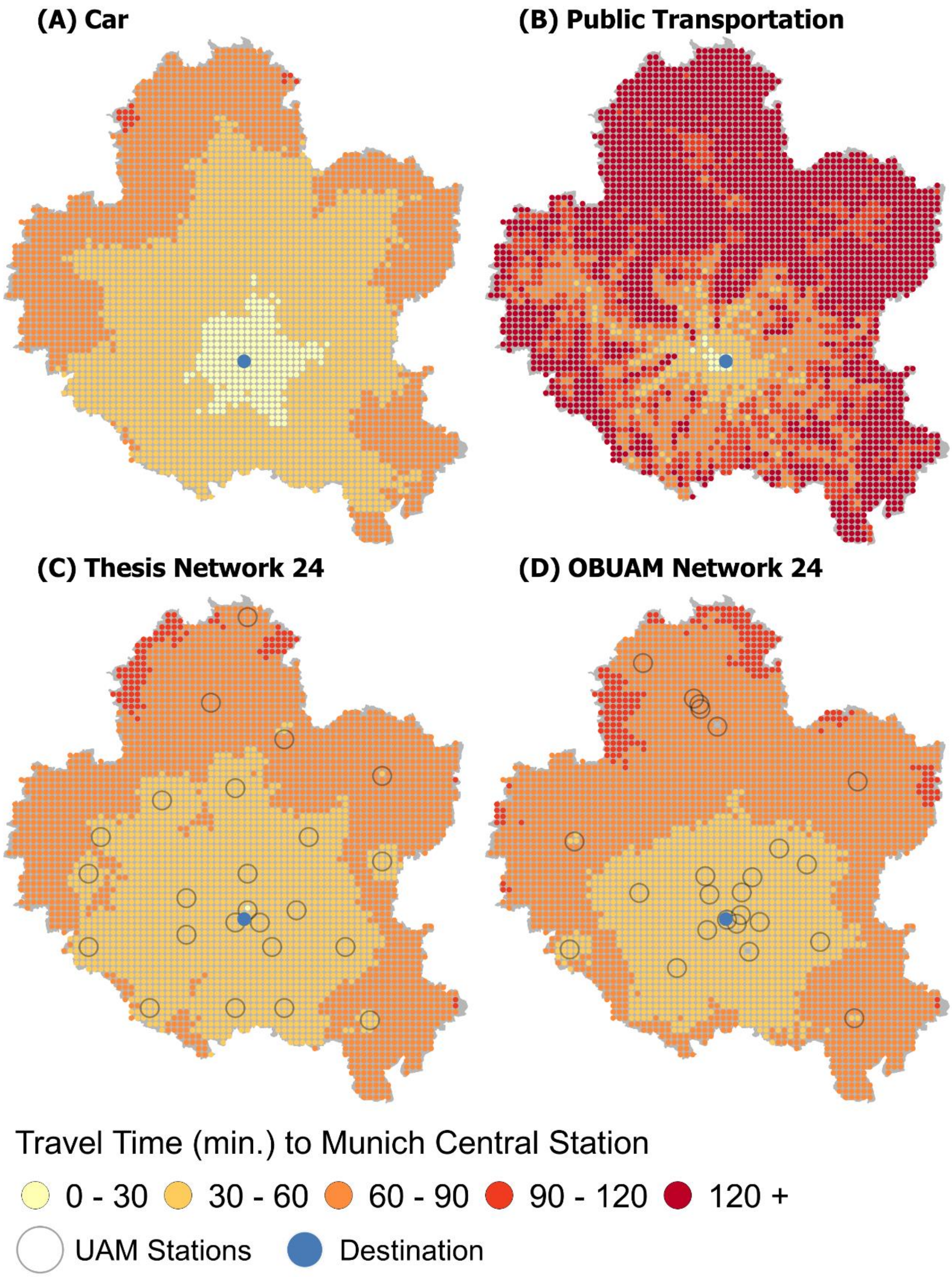

Figure 17A Travel Time Comparisons to Munich Central Station

Maps C and D of Figure 17A show results for the 24-station UAM networks. The Thesis network resulted in providing access in the 30- to 60-minute travel time range to a larger area than the OBUAM network.

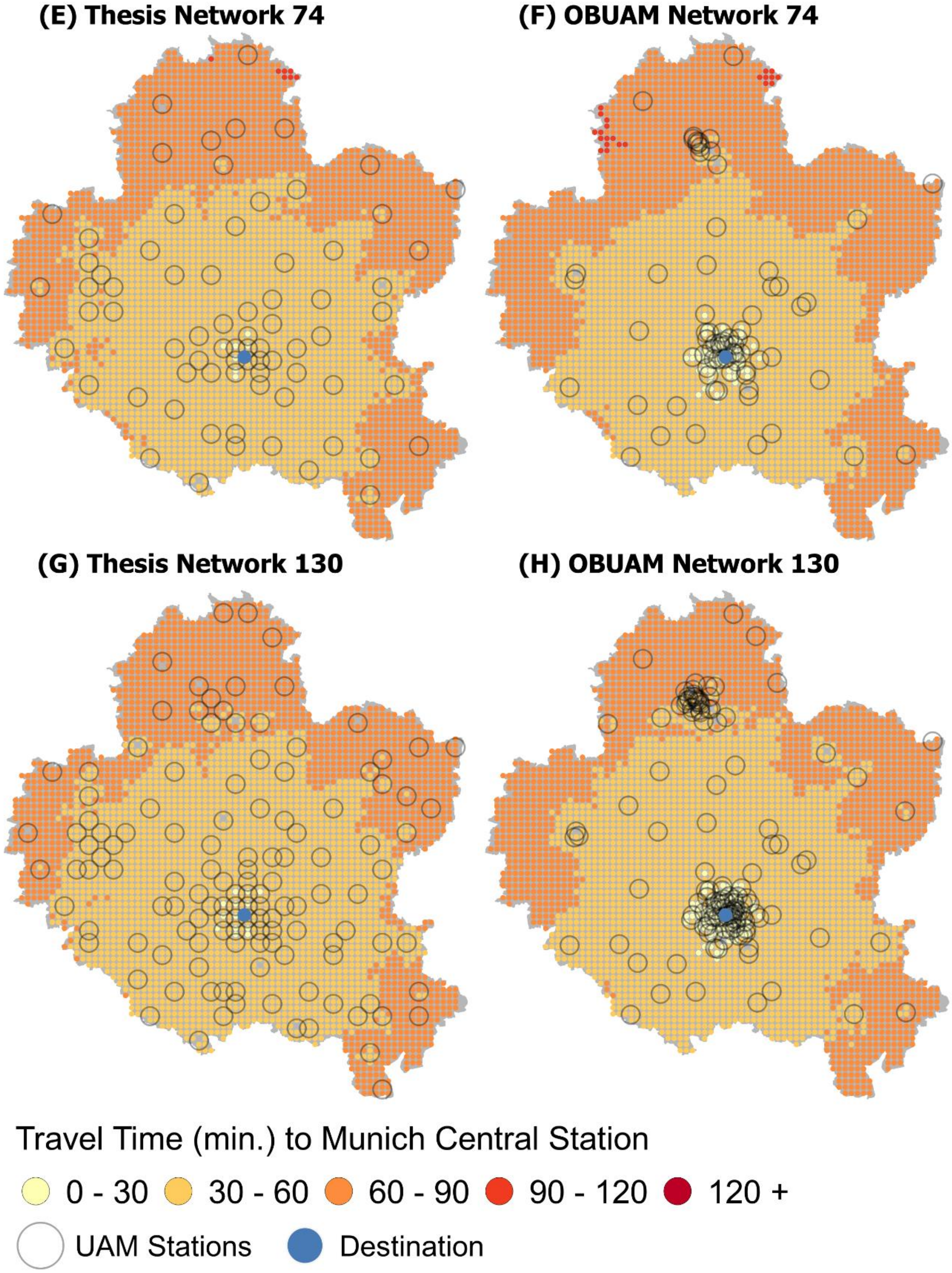

Figure 17B Travel Time Comparisons to Munich Central Station

Maps E and F of Figure 17B show results for the 74-station UAM networks. Though the Thesis network resulted in a slightly larger access area for the 30- to 60-minute travel time range than the OBUAM network, the OBUAM network did provide a larger access area for travel time under 30 minutes (especially in the Munich city center).

Finally, maps G and H of Figure 17B show results for the 130-station UAM networks. Like the 74-station results, the Thesis network resulted in a slightly larger access area for the 30- to 60-minute travel time range than the OBUAM network, however the OBUAM network performed significantly better in the city center.

To further illustrate travel time savings, maps were created that identified areas where UAM was faster than ground transportation (i.e. car and public transportation). The travel time savings to the Munich Central Station are shown below in Figures 18A and 18B.

Maps A and B of Figure 18A show the travel time savings for the 24-station UAM networks. While the Thesis UAM networks do show more travel time savings, both show relatively minor travel time savings when traveling to the Munich Central Station.

Maps C and D of Figure 18A show the travel time savings for the 74-station UAM networks. Compared to the 24-station UAM networks, larger areas in the north and at the periphery of the study area showed travel time savings with UAM.

Finally, Maps E and F of Figure 18B show the travel time savings for the 130-station UAM networks. The Thesis network shows a larger amount of travel time savings in the Augsburg area.

In general, the maps showed that the city of Munich is already well-connected with existing ground transportation. However, UAM could provide travel time savings for the periphery regions of the study area.

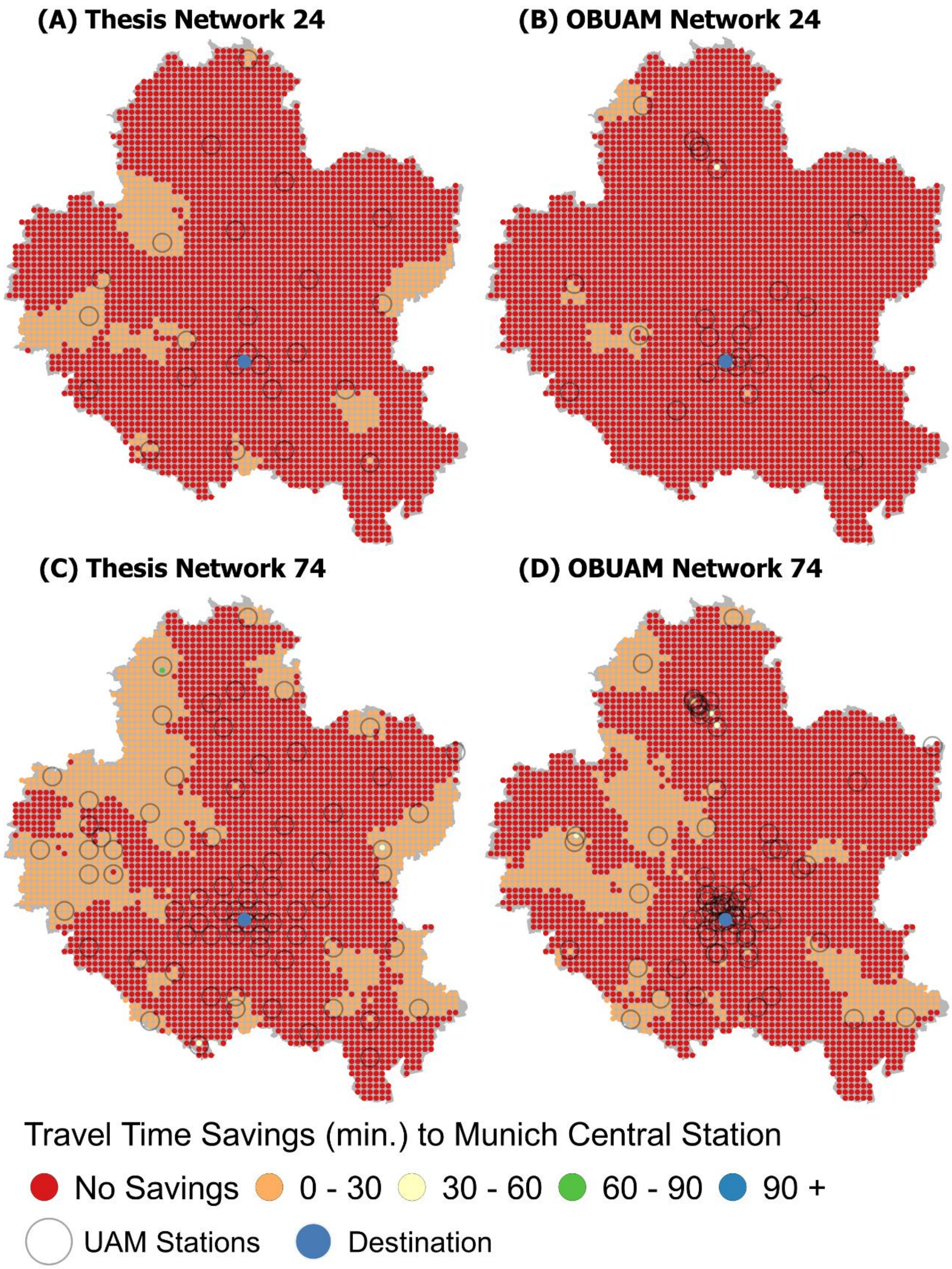

Figure 18A Travel Time Savings to Munich Central Station

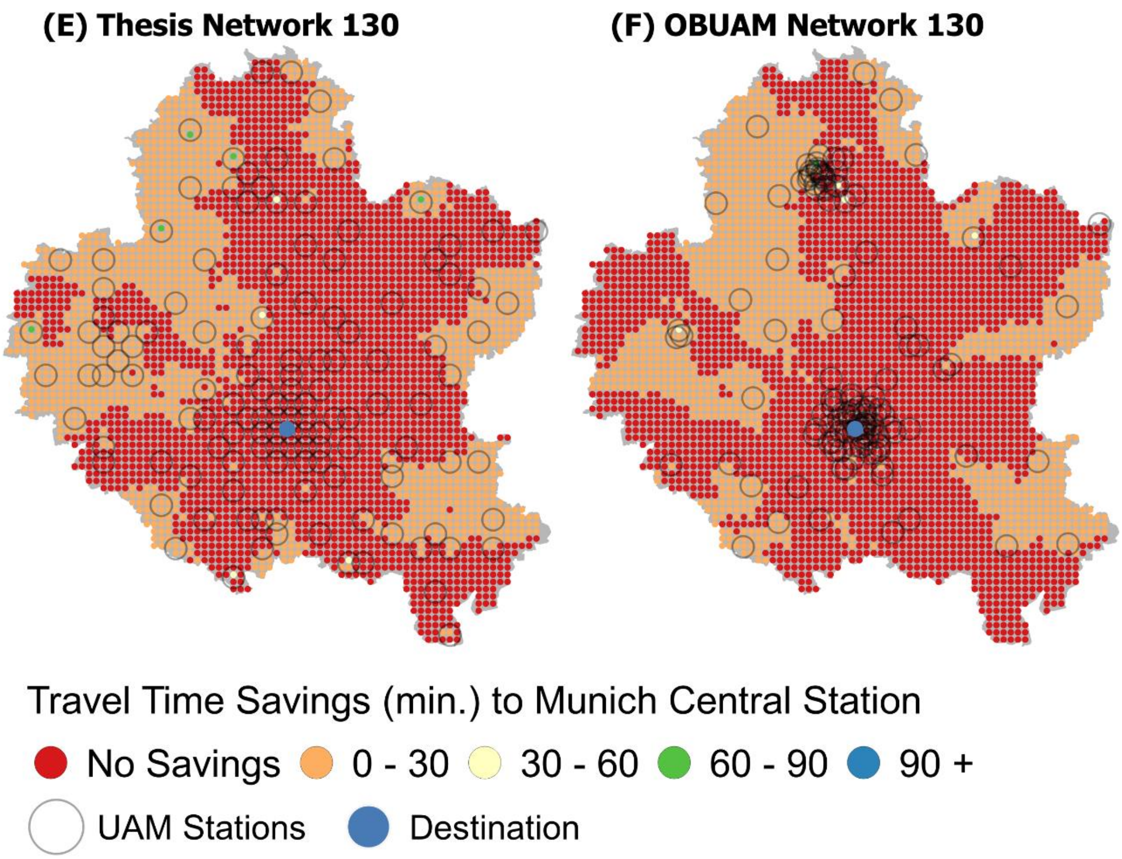

Figure 18B Travel Time Savings to Munich Central Station

5.2.3.2 Travel Times to Augsburg Central Station

The travel time results to the Augsburg Central Station are shown below in Figures 19A and 19B.

In terms of providing the quickest access in the immediate vicinity of the destination, car travel time, shown in map A of Figure 19A, was among the best performing. Travel times clearly increased with the increase of distance to the destination. Public transportation travel time, shown in map B of Figure 19B, was among the worst performing. The distinct patterns shown for public transportation map indicate travel time is dependent on an origin point's distance to a transit station. Compared to the car travel times, the Thesis networks had an advantage in that travel times over 90 minutes were reduced and travel times over 120 minutes were almost non-existent. Further, the 74- and 130-station Thesis networks had similarly sized extents, with car, for travel times in the 30- and 60-minute range. Again, while public transportation was generally the worst performing, it did have a slight advantage over the 24-station Thesis network in providing quicker travel times in the immediate vicinity of the destination.

Maps C and D of Figure 19A show results for the 24-station UAM networks. The results for the OBUAM network indicate origin points directly adjacent the destination performed worse than origin points much further away. The peculiar result is due to the way travel time is calculated by the MATSim UAM extension's calculators [94]. Every origin point within the search radius of a UAM station (here set to 160 km) was forced to take UAM regardless of their distance to the destination. Therefore, the origin points immediately around the destination were required to first travel to the nearest UAM station and then travel back to the destination. Because the Thesis network had more than 1 UAM station near the destination, the travel time results performed better around the Augsburg Central Station. The OBUAM network, however, did perform better than the Thesis network given it had less amount of origin points traveling more than 90 minutes.

Maps E and F of Figure 19B show results for the 74-station UAM networks. The results for the OBUAM network performed better than the Thesis network given there were larger areas of access for both the 0- to 30- and 30- to 60-minute travel time ranges. Additionally, the OBUAM network had less origin points traveling more than 90 minutes.

Finally, maps G and H of Figure 19B show results for the 130-station UAM networks. Like the 74-station results, the OBUAM network performed better than the Thesis network in terms of providing faster travel times to the destination. The OBUAM network also had less origin points traveling more than 90 minutes.

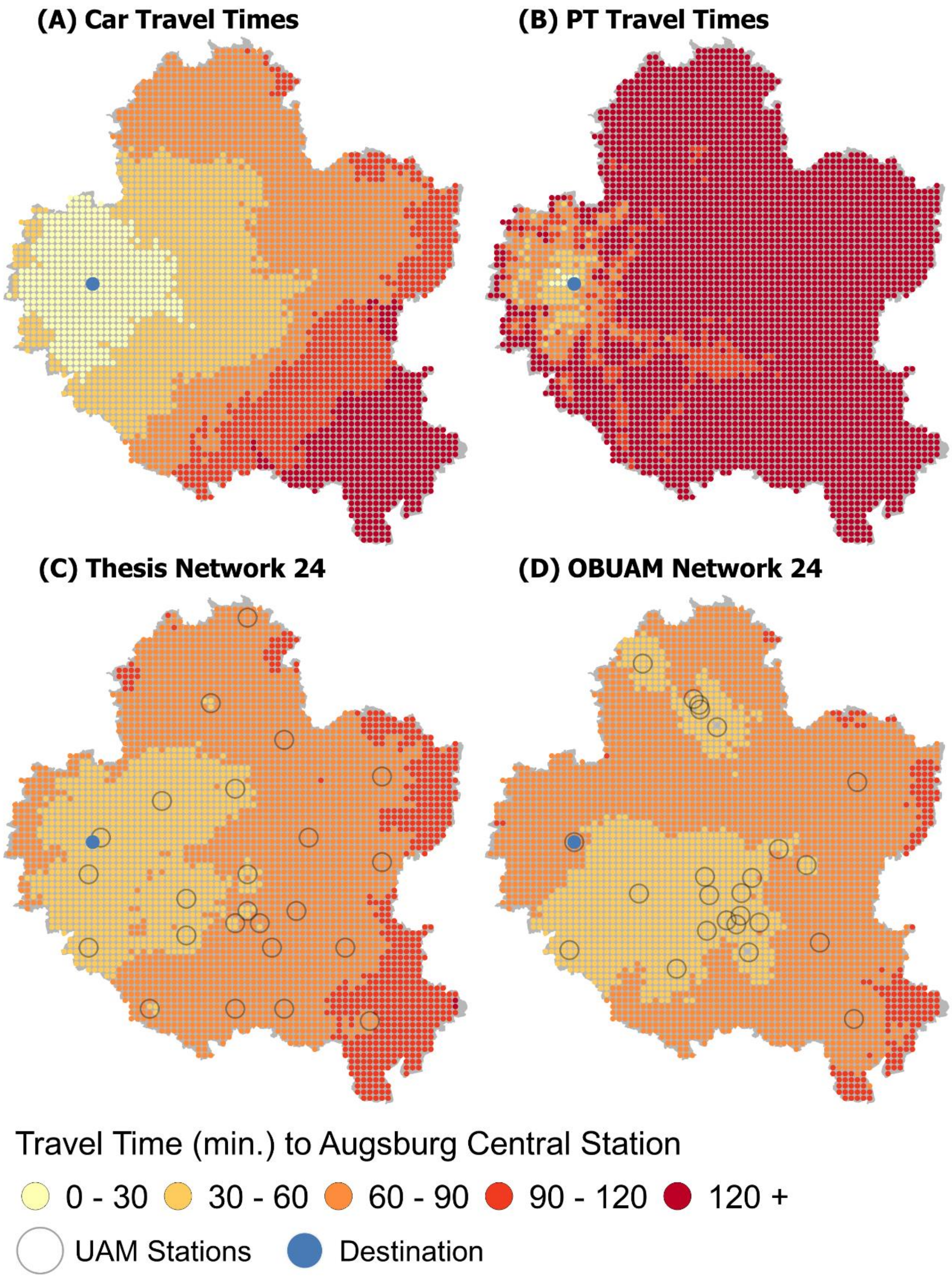

Figure 19A Travel Time Comparisons to Augsburg Central Station

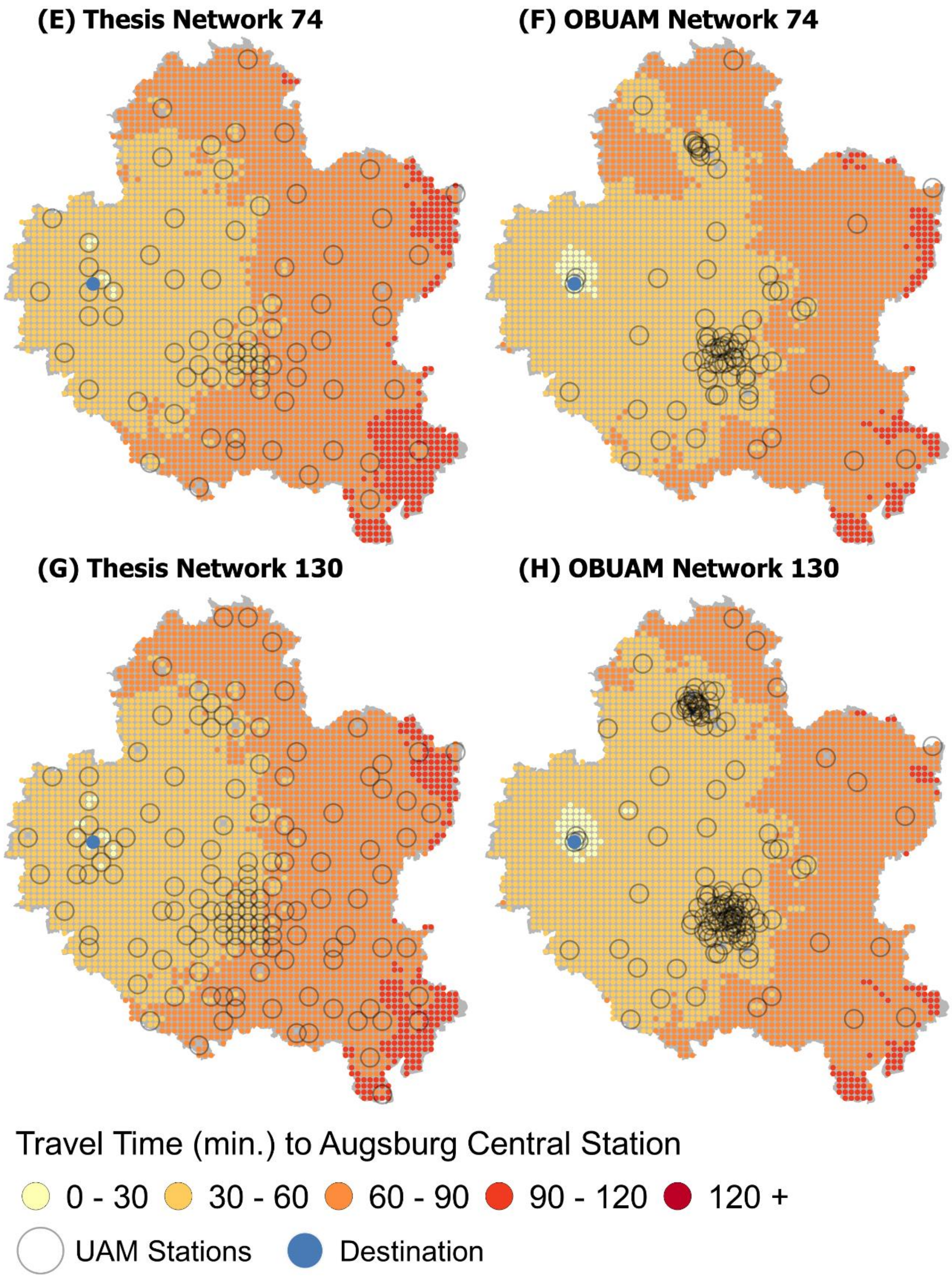

Figure 19B Travel Time Comparisons to Augsburg Central Station

To further illustrate travel time savings, maps were created that identified areas where UAM was faster than ground transportation (i.e. car and public transportation). The travel time savings to the Augsburg Central Station are shown below in Figures 20A and 20B.

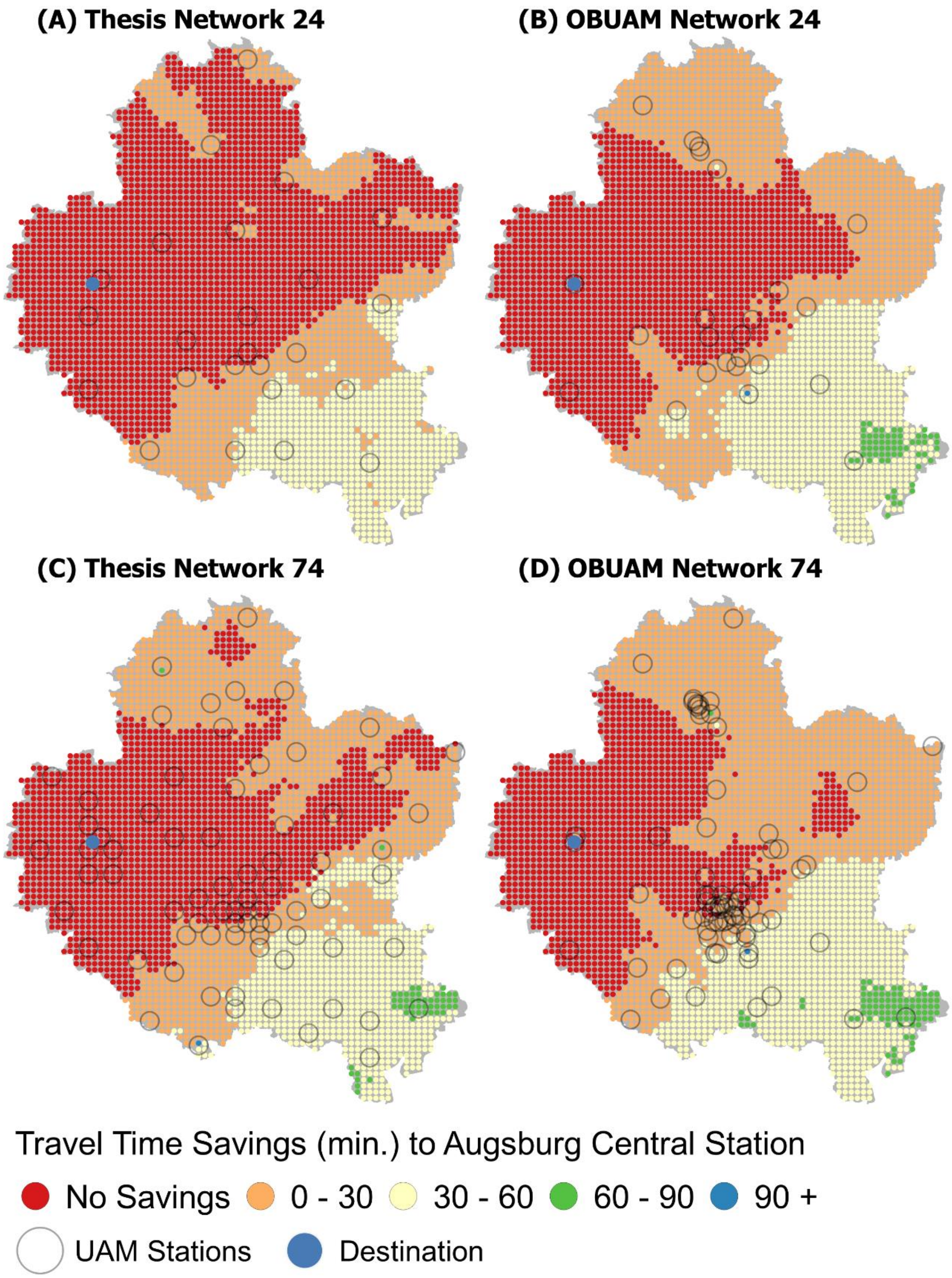

Figure 20A Travel Time Savings to Augsburg Central Station

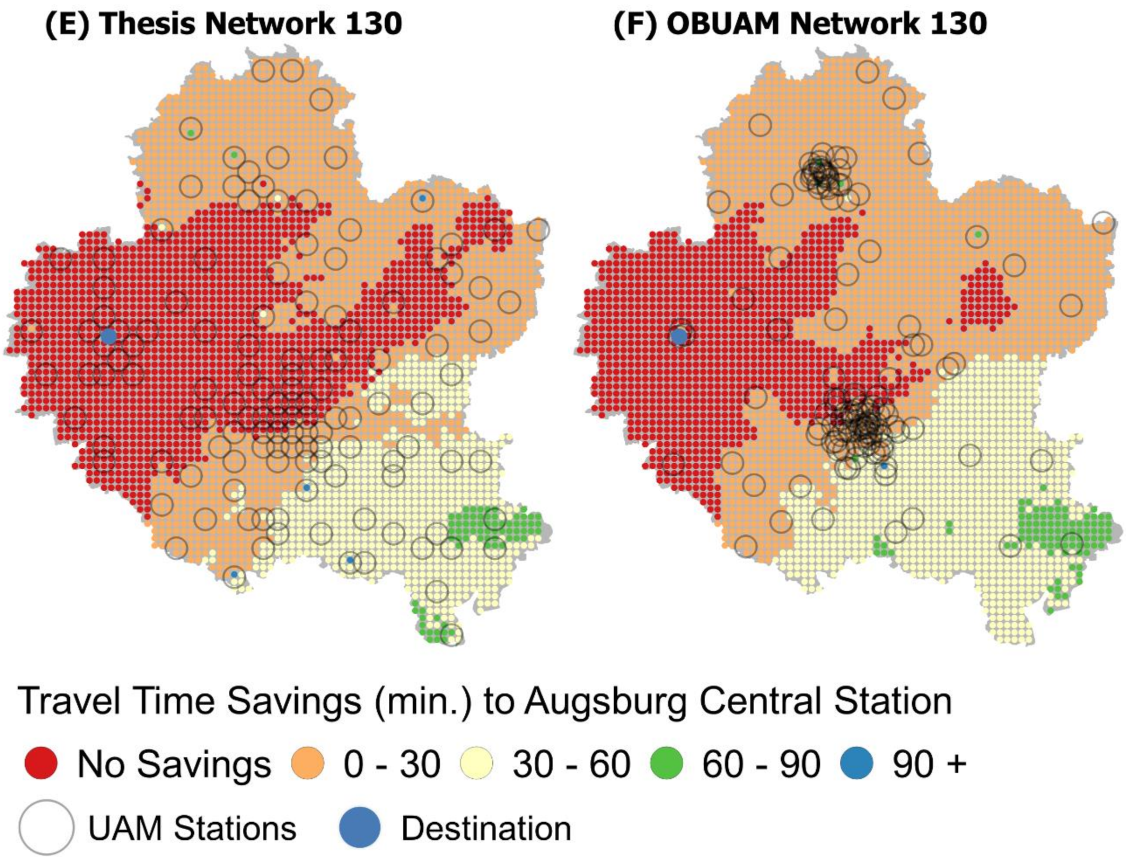

Figure 20B Travel Time Savings to Augsburg Central Station

Maps A and B of Figure 20A show the travel time savings for the 24-station UAM networks. The OBUAM network provided larger travel time savings, especially in the southeastern region of the study area.

Maps C and D of Figure 20A show the travel time savings for the 74-station UAM networks. Like the 24-station station networks, the OBUAM network provided larger travel time savings.

Finally, maps E and F of Figure 20A show the travel time savings for the 130-station UAM networks. Again, the OBUAM networks yielded larger travel time savings.

Compared to the Munich Central Station travel time savings, traveling to Augsburg via UAM could provide larger travel time savings, especially if traveling from the southeastern region of the study area.

5.2.3.3 Travel Times to Munich Airport

The travel time results to the Munich Airport are shown below in Figures 21A and 21B.

Map A of Figure 21A show car travel times were again found to be the best performing in terms of providing the largest amount of travel time under 30 minutes. Conversely, public transportation travel times, shown in map B of Figure 19A, were among the worst performing. The resulting radial patterns for public transportation show travel time is dependent on proximity to transit stations. When compared to the Thesis UAM networks, the car travel times had a consistent advantage for the northernmost region of the study area. However, the Thesis UAM network travel times did have a reduction in travel times over 90 minutes. Like the previous 2 set of results, the public transportation network provided a very minimal advantage in the area immediately around the destination in providing quicker travel times.

Maps C and D of Figure 21A show results for the 24-station UAM networks. The OBUAM network travel times resulted in a more even and larger distribution of travel time within 30 and 60 minutes. Map D also showed small areas near the destination with travel times under 30 minutes.

Maps E and F of Figure 21B show results for the 74-station UAM networks. The OBUAM network was found to produce a larger distribution of travel times within 30 and 60 minutes. There was also a larger area with travel times under 30 minutes near the destination.

Finally, maps G and H of Figure 21B show the results of the 130-station UAM networks. The results were found to produce a similar distribution of travel time ranging between 30 and 60 minutes. However, the OBUAM network produced travel times under 30 minutes near the destination.

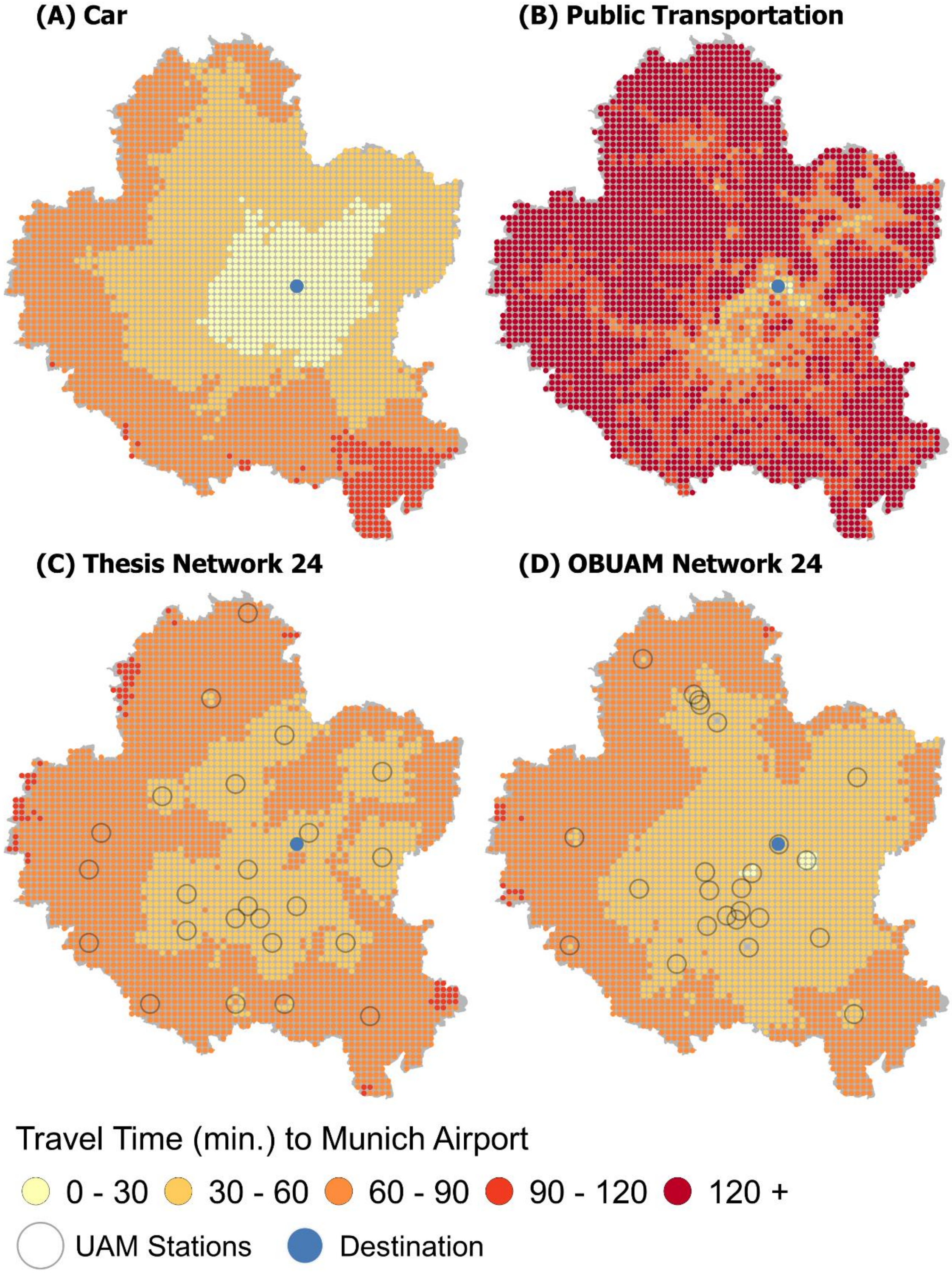

Figure 21A Travel Time Comparisons to Munich Airport

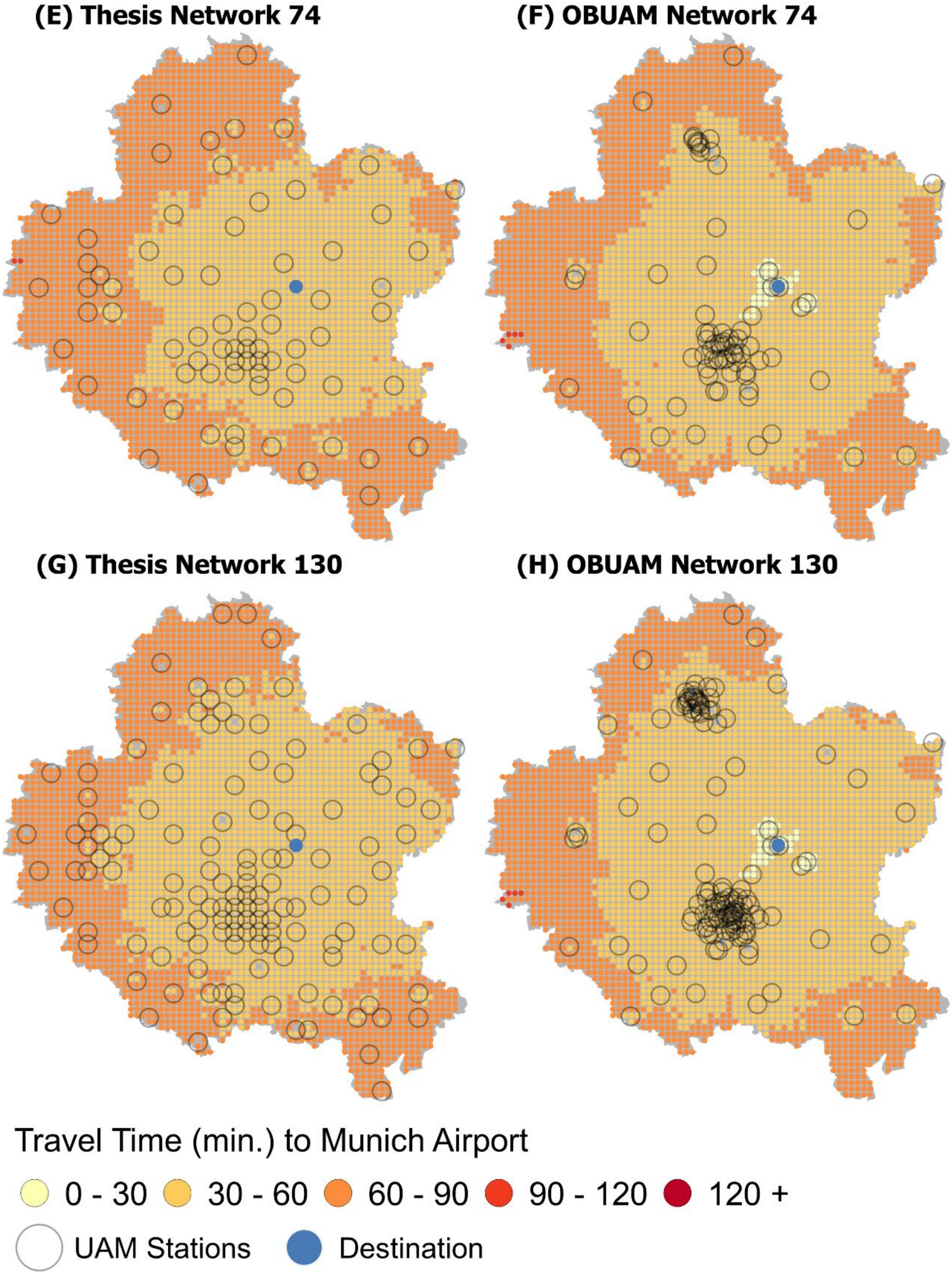

Figure 21B Travel Time Comparisons to Munich Airport

To further illustrate travel time savings, maps were created that identified areas where UAM was faster than ground transportation (i.e. car and public transportation). The travel time savings to the Munich Airport are shown below in Figures 22A and 22B.

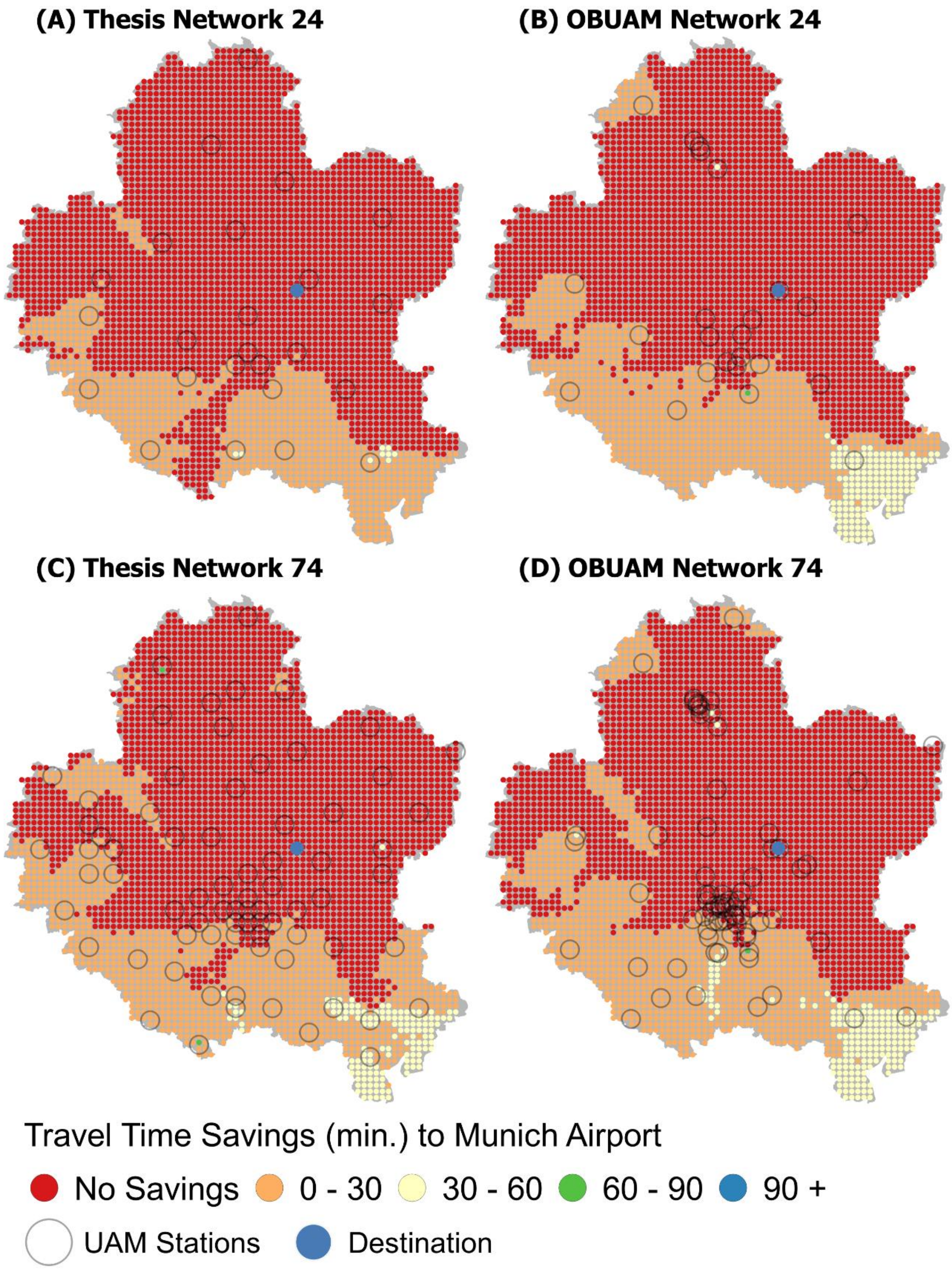

Figure 22A Travel Time Savings to Munich Airport

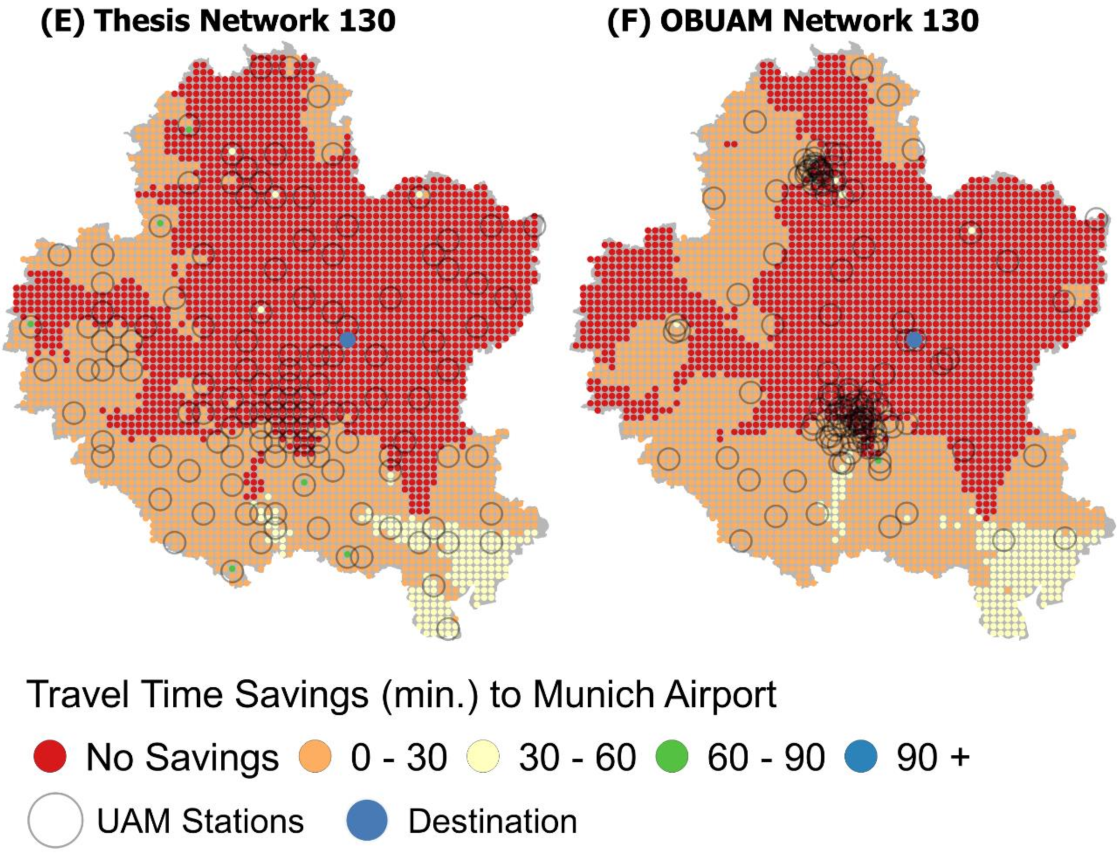

Figure 22B Travel Time Savings to Munich Airport

Maps A and B of Figure 22A show the travel time savings for the 24-station UAM networks. The results indicate the southern region of the study area could potentially benefit from UAM when traveling to the Munich Airport. The OBUAM network had an advantage over the Thesis network in the southeastern region of the study area.

Maps C and D of Figure 22A show the travel time savings for the 74-station UAM networks. The results for both networks are similar and like the 24-station network results, the southern region of the study area could potentially benefit the most from UAM when traveling to the Munich Airport.

Finally, maps E and F of Figure 22B show the travel time savings for the 130-station UAM networks. Again, the southern region of the study area could benefit the most from UAM. The Thesis network showed a slight advantage for the Augsburg area. However, the OBUAM network could provide faster travel times to the southern half of Munich's city center.

In general, the southern region of the study area could benefit the most from UAM when traveling to the Munich Airport.

6 CONCLUSION

6.1 Discussion of Results

The mode choice modeling results indicated the highest amount of incremental UAM demand was for the range between 5 and 12 UAM stations. For said range, UAM demand increased from just over 9,000 to just under 54,000 UAM trips, which corresponded to a mode share of about 0.09 and 0.55%, respectively. In turn, the range between 13 and 75 UAM stations generated a more gradual increase in demand with total trips ranging between 54,000 and about 99,200 UAM trips, which corresponded to a mode share of about 0.55 and 1%, respectively. These results were comparatively higher than the results found by Ploetner et al. [8] where their 74-station network produced a UAM mode share of 0.5%, and as they pointed out, such low mode shares indicate UAM may not significantly alter existing mobility patterns or conditions. Additionally, the range between 15 and 35 stations was found to produce fluctuations in UAM demand. A reason for such fluctuations were likely due to the location of the UAM stations. Such results indicate station location is more influential to demand than number of stations. Overall, the resulting incremental UAM demand did not show a critical point or exact network size where demand stagnated, however the range between 5 and 12 stations did show the highest rate of incremental UAM demand. Finally, resulting trip distances were consistent with previous studies [8, 14, 24] in showing a majority of UAM trips were for shorter distance trips.

When comparing the UAM demand between the Thesis and OBUAM networks, the demand generated by the Thesis networks was larger for all network sizes. The main difference between the 2 sets of networks was the proximity of stations and spatial distribution throughout the study area. The Thesis networks were significantly more spread out, however there were general similarities in station placements for both sets of networks. For example, a high number of stations were unsurprisingly located within or around the Munich, Augsburg and Ingolstadt city centers. These are the largest cities in the study area and hence contained the largest amount of demand to which stations were attracted to. Further, the top 3 Thesis-network stations were found to take in a larger amount of demand as compared to the OBUAM-network stations. Higher spatial distribution therefore led to areas of high demand being served by of a lower number of stations. These results were reasonable given the Thesis networks were allocated with the location-allocation solver type maximize coverage which allocated stations in such a way that all demand points were served while maximizing demand per station (maximize coverage) and/or minimizing weighted distances (minimize impedance).

The travel time comparison results indicated UAM benefits could be realized for longer distance trips. This result was consistent with previous UAM station placement studies [3, 8, 24]. The travel time maps showed that the Munich Central Station and Munich Airport are already well connected by existing ground transportation, especially car. The largest amount of travel time savings was achieved when traveling to the Augsburg Central Station. Specifically, traveling to Augsburg from the southwestern region of the study area (around Rosenheim) saw travel time savings of up to more than 90 minutes when traveling via UAM. The south and southwestern regions of the study area could also benefit from UAM when traveling to the Munich Airport with travel time savings found to go over 60 minutes. In general, the travel time savings maps showed that, at least for the 3 identified destinations, ground transportation is faster than UAM. While the largest amount of travel time savings was realized when traveling to the Augsburg Central Station via the Thesis' 130-station network, the map (map E of Figure 20B) indicated a large portion of the study area experienced no travel time savings. This could perhaps indicate the study area is a bit small to implement UAM at this scale. Increasing the size would likely lead to longer distance trips where travel time savings from UAM could become more widespread.

The manually selected OBUAM networks were generally found to produce greater travel time savings than the semi-automated Thesis networks. This was in great part due to the exact placement of the OBUAM network stations. The locations of OBUAM-network stations were carefully considered by experts [8] and often placed near major roads and/or public transportation nodes. Further, there was always an OBUAM station allocated at the tested destination sites for travel time comparisons. The OBUAM stations were therefore allocated in areas with high accessibility. While Thesis-network stations were allocated to areas of high demand, they were often allocated to areas with low connectivity. The Thesis-network station locations were constrained by the initial set of candidate facilities (shown in Appendix D), which were evenly spread out throughout the entire study area. Like UAM demand, station location is more influential than number of stations for travel time savings. This can be seen in the southeastern region of maps E and F of Figure 20B or maps C and D of Figure 22A where the Thesis UAM networks offered more stations, however generated lower travel times. These results are consistent with Lim and Hwang [20] who found that travel time savings are maximized with appropriately located UAM stations.

To conclude, the station allocation procedure employed in this thesis generated UAM networks that were evenly distributed throughout the study area. This resulted in comparatively higher UAM demand than the manually allocated OBUAM networks. However, when comparing travel times, the OBUAM network had apparent advantages due to their carefully considered station placements.

6.2 Limitations

The stations in this thesis were allocated without consideration of restricted airspace or land-use. The stations were essentially free to be allocated anywhere in the study area (except lakes and forests) where demand was satisfied. Further, the generated flight paths were straight station-to-station routes that often traversed over population. Some station allocation studies [3, 7, 22, 23] discussed in Section 2.2 did consider airspace restrictions while Ploetner et al. [8] explored flight paths that were restricted to fly over areas of low population density; similar to how existing helicopter routes in some US cities are set up [1]. UAM will likely be subject to several regulatory hurdles for cities and the public to accept its implementation. Noise, visual disturbances and emissions are all examples of possible negative effects from UAM [1]. Rothfeld et al. [2] indicated such byproducts of UAM should be explored in more detail. In addition to no airspace or land-use restrictions, the mode-choice modeling was conducted with no UAM station capacity restrictions and with a very large fleet size. The mode-choice modeling was therefore conducted for a scenario where a UAM vehicle is always readily available and wait time is nonexistent. While disregarding station capacity was consistent with previous studies [8, 21, 24], setting limits on fleet size was found to significantly increase UAM travel times, reduce UAM demand [14] and/or generate more demand than the supply of UAM vehicles could handle [8].

The location-allocation solver only considered car as a mode of a travel between demand points and potential stations. This is a limitation of the software where only a single impedance can be set at a time. Therefore, even though ESRI's ArcMap has the capability to include public transportation in infrastructure networks (or network datasets), the location-allocation solver would only be able to consider either, for example, travel time via car or via public transportation, but not both simultaneously. This is a limitation because studies such as Rothfeld et al. [2] or Ploetner et al. [8] have indicated UAM should be integrated as a multi-modal system.

As discussed in Section 6.1, the manually selected UAM networks generally outperformed the Thesis networks given their locations were carefully considered and often placed in highly accessible sites. The Thesis-network sites were pre-determined and limited to just under 1,000 evenly distributed points. This resulted in potential UAM station sites to often be located at arbitrary locations. Therefore, 1,000 evenly distributed points, as potential facility sites, were found to be too coarse for the size of the study area.

Finally, as was presented in Section 4.4.3, the location-allocation solver results were likely undesirably influenced by a zone structure error visualized in Figure 11. While going through all 5,000 zones is unwieldly to determine other such errors, simply disregarding empty (i.e. no land-use or socio-economic data) zones during the data collection and preparation step (Chapter 3) would have remedied the problem. As discussed, the error was unfortunately found towards the end of the thesis after all subsequent steps and analysis had been conducted.

6.3 Future Work

As described above in Section 6.1, the Thesis networks performed better than the OBUAM networks when considering UAM demand. However, the OBUAM networks provided greater travel time savings due to their carefully considered station placements. The OBUAM stations were allocated in areas of higher connectivity. Therefore, an interesting exploration could be the combination of these 2 methods where a few stations are manually placed in areas of high connectivity or known demand and then subsequent stations are allocated using the semi-automated location-allocation procedure used for the Thesis networks. As explained in Section 4.5.1 ESRI's location-allocation [88, 90] allows facilities to be classified as candidate or required. This could mitigate situations where UAM stations are allocated in poorly connected locations; an occurrence common to the resulting Thesis-network stations.

If maximizing UAM demand is the goal, a similar procedure could consist of running the location-allocation solver, fixing the allocated stations and again running the location-allocation solver with a single, or very small, increment in number of stations to find. Such UAM network creation could represent short-, medium- or long-term UAM implementation plans. The short-term UAM network stations would correspond to the initial set of stations that would produce the largest amount of potential UAM demand and could accommodate low-density networks early UAM operations are envisioned to serve [1].

Finally, the enhanced MITO model, that integrated the MATSim UAM extension, developed in Ploetner et al [8] was not used to full capacity. Only the MITO portion of the model was used without utilizing the feedback loop (described in Section 2.1.3) with the MATSim UAM extension's traffic assignment capabilities. Running MITO for all 70+ scenarios proved to be time consuming and required a significant amount of processing power. Adding the MATSim feedback loop would have surely increased computational requirements. Determining mode choice with this feedback loop could perhaps provide more realistic levels of demand and could possibly alter the incremental UAM demand pattern (Figure 14).

7 REFERENCES

[1] D. P. Thipphavong *et al.,* “Urban Air Mobility Airspace Integration Concepts and Considerations,” in *18th Aviation Technology, Integration, and Operations Conference (AIAA Aviation Forum 2018)*, Atlanta, GA, USA, 2018.

[2] R. Rothfeld, A. Straubinger, M. Fu, C. Al Haddad, and C. Antoniou, “Urban air mobility,” in *Demand for Emerging Transportation Systems: Modeling Adoption, Satisfaction, and Mobility Patterns*, C. Antoniou, D. Efthymiou, and E. Chaniotakis, Eds., Amsterdam: Elsevier, 2020, pp. 267–284.

[3] J. Holden and N. Goel, “Fast-Forwarding to a Future of On-Demand Urban Air Transportation,” Uber Elevate, Oct. 2016. [Online] Available: https://www.uber.com/elevate.pdf.

[4] M. D. Patterson, K. R. Antcliff, and L. W. Kohlman, “A Proposed Approach to Studying Urban Air Mobility Missions Including an Initial Exploration of Mission Requirements,” in *75th Annual Forum and Technology Display*, Phoenix, AZ, USA, 2018.

[5] R. L. Rothfeld, M. Balać, K. O. Ploetner, and C. Antoniou, “Agent-Based Simulation of Urban Air Mobility,” in *18th Aviation Technology, Integration, and Operations Conference (AIAA Aviation Forum 2018)*, Atlanta, GA, USA, 2018.

[6] S. Baur, S. Schickram, A. Homulenko, N. Martinez, and A. Dyskin, “Urban Air Mobility: The Rise of A New Mode of Transportation,” Roland Berger, Munich, Germany, Nov. 2018. [Online] Available: https://www.rolandberger.com/en/Publications/Passenger-drones-ready-for-take-off.html. Accessed on: July 2019.

[7] D. N. Fadhil, “A GIS-based Analysis for Selecting Ground Infrastructure Locations for Urban Air Mobility,” M.S. Thesis, Department of Civil, Geo and Environmental Engineering, Technical University of Munich (TUM), Munich, Germany, 2018.

[8] K. O. Ploetner *et al.,* “Long-Term Application of Urban Air Mobility Complementing Public Transport: An Upper Bavaria Example,” in *Deutscher Luft- und Raumfahrtkongress 2019 [German Aerospace Congress 2019]*, Darmstadt, Germany, 2019.

[9] Federal Office for Building and Regional Planning, “Spatial Development and Spatial Planning in Germany,” Federal Office for Building and Regional Planning, Bonn, Germany, Mar. 2001. [Online] Available: https://www.bbsr.bund.de/BBSR/EN/Publications/CompletedSeries/Berichte/2000_2009/BrochureSpatialDevelopment.html?nn=393166. Accessed on: December 2019.

[10] E. C. P. Neto, D. M. Baum, Júnior, Jorge Rady de Almeida, J. B. C. Junior, and P. S. Cugnasca, “Trajectory-Based Urban Air Mobility (UAM) Operations Simulator (TUS),” *CoRR*, vol. abs/1908.08651, 2019.

[11] M. Shamiyeh, J. Bijewitz, and M. Hornung, “A Review of Recent Personal Air Vehicle Concepts,” in *6th Council of European Airspace Societies (CEAS) Aerospace Conference*, Bucharest, Romania, 2017, pp. 1–16.

[12] Y. Liu, M. Kreimeier, E. Stumpf, Y. Zhou, and H. Liu, “Overview of Recent Endeavors on Personal Aerial Vehicles: A Focus on the US and Europe led Research Activities,” *Progress in Aerospace Sciences*, vol. 91, pp. 53–66, 2017.

[13] A. Horni, K. Nagel, and K. W. Axhausen, Eds., *Multi-Agent Transport Simulation MATSim*. London: Ubiquity Press, 2016.

[14] R. L. Rothfeld, M. Balać, K. O. Ploetner, and C. Antoniou, “Initial Analysis of Urban Air Mobility’s Transport Performance in Sioux Falls,” in *18th Aviation Technology, Integration, and Operations Conference (AIAA Aviation Forum 2018)*, Atlanta, GA, USA, 2018.

[15] R. Moeckel, N. Kuhnel, C. Llorca, A. T. Morenoa, and H. Rayaprolu, “Microscopic Travel Demand Modeling: Using the Agility of Agent-Based Modeling Without the Complexity of Activity-Based Models,” in *Transportation Research Board Annual Meeting 2019*, Washington, D.C., USA, 2019.

[16] A. Moreno and R. Moeckel, “Population Synthesis Handling Three Geographical Resolutions,” *IJGI*, vol. 7, no. 5, p. 174, 2018.

[17] K. R. Antcliff, M. D. Moore, and K. H. Goodrich, “Silicon Valley as an Early Adopter for On-Demand Civil VTOL Operations,” in *16th Aviation Technology, Integration, and Operations Conference (AIAA Aviation Forum 2016)*, Washington, D.C., USA, 2016.

[18] T. Otte, N. Metzner, J. Lipp, M. S. Schwienhorst, A. F. Solvay, and T. Meisen, “User-centered Integration of Automated Air Mobility into Urban Transportation Networks,” in *2018 IEEE/AIAA 37th Digital Avionics Systems Conference (DASC)*, London, 2018, pp. 1–10.

[19] J. Malczewski and C. Rinner, *Multicriteria Decision Analysis in Geographic Information Science*, 2015.

[20] E. Lim and H. Hwang, “The Selection of Vertiport Location for On-Demand Mobility and Its Application to Seoul Metro Area,” *International Journal of Aeronautical and Space Sciences*, vol. 20, no. 1, pp. 260–272, https://doi.org/10.1007/s42405-018-0117-0, 2019.

[21] S. Rath and J. Y. J. Chow, “Air Taxi Skyport Location Problem for Airport Access,” *Computing Research Repository (CoRR)*, vol. abs/1904.01497, 2019.

[22] N. Syed *et al.,* “Preliminary Considerations for ODM Air Traffic Management based on Analysis of Commuter Passenger Demand and Travel Patterns for the Silicon Valley Region of California,” in *17th Aviation Technology, Integration, and Operations Conference (AIAA Aviation Forum 2017)*, Denver, Colorado, USA, 2017.

[23] B. German, M. Daskilewicz, T. K. Hamilton, and M. M. Warren, “Cargo Delivery in by Passenger eVTOL Aircraft: A Case Study in the San Francisco Bay Area,” in *2018 AIAA Aerospace Sciences Meeting*, Kissimmee, Florida, USA, 2018.

[24] M. Daskilewicz, B. German, M. Warren, L. A. Garrow, S.-S. Boddupalli, and T. H. Douthat, “Progress in Vertiport Placement and Estimating Aircraft Range Requirements for eVTOL Daily Commuting,” in *18th Aviation*

Technology, Integration, and Operations Conference (AIAA Aviation Forum 2018), Atlanta, GA, USA, 2018.

[25] J. Malczewski, *GIS and Multicriteria Decision Analysis*. New York: J. Wiley & Sons, 1999.

[26] J. Malczewski, “GIS-based Multicriteria Decision Analysis: A Survey of the Literature,” *International Journal of Geographical Information Science*, vol. 20, no. 7, pp. 703–726, 2006.

[27] S. Drobne and A. Lisec, “Multi-attribute Decision Analysis in GIS: Weighted Linear Combination and Ordered Weighted Averaging,” *Informatica (Slovenia)*, vol. 33, pp. 459–474, 2009.

[28] H. Voogd, *Multicriteria Evaluation for Urban and Regional Planning*. London: Pion, 1983.

[29] C. Kao, “Weight Determination for Consistently Ranking Alternatives in Multiple Criteria Decision Analysis,” *Applied Mathematical Modelling*, vol. 34, no. 7, pp. 1779–1787, http://www.sciencedirect.com/science/article/pii/S0307904X0900300X, 2010.

[30] P. M. Macharia and C. N. Mundia, “GIS Analysis and Spatial Modelling for Optimal Oil Pipeline Route Location: A Case Study of Proposed Isiolo Nakuru Pipeline Route,” *International Journal of Science and Research*, vol. 3, no. 12, 1227-1231, 2014.

[31] J. Ma, Z.-P. Fan, and L.-H. Huang, “A Subjective and Objective Integrated Approach to Determine Attribute Weights,” *European Journal of Operational Research*, vol. 112, no. 2, pp. 397–404, http://www.sciencedirect.com/science/article/pii/S0377221798001416, 1999.

[32] N. H. Zardari, *Weighting Methods and their Effects on Multi-Criteria Decision Making Model Outcomes in Water Resources Management*. Cham: Springer, 2014.

[33] M. Şahin and H. Yurdugül, “A Content Analysis Study on the Use of Analytic Hierarchy Process in Educational Studies,” *Eğitimde ve Psikolojide*

Ölçme ve Değerlendirme Dergisi [Journal of Measurement and Evaluation in Education and Psychology], vol. 9, no. 4, pp. 376–392, 2018.

[34] T. L. Saaty, “Fundamentals of the Analytic Hierarchy Process,” in *Managing Forest Ecosystems, The Analytic Hierarchy Process in Natural Resource and Environmental Decision Making*, K. von Gadow et al., Eds., Dordrecht: Springer Netherlands, 2001, pp. 15–35.

[35] R. C. Estoque, “Analytic Hierarchy Process in Geospatial Analysis,” in *Progress in Geospatial Analysis*, Y. Murayama, Ed., Tokyo, New York: Springer, 2012.

[36] T. L. Saaty, “Axiomatic Foundation of the Analytic Hierarchy Process,” *Management Science*, vol. 32, no. 7, pp. 841–855, www.jstor.org/stable/2631765, 1986.

[37] T. Saaty, “Decision Making with the Analytic Hierarchy Process,” *Int. J. Services Sciences Int. J. Services Sciences*, vol. 1, no. 1, pp. 83–98, 2008.

[38] T. L. Saaty, *The Analytic Hierarchy Process: Planning, Priority Setting, Resource Allocation*. New York, London: McGraw-Hill, 1980.

[39] E. Forman and K. Peniwati, “Aggregating Individual Judgments and Priorities with the Analytic Hierarchy Process,” *European Journal of Operational Research*, vol. 108, no. 1, pp. 165–169, http://www.sciencedirect.com/science/article/pii/S0377221797002440, 1998.

[40] W. Ossadnik, S. Schinke, and R. H. Kaspar, “Group Aggregation Techniques for Analytic Hierarchy Process and Analytic Network Process: A Comparative Analysis,” *Group Decis Negot*, vol. 25, no. 2, pp. 421–457, 2016.

[41] E. Kazimieras Zavadskas, J. Antucheviciene, and S. Kar, “Multi-Objective and Multi-Attribute Optimization for Sustainable Development Decision Aiding,” *Sustainability*, vol. 11, no. 11, p. 3069, 2019.

[42] C.-L. Hwang and K. Yoon, *Multiple Attribute Decision Making: Methods and Applications A State-of-the-Art Survey (Lecture Notes in Economics and Mathematical Systems)*. Berlin, Germany: Springer Verlag, 1981.

[43] J. R. Beaumont, “Location-Allocation Problems in a Plane a Review of Some Models,” *Socio-Economic Planning Sciences*, vol. 15, no. 5, pp. 217–229, 1981.

[44] R. L. Church, “Location Modelling and GIS,” in *Geographical Information Systems: Principles, Techniques, Management, and Applications*, P. A. Longley, M. F. Goodchild, D. J. Maguire, and D. W. Rhind, Eds., 2nd ed., New York, Chichester: Wiley, 2005, pp. 293–303.

[45] R. Church and C. ReVelle, “The Maximal Covering Location Problem,” *Papers of the Regional Science Association*, vol. 32, no. 1, pp. 101–118, 1974.

[46] J. C. García-Palomares, J. Gutiérrez, and M. Latorre, “Optimizing the Location of Stations in Bike-Sharing Programs: A GIS Approach,” *Applied Geography*, vol. 35, no. 1-2, pp. 235–246, 2012.

[47] R. Church and F. A. Medrano, “Location-Allocation Modeling and GIS,” in *The Geographic Information Science & Technology Body of Knowledge*, D. DiBiase et al., Eds., Washington, D.C.: Association of American Geographers, 2006.

[48] T. L. Lei, R. L. Church, and Z. Lei, “A Unified Approach for Location-Allocation Analysis: Integrating GIS, Distributed Computing and Spatial Optimization,” *International Journal of Geographical Information Science*, vol. 30, no. 3, pp. 515–534, 2016.

[49] R. L. Church, “Geographical Information Systems and Location Science,” *Computers & Operations Research*, vol. 29, no. 6, pp. 541–562, 2002.

[50] ESRI, *Algorithms Used by the ArcGIS Network Analyst Extension.* [Online] Available: http://desktop.arcgis.com/en/arcmap/latest/extensions/network-analyst/algorithms-used-by-network-analyst.htm. Accessed on: December 2019.

[51] P. J. Densham and G. Rushton, “Strategies for Solving Large Location-Allocation Problems by Heuristic Methods,” *Environ Plan A*, vol. 24, no. 2, pp. 289–304, 1992.

[52] S. M. S. Mapa and R. d. S. Lima, “Combining Geographic Information Systems for Transportation and Mixed Integer Linear Programming in

Facility Location-Allocation Problems," *JSEA*, vol. 07, no. 10, pp. 844–858, 2014.

[53] ESRI Academy, *Introduction to Surface Modeling Using ArcGIS.* [Online] Available: https://www.esri.com/training/catalog/57630436851d31e02a43f1b7/introduction-to-surface-modeling-using-arcgis/. Accessed on: October 2019.

[54] L. W. Zhi, "Chapter 15: Spatial Interpolation," California State University, Fresno, November 2012.

[55] C. Vansarochana, N. Tripathi, and R. Clemente, "Finding Appropriate Interpolation Techniques for Topographic Surface Generation for Mudslide Risk Zonation," *Geocarto International*, vol. 24, pp. 313–332, 2009.

[56] C. Childs, "Interpolating Surfaces in ArcGIS Spatial Analyst," ESRI, ArcUser, Jul. 2004. [Online] Available: https://www.esri.com/news/arcuser/0704/summer2004.html. Accessed on: October 2019.

[57] A. Setianto and T. Triandini, "Comparison of Kriging and Inverse Distance Weighted (IDW) Interpolation Methods in Lineament Extraction and Analysis," *Journal of Applied Geology*, vol. 5, no. 1, http://dx.doi.org/10.22146/jag.7204, 2015.

[58] L. Mitas and H. Mitasova, "Spatial Interpolation," in *Geographical Information Systems: Principles, Techniques, Management, and Applications*, P. A. Longley, M. F. Goodchild, D. J. Maguire, and D. W. Rhind, Eds., 2nd ed., New York, Chichester: Wiley, 2005, pp. 481–492.

[59] ESRI, *How IDW works.* [Online] Available: http://desktop.arcgis.com/en/arcmap/latest/tools/3d-analyst-toolbox/how-idw-works.htm. Accessed on: November 2019.

[60] GISGeogrpahy, *Inverse Distance Weighting (IDW) Interpolation.* [Online] Available: https://gisgeography.com/inverse-distance-weighting-idw-interpolation/. Accessed on: November 2019.

[61] ESRI, *How Kernel Density works.* [Online] Available: http://desktop.arcgis.com/en/arcmap/latest/tools/spatial-analyst-toolbox/how-kernel-density-works.htm. Accessed on: November 2019.

[62] K. Kobylińska, R. Cellmer, S. Źróbek, and N. Lepkova, “Using Kernel Density Estimation for Modelling and Simulating Transaction Location,” *International Journal of Strategic Property Management*, vol. 21, no. 1, pp. 29–40, 2017.

[63] J. M. Krisp and O. Špatenková, “Kernel Density Estimations for Visual Analysis of Emergency Response Data,” in *Lecture Notes in Geoinformation and Cartography, Geographic Information and Cartography for Risk and Crisis Management*, M. Konecny, S. Zlatanova, and T. L. Bandrova, Eds., Berlin, Heidelberg: Springer Berlin Heidelberg, 2010, pp. 395–408.

[64] Larry Wasserman, “Statistical Methods for Machine Learning,” Carnegie Mellon University.

[65] J. Molloy and R. Moeckel, “Automated Design of Gradual Zone Systems,” *Open Geospatial Data, Software and Standards*, vol. 2, no. 1, p. 19, https://doi.org/10.1186/s40965-017-0032-5, 2017.

[66] K. Coffel *et al., Guidelines for Providing Access to Public Transportation Stations*. Washington, D.C.: Transportation Research Board, 2012.

[67] TripAdvisor, *Things to Do in Upper Bavaria.* [Online] Available: https://www.tripadvisor.com/Attractions-g1385761-Activities-Upper_Bavaria_Bavaria.html. Accessed on: July 2019.

[68] TripAdvisor, *Everything You Need to Know About the TripAdvisor Popularity Ranking.* [Online] Available: https://www.tripadvisor.com/TripAdvisorInsights/w765. Accessed on: Dec. 17 2019.

[69] OpenStreetMap, *Bayern.* [Online] Available: http://download.geofabrik.de/europe/germany/bayern.html. Accessed on: September 2019.

[70] Bavarian Chambers of Industry and Commerce (Industrie- und Handelskammern in Bayern), *Company Database of the Bavarian Chambers of Commerce and Industry.* [Online] Available: https://firmen-in-bayern.de/sites/fitby/welcome.aspx. Accessed on: July 2019.

[71] M. Minn, *MMQGIS*: Quantum GIS, 2019.

[72] QGIS Development Team (2018), *QGIS Geographic Information System*: Open Source Geospatial Foundation Project, 2018.

[73] K. T. Geurs and B. van Wee, “Accessibility Evaluation of Land-Use and Transport Strategies: Review and Research Directions,” *Journal of Transport Geography*, vol. 12, no. 2, pp. 127–140, 2004.

[74] W. G. Hansen, “How Accessibility Shapes Land Use,” *Journal of the American Institute of Planners*, vol. 25, no. 2, pp. 73–76, 1959.

[75] Travel Forecasting Resources, *Accessibilities.* [Online] Available: http://tfresource.org/Accessibilities. Accessed on: September 2019.

[76] M.-P. Kwan, “Space-Time and Integral Measures of Individual Accessibility: A Comparative Analysis Using a Point-based Framework,” *Geographical Analysis*, vol. 30, no. 3, pp. 191–216, 1998.

[77] D. Foot, *Operational Urban Models*: Routledge, 2017.

[78] M. Batty, *Urban Modelling: Algorithms, Calibrations, Predictions*. Cambridge: Cambridge University Press, 2010.

[79] R Core Team, *R: A Language and Environment for Statistical Computing*. Vienna, Austria: R Foundation for Statistical Computing, 2019.

[80] B. Németh *et al.,* “Comparison of Weighting Methods Used in Multicriteria Decision Analysis Frameworks in Healthcare with Focus on Low- and Middle-Income Countries,” (eng), *Journal of comparative effectiveness research*, vol. 8, no. 4, pp. 195–204, 2019.

[81] S. P. Robbins, *Management,* 4th ed. Englewood Cliffs, N.J.: Prentice Hall, 1994.

[82] G. A. Miller, “The Magical Number Seven, Plus or Minus Two: Some Limits on Our Capacity for Processing Information,” *Psychological Review*, vol. 63, no. 2, pp. 81–97, 1956.

[83] T. L. Saaty and M. S. Ozdemir, “Why the Magic Number Seven Plus or Minus Two,” *Mathematical and Computer Modelling*, vol. 38, no. 3-4, pp. 233–244, 2003.

[84] W. C. Wedley, “Consistency Prediction for Incomplete AHP Matrices,” *Mathematical and Computer Modelling*, vol. 17, no. 4-5, pp. 151–161, 1993.

[85] T. L. Saaty, “A Scaling Method for Priorities in Hierarchical Structures,” *Journal of Mathematical Psychology*, vol. 15, no. 3, pp. 234–281, 1977.

[86] ESRI, *ArcGIS Desktop*. Redlands, CA, USA: Environmental Systems Research Institute, 2019.

[87] ESRI, *IDW.* [Online] Available: https://desktop.arcgis.com/en/arcmap/latest/tools/3d-analyst-toolbox/idw.htm. Accessed on: December 2019.

[88] ESRI, *Location-Allocation Analysis.* [Online] Available: https://desktop.arcgis.com/en/arcmap/latest/extensions/network-analyst/location-allocation.htm. Accessed on: November 2019.

[89] ESRI, *What is a Network Dataset?* [Online] Available: https://desktop.arcgis.com/en/arcmap/latest/extensions/network-analyst/what-is-a-network-dataset.htm. Accessed on: December 2019.

[90] ESRI, *Solve Location Allocation.* [Online] Available: https://pro.arcgis.com/en/pro-app/tool-reference/ready-to-use/itemdesc-solvelocationallocation.htm. Accessed on: December 2019.

[91] ESRI, *What is Model Builder?* [Online] Available: https://desktop.arcgis.com/en/arcmap/latest/analyze/modelbuilder/what-is-modelbuilder.htm. Accessed on: December 2019.

[92] ESRI, *Calculate Locations.* [Online] Available: https://desktop.arcgis.com/en/arcmap/latest/tools/network-analyst-toolbox/calculate-locations.htm. Accessed on: December 2019.

[93] R. L. Church and C. S. ReVelle, “Theoretical and Computational Links between the p-Median, Location Set-covering, and the Maximal Covering Location Problem,” *Geographical Analysis*, vol. 8, no. 4, pp. 406–415, 1976.

[94] R. Rothfeld and M. Balac, *MATSim-UAM.* [Online] Available: https://bauhausluftfahrt.github.io/MATSim-UAM/. Accessed on: July 2019.

[95] R. Moeckel, *MITO.* [Online] Available: https://wiki.tum.de/display/msmmodels/MITO. Accessed on: January 2020.

[96] Bavaria State Office for Statistics, *Statistics.* [Online] Available: https://www.statistik.bayern.de/statistik/index.html.

[97] TomTom, *Munich: Munich in the Traffic Index.* [Online] Available: https://www.tomtom.com/en_gb/traffic-index/munich-traffic#statistics. Accessed on: Dec. 20 2019.

[98] TomTom, *Augsburg: Augsburg in the Traffic Index.* [Online] Available: https://www.tomtom.com/en_gb/traffic-index/augsburg-traffic. Accessed on: Jan. 06 2020.

8 APPENDICES

APPENDIX A POINTS OF INTEREST

The sites considered for the points of interest factor were the following:

Marienplatz	Hofgarten
Englischer Garten	Deutsches Museum
KZ-Gedenkstätte Dachau	Frauenkirche
Asamkirche	Odeonsplatz
Chiemsee	Max-Joseph-Platz
New Town Hall Munich	Karlsplatz/Stachus
Theresienwiese (Oktoberfest)	Eisbachwelle
Hellabrunn Zoo	St. Martin Church
Alte Pinakothek	Trausnitz Castle
Viktualienmarkt	Botanical Garden at Nymphenburg
Nymphenburg Palace	Augsburg Zoo
Allianz Arena	Augsburger Puppenkiste
Lake Starnberger	Fuggerei
Munich Residence	Augbsburg Town Hall
St. Peter’s Church	Augsburg Cathedral
Olympiapark	Weihenstephan
BMW-World	Erdinger Weissbräu
Neue Pinakothek	Erding Thermal Baths
Andechs Monastery	Ingolstadt Altstadt
Pinakothek der Moderne	Audi Museum + HQ
Chinese Tower	Ingolstadt Village
Königsplatz	BMW Zentrale

APPENDIX B FACTOR HEATMAPS

B1. Population

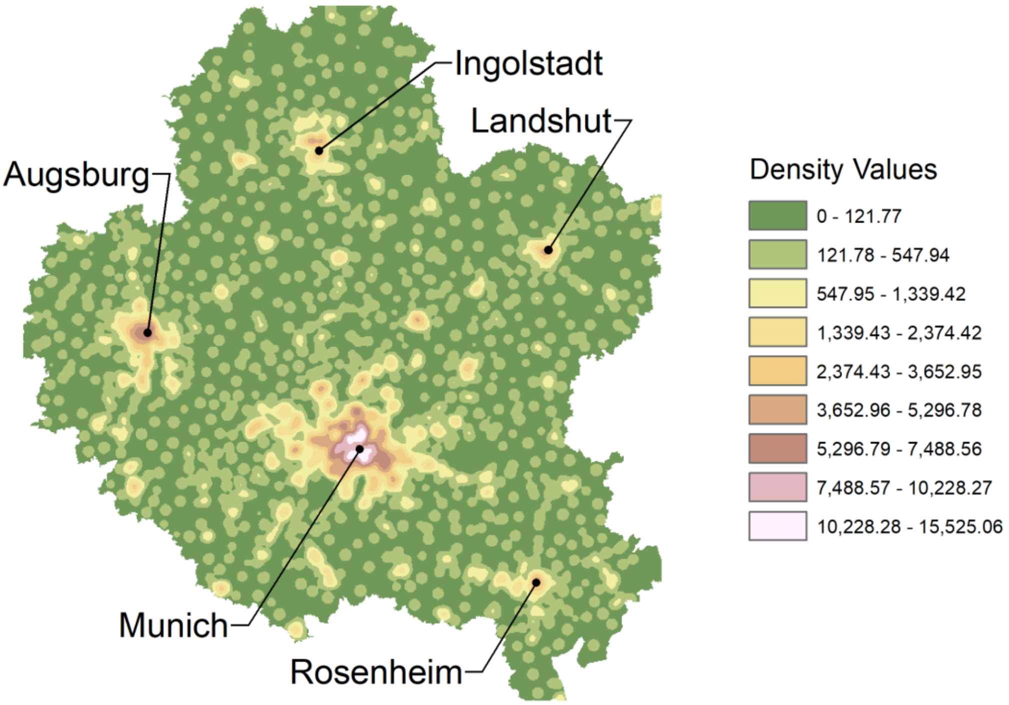

B2. Employment

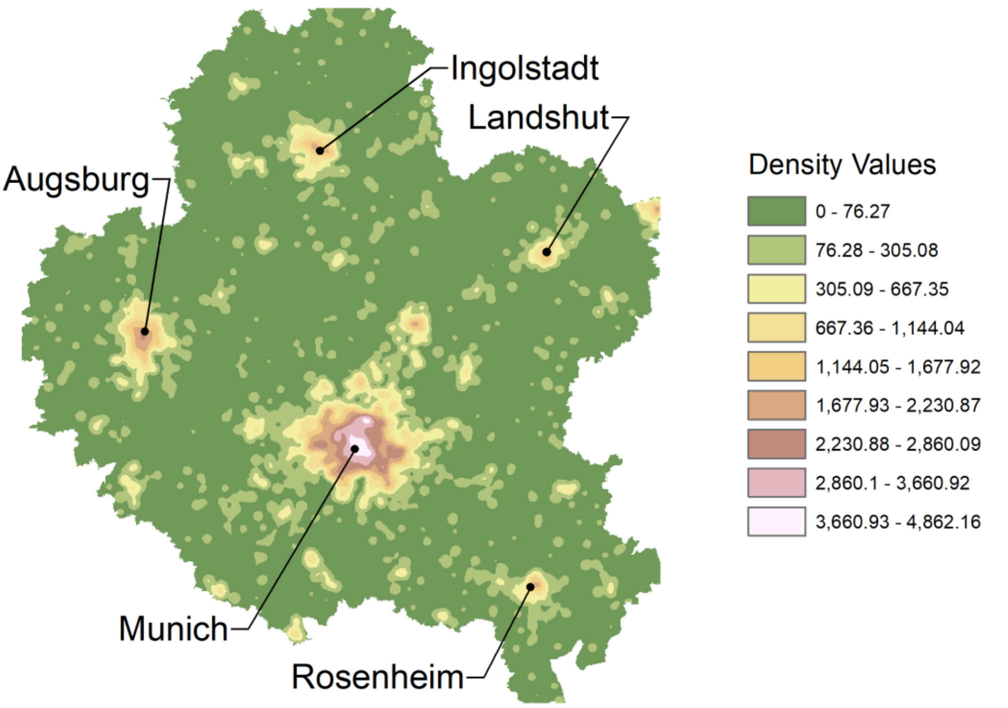

B3. Points of Interest

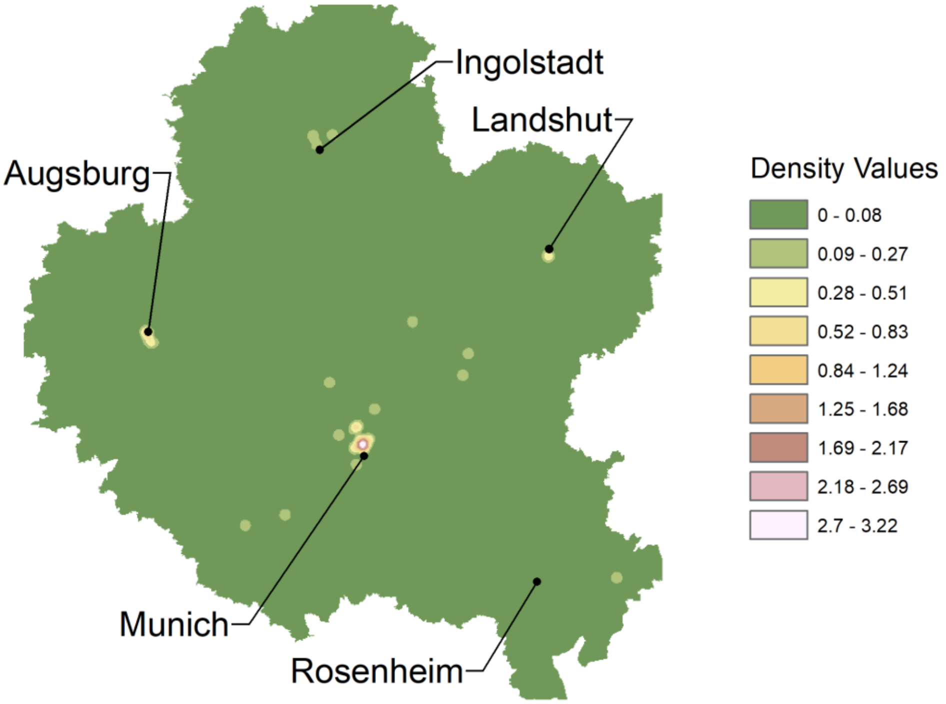

B4. Transportation Nodes

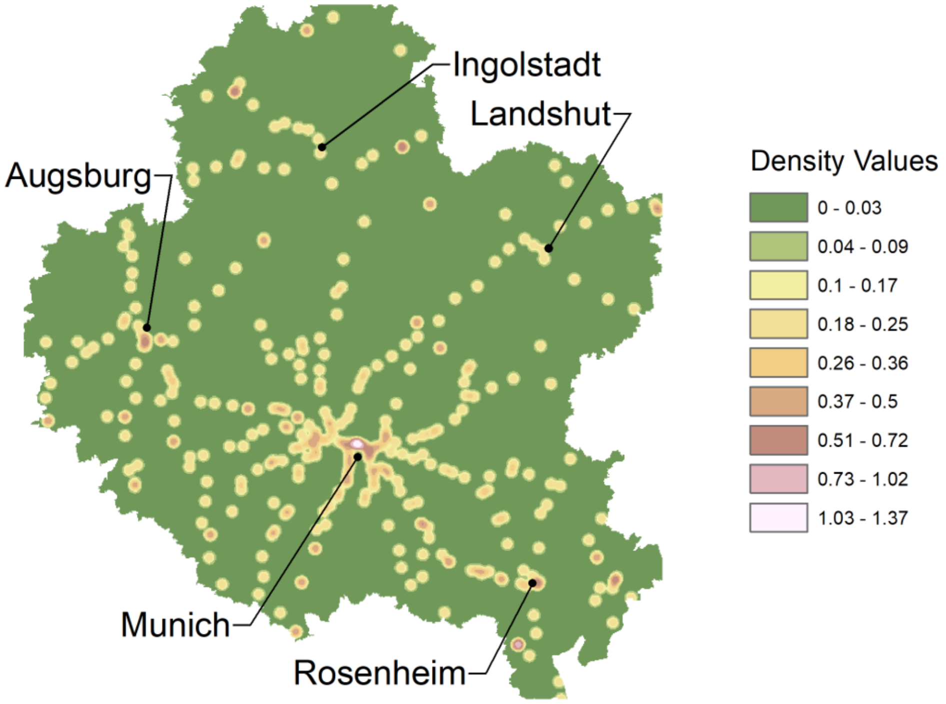

B5. Company Headquarters

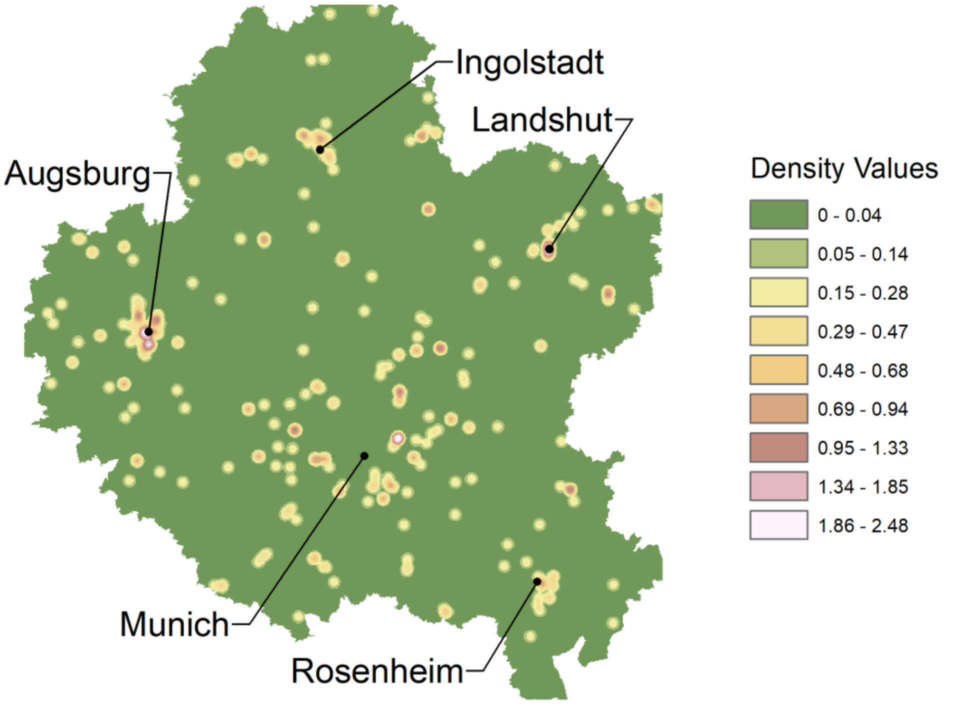

B6. Travel Demand

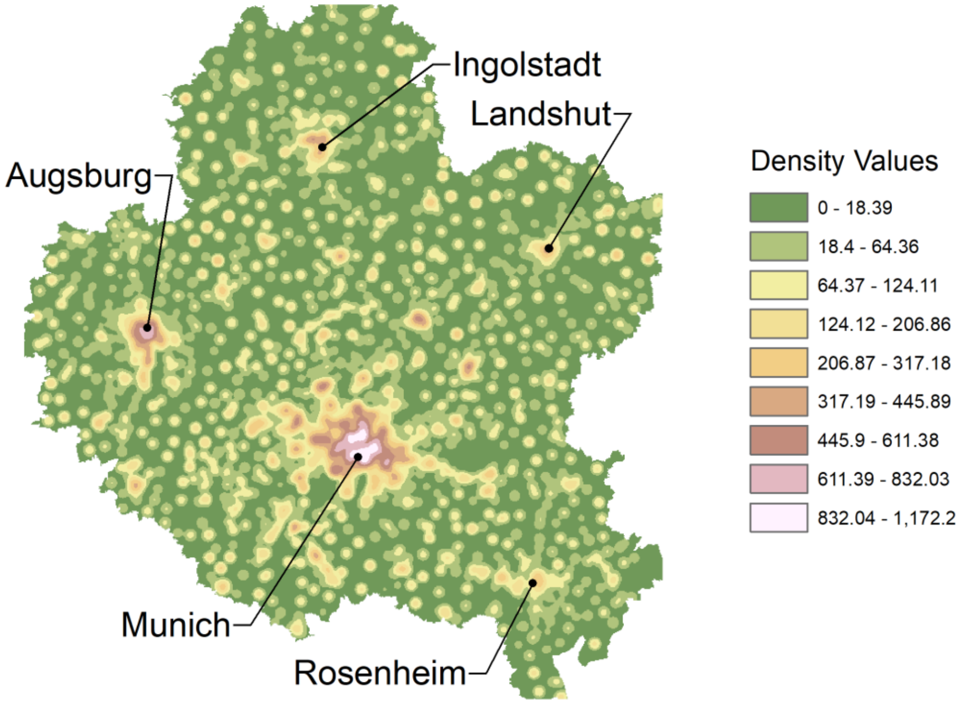

B7. Car Accessibility to Population

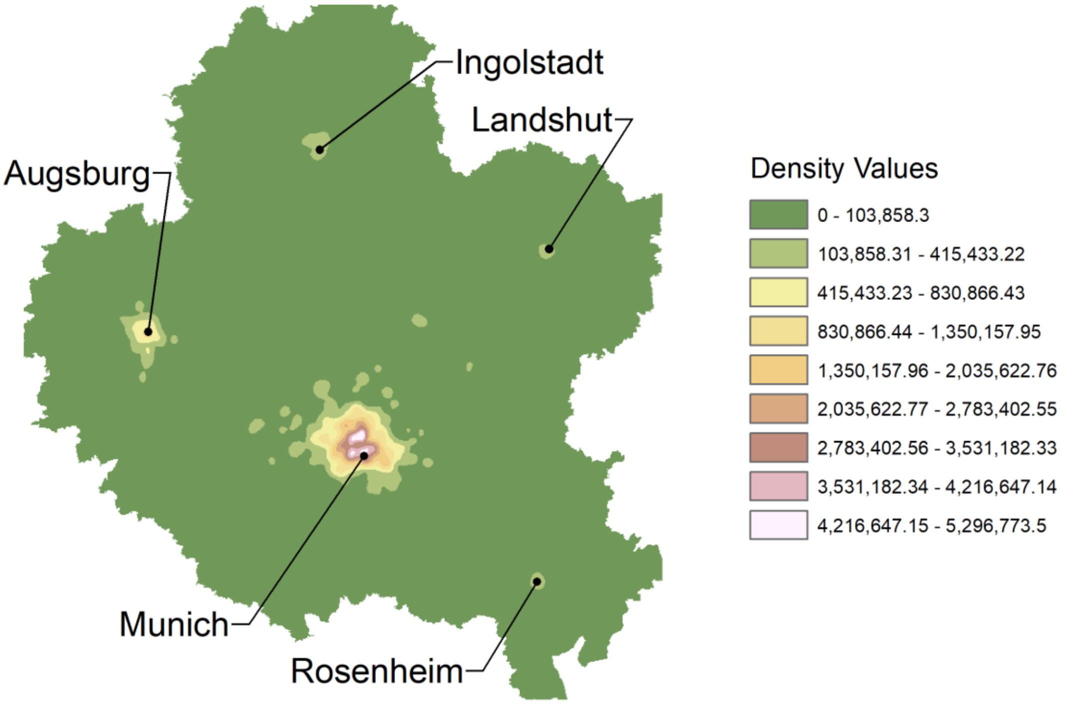

B8. Car Accessibility to Employment

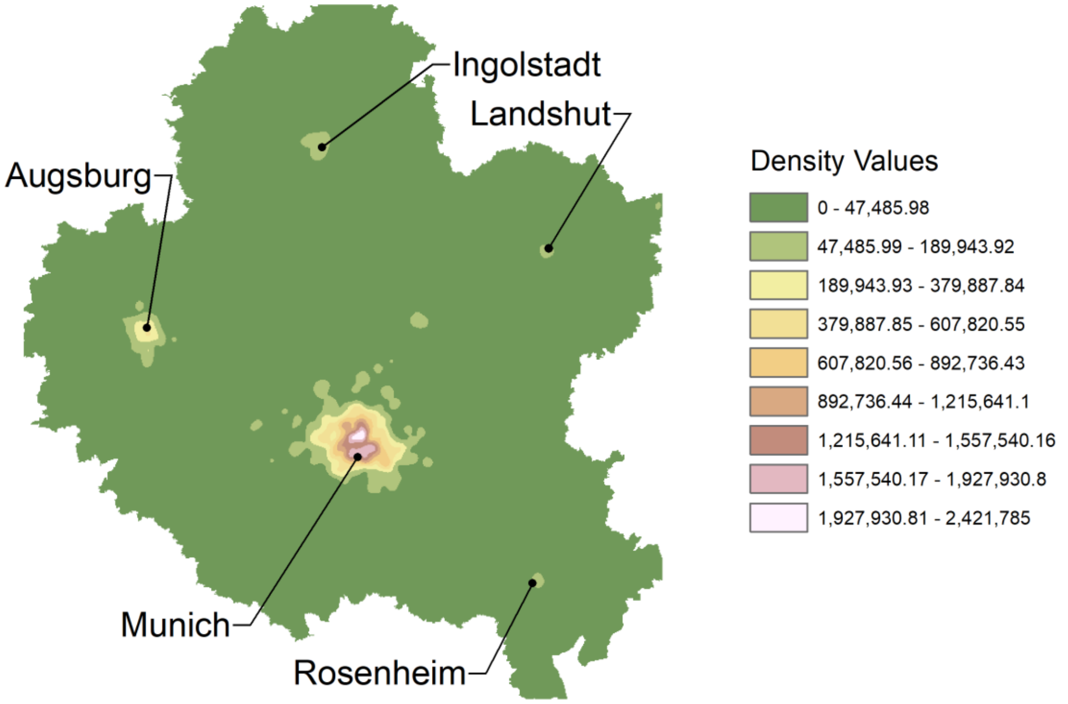

B9. PT Accessibility to Population

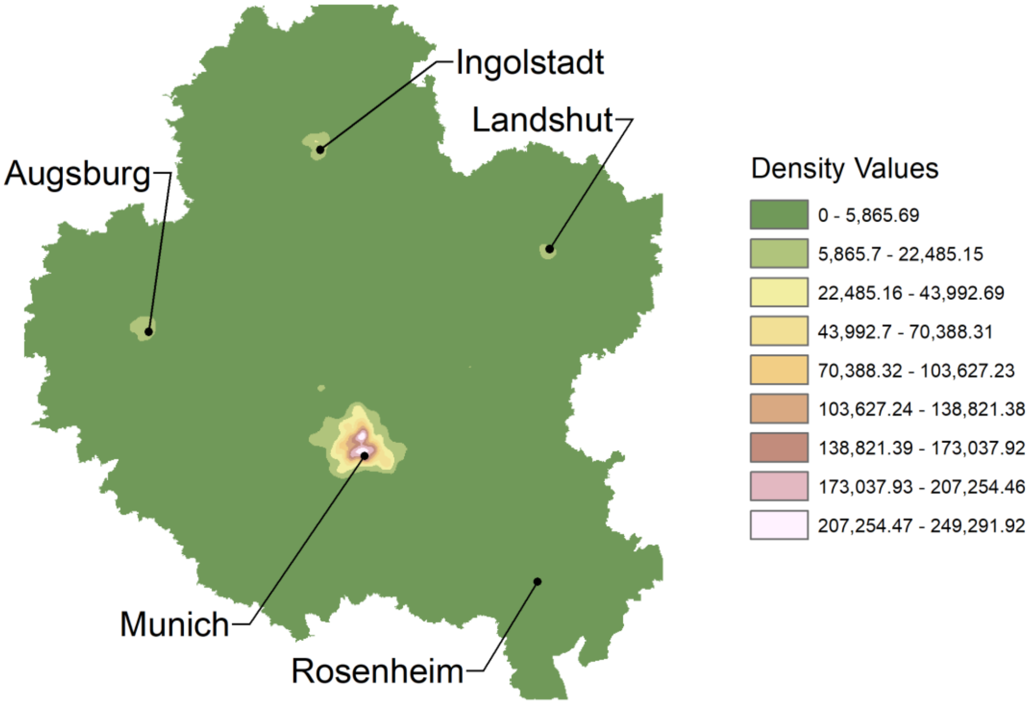

B10. PT Accessibility to Employment

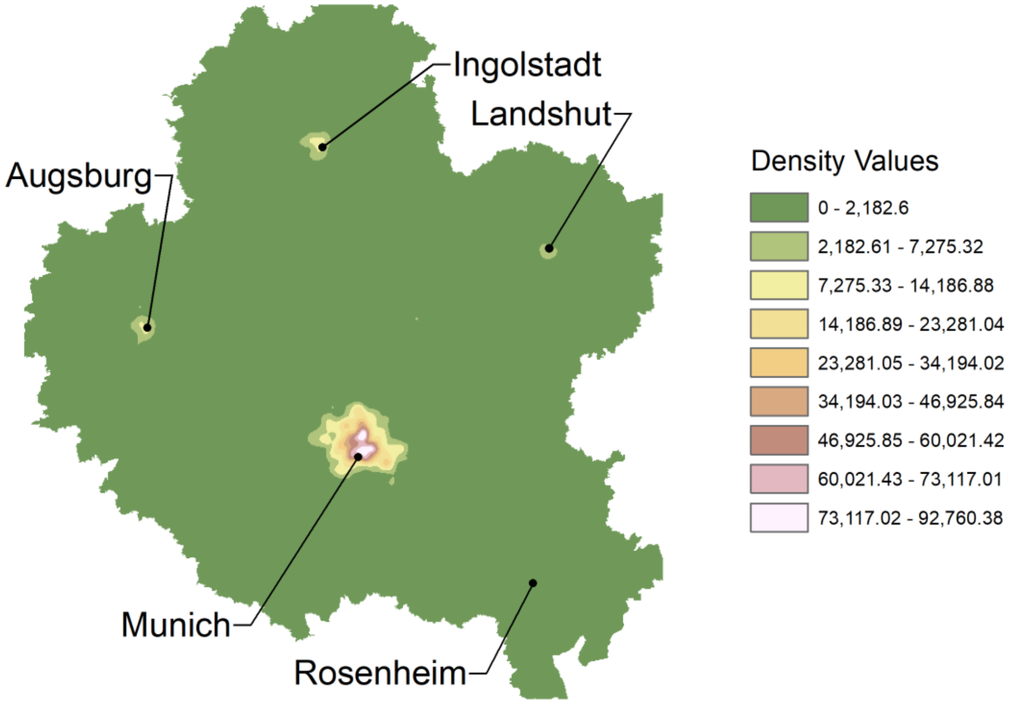

APPENDIX C AHP QUESTIONNAIRE

C1. Pairwise Comparison

No.	Is factor 1 or 2 more important?				Status 1	Equal	By how much more?	Status 2
		Factor 1		Factor 2				
1	□	Population	□	Employment	Pending			Pending
2	□	Population	□	POI	Pending			Pending
3	□	Population	□	Transport Nodes	Pending			Pending
4	□	Population	□	Company HQs	Pending			Pending
5	□	Population	□	Total O/D	Pending			Pending
6	□	Population	□	Car Accessibility to Employment	Pending			Pending
7	□	Population	□	Car Accessibility to Population	Pending			Pending
8	□	Population	□	PT Accessibility to Employment	Pending			Pending
9	□	Population	□	PT Accessibility to Population	Pending			Pending
10	□	Employment	□	POI	Pending			Pending
11	□	Employment	□	Transport Nodes	Pending			Pending
12	□	Employment	□	Company HQs	Pending			Pending
13	□	Employment	□	Total O/D	Pending			Pending
14	□	Employment	□	Car Accessibility to Employment	Pending			Pending
15	□	Employment	□	Car Accessibility to Population	Pending			Pending
16	□	Employment	□	PT Accessibility to Employment	Pending			Pending
17	□	Employment	□	PT Accessibility to Population	Pending			Pending
18	□	POI	□	Transport Nodes	Pending			Pending
19	□	POI	□	Company HQs	Pending			Pending
20	□	POI	□	Total O/D	Pending			Pending
21	□	POI	□	Car Accessibility to Employment	Pending			Pending
22	□	POI	□	Car Accessibility to Population	Pending			Pending
23	□	POI	□	PT Accessibility to Employment	Pending			Pending
24	□	POI	□	PT Accessibility to Population	Pending			Pending
25	□	Transport Nodes	□	Company HQs	Pending			Pending
26	□	Transport Nodes	□	Total O/D	Pending			Pending
27	□	Transport Nodes	□	Car Accessibility to Employment	Pending			Pending
28	□	Transport Nodes	□	Car Accessibility to Population	Pending			Pending
29	□	Transport Nodes	□	PT Accessibility to Employment	Pending			Pending
30	□	Transport Nodes	□	PT Accessibility to Population	Pending			Pending
31	□	Company HQs	□	Total O/D	Pending			Pending
32	□	Company HQs	□	Car Accessibility to Employment	Pending			Pending
33	□	Company HQs	□	Car Accessibility to Population	Pending			Pending
34	□	Company HQs	□	PT Accessibility to Employment	Pending			Pending
35	□	Company HQs	□	PT Accessibility to Population	Pending			Pending
36	□	Total O/D	□	Car Accessibility to Employment	Pending			Pending
37	□	Total O/D	□	Car Accessibility to Population	Pending			Pending
38	□	Total O/D	□	PT Accessibility to Employment	Pending			Pending
39	□	Total O/D	□	PT Accessibility to Population	Pending			Pending
40	□	Car Accessibility to Employment	□	Car Accessibility to Population	Pending			Pending
41	□	Car Accessibility to Employment	□	PT Accessibility to Employment	Pending			Pending
42	□	Car Accessibility to Employment	□	PT Accessibility to Population	Pending			Pending
43	□	Car Accessibility to Population	□	PT Accessibility to Employment	Pending			Pending
44	□	Car Accessibility to Population	□	PT Accessibility to Population	Pending			Pending
45	□	PT Accessibility to Employment	□	PT Accessibility to Population	Pending			Pending

C2. Comparison Matrix

Comparison Matrix - All Factors										
FACTORS	Pop	Emp	POI	Transport	CompHQ	TotOD	CarAccEmp	CarAccPop	PtAccEmp	PtAccPop
Pop	1	1	1	1	1	1	1	1	1	1
Emp	1	1	1	1	1	1	1	1	1	1
POI	1	1	1	1	1	1	1	1	1	1
Transport	1	1	1	1	1	1	1	1	1	1
CompHQ	1	1	1	1	1	1	1	1	1	1
TotOD	1	1	1	1	1	1	1	1	1	1
CarAccEmp	1	1	1	1	1	1	1	1	1	1
CarAccPop	1	1	1	1	1	1	1	1	1	1
PtAccEmp	1	1	1	1	1	1	1	1	1	1
PtAccPop	1	1	1	1	1	1	1	1	1	1
sum	10	10	10	10	10	10	10	10	10	10

C3. Priority Vector

Normalized Relative Weight Matrix - All Factors											Eigenvector
FACTORS	Pop	Emp	POI	Transport	CompHQ	TotOD	CarAccEmp	CarAccPop	PtAccEmp	PtAccPop	
Pop	0.1	0.1	0.1	0.1	0.1	0.1	0.1	0.1	0.1	0.1	0.1
Emp	0.1	0.1	0.1	0.1	0.1	0.1	0.1	0.1	0.1	0.1	0.1
POI	0.1	0.1	0.1	0.1	0.1	0.1	0.1	0.1	0.1	0.1	0.1
Transport	0.1	0.1	0.1	0.1	0.1	0.1	0.1	0.1	0.1	0.1	0.1
CompHQ	0.1	0.1	0.1	0.1	0.1	0.1	0.1	0.1	0.1	0.1	0.1
TotOD	0.1	0.1	0.1	0.1	0.1	0.1	0.1	0.1	0.1	0.1	0.1
CarAccEmp	0.1	0.1	0.1	0.1	0.1	0.1	0.1	0.1	0.1	0.1	0.1
CarAccPop	0.1	0.1	0.1	0.1	0.1	0.1	0.1	0.1	0.1	0.1	0.1
PtAccEmp	0.1	0.1	0.1	0.1	0.1	0.1	0.1	0.1	0.1	0.1	0.1
PtAccPop	0.1	0.1	0.1	0.1	0.1	0.1	0.1	0.1	0.1	0.1	0.1

C4. Consistency

Consistencies - All Factors										
Factors	*Pop*	*Emp*	*POI*	*Transport*	*CompHQ*	*TotOD*	*CarAccEmp*	*CarAccPop*	*PtAccEmp*	*PtAccPop*
Eigenvector	0.1	0.1	0.1	0.1	0.1	0.1	0.1	0.1	0.1	0.1
sum	10	10	10	10	10	10	10	10	10	10
Maximum Eigenvalue	10									
Consistency Index (CI)	-1.97373E-16									
Random Consistency Index (RI)	1.49									
Consistency Ratio (CR)	0%									

APPENDIX D DEMAND POINTS AND FACILITIES

D1. Demand Points

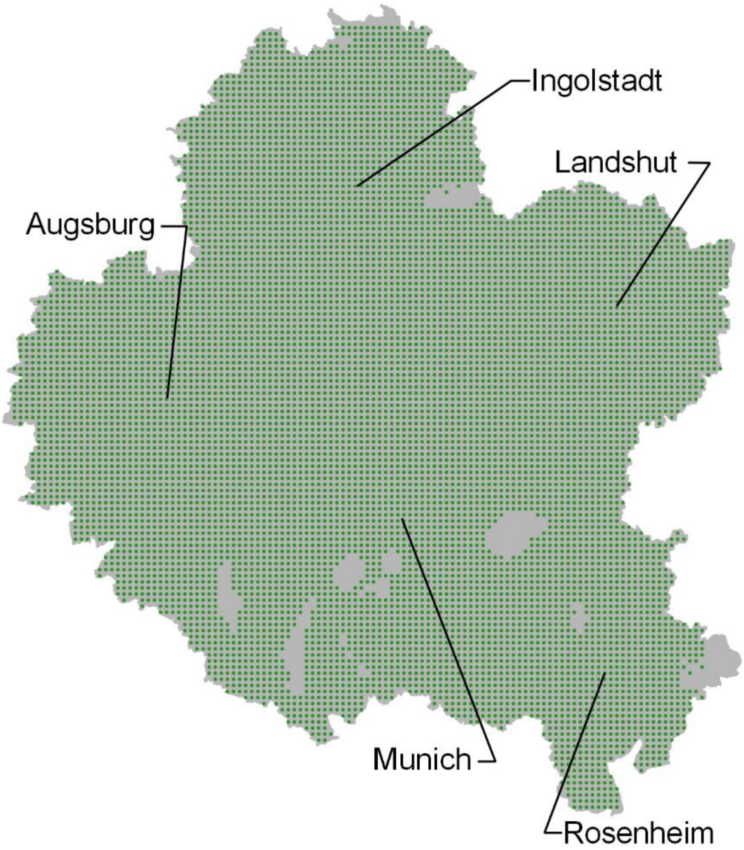

D2. Facilities

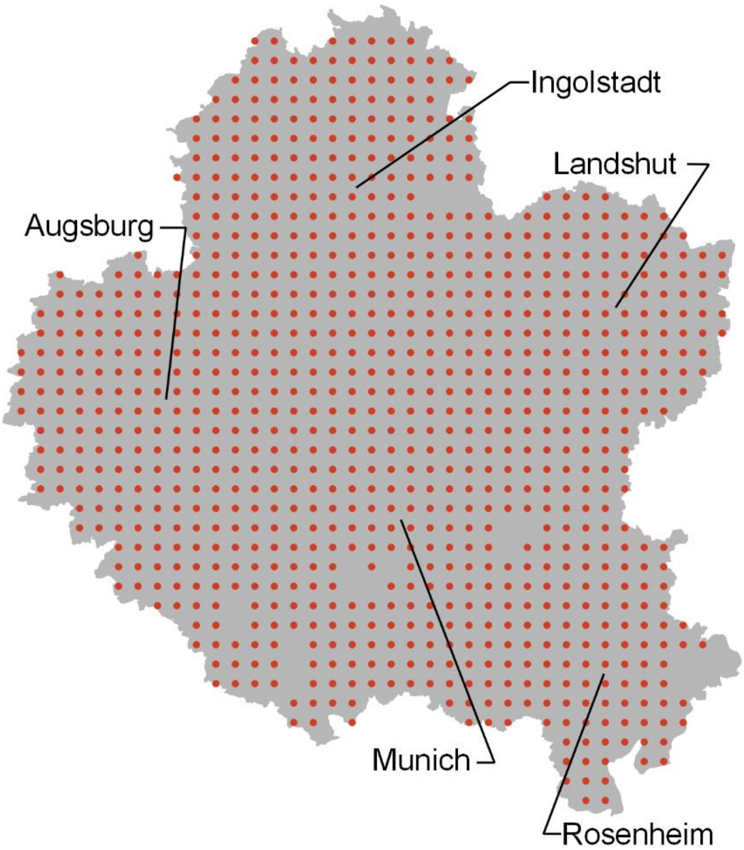

APPENDIX E LOCATION-ALLOCATION MODEL BUILDER

The model builder figure was broken up into 2 separate images below. Ellipsoid shapes correspond to variables (inputs/outputs) while rounded squares correspond to ESRI tools. The by, to and from values on the left correspond to the iterator values and represented the number of stations to find. The output layer variable corresponds to the naming of all generated files and workspace variable to the save location of said files. Required inputs are shown in blue and correspond, from left to right, to the network dataset (i.e. roads), input demand (i.e. demand points) and input facilities. Other inputs included the location-allocation problem type (e.g. minimize impedance or maximize coverage) and impedance cutoff values. The bottom image shows the model's segregation and saving procedures for generated files.

E1. Location-Allocation Model Builder

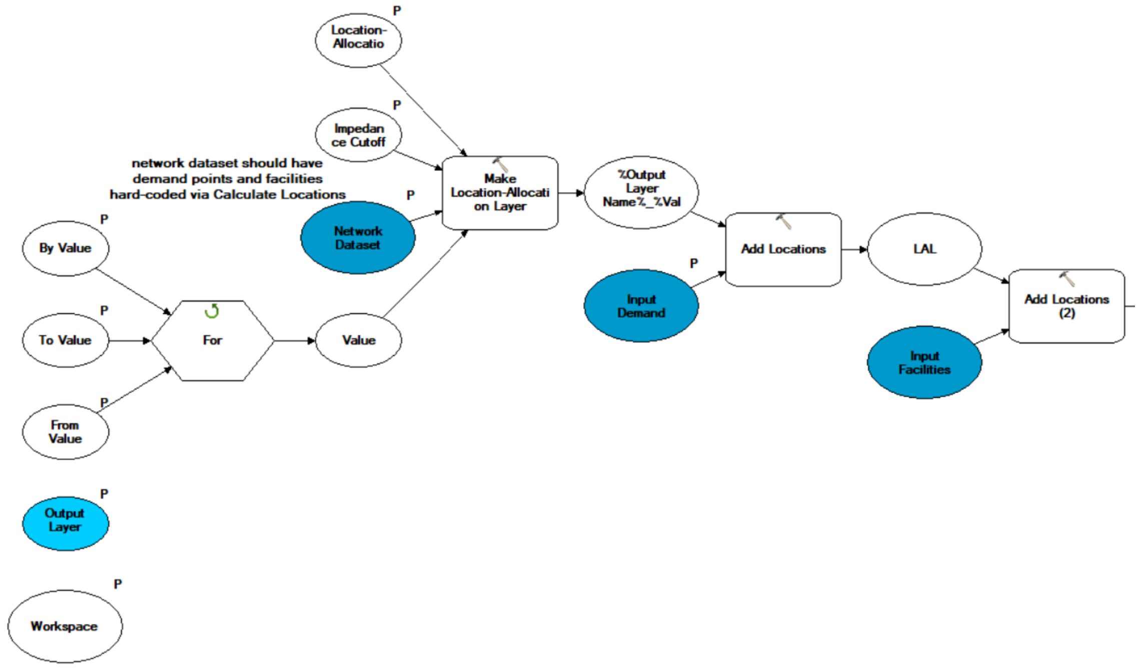

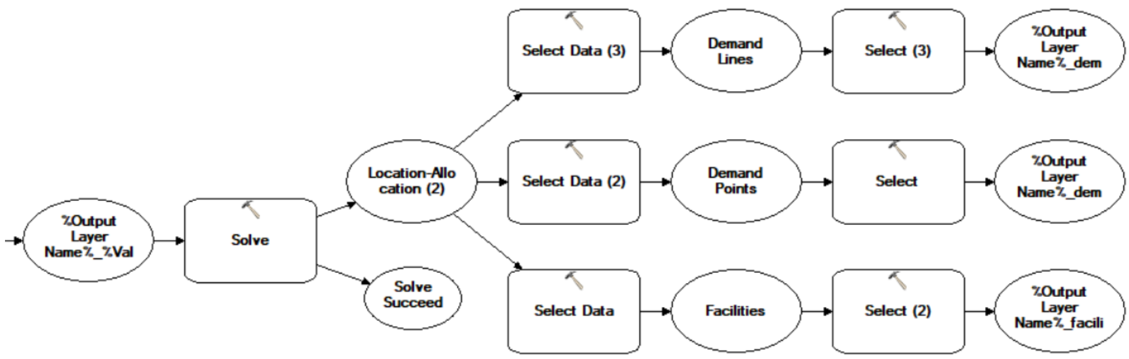

Statement of Independent Work

I hereby confirm that this thesis was written independently by myself without the use of any sources beyond those cited, and all passages and ideas taken from other sources are cited accordingly.

Munich, January 15th, 2020

Secundino Arellano III